Subcooled Pool Boiling CHFs for Various Liquids due to Steady and Transient Heat Input

Park, Jongdoc

(Degree)
博士（工学）

(Date of Degree)
2006-03-25

(Date of Publication)
2009-02-19

(Resource Type)
doctoral thesis

(Report Number)
甲3574

(URL)
https://hdl.handle.net/20.500.14094/D1003574

Kobe University
Doctoral Dissertation

Subcooled Pool Boiling CHFs for Various Liquids due to Steady and Transient Heat Input

January 2006

Kobe University
Graduate School of Science and Technology

Division of Ocean Mechanical and Energy Engineering

Jongdoc PARK

Subcooled Pool Boiling CHFs for Various Liquids due to Steady and Transient Heat Input

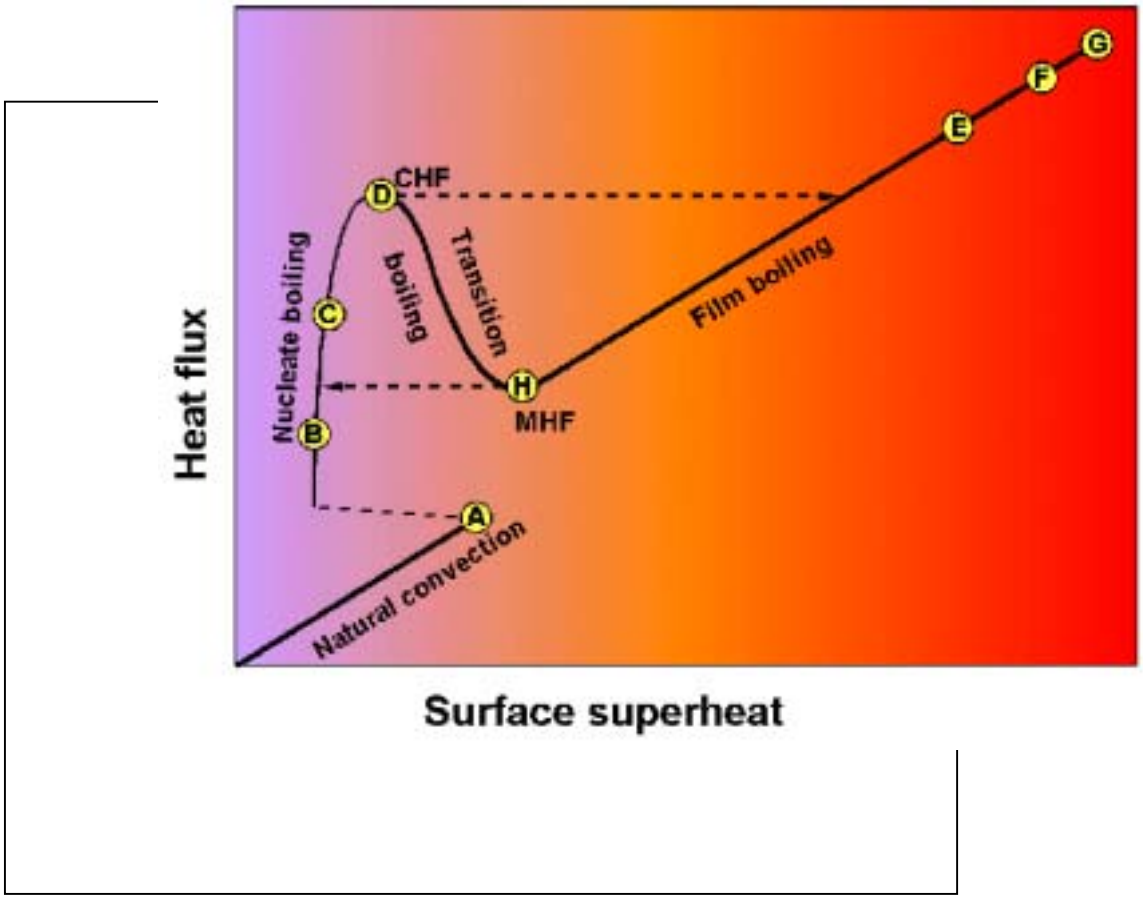

Januray 2006

Jongdoc PARK

Contents

Nomenclature

c_p	Specific heat at constant pressure, J/(kgK)
D	Cylinder diameter, m
K_0	Modified Bessel function of the second kind of zero-order
K_{1st}	Modified Bessel function of the second kind of first-order
K_1	Coefficient in Eq. (3.5)
K_2	Coefficient in Eq. (3.4)
K_3	Coefficient in Eq. (3.6)
K_4	Coefficient in Eq. (3.7)
k	Thermal conductivity, W/(mK)
L'	Non-dimensional length
p	Pressure, Pa
$p_{cr,l}$	Critical pressure of liquid
Q	Heat generation rate, W/m^3
Q_o	Initial heat generation rate, W/m^3
q_{cr}	Critical heat flux, W/m^2
$q_{cr,sat}$	q_{cr} for saturated condition, W/m^2
$q^*_{cr,sat}$	q_{cr} due to HSN for saturated condition, W/m^2
$q_{cr,sub}$	q_{cr} for subcooled condition, W/m^2
q_{st}	Steady-state critical heat flux, W/m^2
$q_{st,sub}$	q_{st} for subcooled condition, W/m^2
q_{in}	Boiling initiation heat flux, W/m^2
T_B	Bulk liquid temperature, K
T_w	Heater surface temperature, K

ΔT_{in} Incipient boiling surface superheat, K

$\Delta T_{sat} = (T_w - T_{sat})$, Surface superheat, K

$\Delta T_{sub} = (T_{sat} - T_B)$, Liquid subcooling, K

t Time, s

Greek symbols

ρ Density, kg/ m^3

σ Surface tension, N/m

τ Period, s

Subscript

B Bulk

l Liquid

v Vapor

Abbreviations

CHF	Critical heat flux
CS	Commercially-available surface of heater
FDNB	Fully-developed nucleate boiling
HI	Hydrodynamic instability
HSN	Heterogeneous spontaneous nucleation
MS	Heater surface like mirror
Period	The e-fold time corresponding to heat generation rate with the exponential increasing rates from quasi-steady to rapid ones.
RS	Roughly-finished surface of heater

1. Introduction

1.1 Background of CHF research

The critical heat flux (CHF) in boiling heat transfer was vivid in the research history of CHF after the first treatment of CHF in the study of heat transfer was performed by Professor Nukiyama in 1934. Immediately following this, many opinions and theories on CHF were made publicly. However, almost all of that made publicly became forgotten in history because there was constant controversy between theories. When an experiment fact appeared to support a new theory, another new theory was opposed to the existing one in succession. It can put the significance of the theories and opinions forgotten to the derived things such as the experiment method, the experiment fact and the idea etc. brought up in experiment process in order to verify their theory, rather than contribution to CHF. Only these derivatives have been the world of the CHF research that is extremely prospered in the present.

The sound development of knowledge for generalized saturated and subcooled pool boiling CHF mechanisms and those correlations for various test heater configurations and surface conditions in water and wetting liquid such as ethanol, liquid nitrogen, liquid helium and Fluorinert (FC liquids) etc, for wide range of subcoolings and pressures due to steady and transient heat inputs is becoming increasingly important not only for the academic knowledge on the complex transition phenomena but also for the fundamental database of following problems: the transient thermal response of reactivity accident and the engineering safety evaluation of a nuclear reactor, the design such as the high heat flux cooling systems using subcooled water pool boiling, the super-conducting magnets cooled by liquid helium and liquid nitrogen, the thermal control of microelectronic assemblies cooled by FC liquids for future super-computers and so

on. Furthermore, the evaluation of the pool boiling CHF becomes the database for the derivation of subcooled flow boiling CHF correlations based on the pool boiling ones, and it is also an essential problem when the liquid flow in the cooling equipment stops due to accidents.

Many aspects of saturated and subcooled pool boiling CHF have been investigated by many researchers for pressures, subcoolings, test heater configurations, surface conditions, thermal properties, etc., assuming a CHF model mainly based on a kind of hydrodynamic instability at CHF. Recently the saturated and subcooled pool boiling CHF for a horizontal cylinder in water and wetting liquids were measured for comparatively wide range of pressures and subcoolings. It was clarified that the CHFs measured were mainly divided into two mechanisms for lower and higher subcooling at a pressure as a typical case. It was assumed that the former and latter CHFs occur due to hydrodynamic instability (HI) and explosive-like heterogeneous spontaneous nucleation (HSN) on the cylinder surface respectively though the CHFs for subcooling occur only due to the HI or only due to the HSN depending on subcooling, pressure and liquid.

Recently the author analyzed in detail the flow boiling CHF data from some researchers. From the analysis, it was clarified that a maximum value existed in the CHFs as it becomes higher in the subcooling. That is, the maximum phenomenon of this flow boiling CHF data is an important matter from the viewpoint of engineering safety evaluation for cooling systems with high heat flux by increasing the subcooling. It is a result of the introduction of a new physical model to CHF due to the HSN described here, and it is certainly possible to contribute to the explanation of a general CHF mechanism for the cases without and with the flow that can be applied to wide range of liquids. Moreover, it is possible to clarify the effect that not only the heater surface condition but also the heater material and configuration have on the pool and the flow boiling CHF, and to accumulate the CHF database in a new viewpoint.

1.1 Background of CHF research

The scientific research on a steady-state boiling heat transfer has not been completely solved though there were many reports on it. There exists only a few researches on transient boiling heat transfer phenomena. The previous research on the transient boiling heat transfer was aimed to obtain critical heat flux, and the mechanism for CHF was divided into three: (1) The disappearance of liquid film due to evaporation under the steam block during nucleate boiling. (2) Fullness occupancy of the primary air bubbles on the surface of heater. (3) Bubble heat transfer and occupancy due to homogeneous spontaneous nucleation.

The typical trend of the CHF values in relation to the periods meaning of heat generation rate is as follows: the CHF gradually increases with a decrease in period up to the maximum CHF from the steady state one corresponding to the CHF for a period of 20 s, and then the CHF decreases down to the minimum one and again increases with a decrease in period. This trend suggests that there exists another mechanism of CHFs for shorter periods different from the thermal-hydrodynamic instability (HI) model firstly suggested by Kutateladze (1959) and Zuber (1959). The CHFs for the shorter periods at which direct or semi-direct transitions to film boiling occurred in transient conduction regime due to a quasi-steady- state or transient heat input for the liquids including water. A direct transition from non-boiling convective regime to film boiling one was reported by Avksentyuk and Mamontova (1973) and Kutateladze et al. (1973) in liquid metals and wetting liquids as some peculiarities of CHF. However, the mechanism of CHFs for the transient heat inputs with shorter periods remained unresolved for a long time.

The direct transition from a non-boiling regime such as natural convection and transient conduction regimes to film boiling without nucleate boiling was observed by Sakurai et al. (1992, 1993). They carried out the experiments of the CHFs for the transient heat inputs with various periods on a platinum horizontal cylinder in liquid nitrogen at various pressures, and found that direct transition to film boiling occurred in transient conduction

regime. It was assumed that the transitions occurred due to the levitation of liquid on the cylinder surface by the explosive-like heterogeneous spontaneous nucleation (HSN) in originally flooded cavities without the contribution of the active cavities entraining vapors for boiling incipience. All the cavities on the surface that could serve as nucleation sites would initially be flooded since the liquid surface tension is so low that vapor are not entrained in surface cavities and there is no dissolved gas in liquid nitrogen except for possible trace amounts of helium, hydrogen and neon. The explosive-like HSN assumed in originally flooded cavities on a horizontal cylinder in the wetting liquid of liquid nitrogen at which heat transfer crisis occurs was first observed without nucleate boiling under natural convection regime at atmospheric pressure due to steadily increasing heat input at a certain HSN surface superheat which is considerably lower than the corresponding the HSN on a flat surface and the homogeneous spontaneous nucleation at surface superheats theoretically obtained.

The measured CHFs related to subcoolings for water, liquid nitrogen and liquid helium with pressures as a parameter disagreed with the corresponding values derived from the existing correlations given by Kutateladze (1959) based on the model of CHF resulting from hydrodynamic instability. However, those data were well described by the newly derived subcooled pool boiling CHF correlations derived by Sakurai et al. (1993) by assuming that CHFs occur due to the hydrodynamic instability (HI), or the heterogeneous spontaneous nucleation (HSN) in originally flooded cavities with liquid on the test heater surface. Recently Chang et al. (1998) measured CHF and corresponding surface superheat at which the transition from natural convection regime to film boiling in a pool of FC-87, and also measured minimum film boiling heat flux and corresponding surface superheat. They confirmed that both surface superheats at the transition point from natural convection region to film boiling, and the collapse point of minimum film boiling caused by steadily increasing and decreasing heat inputs

respectively, agreed with each other. They concluded that the film boiling incipience at the transition point and minimum film boiling at collapse point occur due to the lower limit of HSN in wetting liquid of FC-72 and FC-87 based on the theory of Sakurai et al. (1996, 2000). Takahashi et al. (1999) has measured the dynamic heat transfer processes due to an exponential heat input for a 1.2 mm diameter horizontal cylinder in a pool of FC-72 at the pressures of 101.3 kPa and 150 kPa. They have assumed that the mechanism of the direct transition from non-boiling regime to film boiling regime is a consequence of the HSN.

The present work is to make clear the transition phenomena to film boiling at steady and transient CHF in non-wetting and wetting liquids. The generalized mechanism for the transitions to film boiling from single-phase conduction or transient conduction and fully or insufficiently developed nucleate boiling due to exponential heat generation rates for wide range of subcoolings and pressures were investigated in water, ethanol and FC-72, adding the photographic approach on the vapor bubble and vapor film behavior on the cylinder surface by using a high-speed video camera.

1.2 Outline of the present work

In Chapter 1, it describes the background of the critical heat flux in heat transfer by boiling. Especially, it pays attention to a physical model of the new CHF mechanism proposed by Sakurai et al. The research background of steady and transient CHFs is described. Moreover, the purpose of this research is described at the end.

In Chapter 2, the schematic diagram of the experimental apparatus is shown. More details, it describes that boiling apparatus, heaters used in the experiment, the experimental method and procedure and so on.

In Chapter 3, it contains steady-state and transient boiling heat transfer characteristics

caused by an exponential heat generation rates with various periods, which are investigated. Steady-state and transient critical heat fluxes (CHFs) are measured using a 1.0 mm diameter horizontal cylinder as a test heater in a pool of water and highly wetting liquids, such as ethanol and FC-72, over periods ranging from about 5 ms to 50 s for wide range of subcoolings and pressures. In this Chapter, it is confirmed that boiling heat transfer processes from non-boiling to film boiling or to fully-developed nucleate boiling (FDNB) are completely different from each other depending on the experimental liquids. Also it is recognized they depend on the heat generation rates shown with period. The trend of critical heat flux (CHF) values in relation to the periods is divided into three groups: first group for the longer period, second group for the shorter and third group for the intermediate one.

In Chapter 4, the purpose of this research is to investigate the effect of the surface conditions of the test cylinders such as the commercially-available surface (CS) and the roughly-finished surface (RS) in saturated and subcooled liquids at various pressures on the transient pool boiling CHFs caused by the exponential heat generation rates with various periods. In this Chapter, it is clarified that the trend of CHF for the shorter periods meaning of higher heat generation rate is significantly affected by the test cylinder surface conditions in a pool of water, ethanol and FC-72. From the results, it is suggested that more study on the diverse surface conditions such as the cavity size distribution and surface energy on the CHF is necessary for a wider range of subcoolings and pressures.

In Chapter 5, it contains the behavior of vapor bubbles and vapor film during the transition from non-boiling and nucleate boiling regime to film boiling due to increasing heat inputs, which are examined by photographs taken by a high-speed video camera. The purpose of this work is to make clear the transition phenomena to film boiling in several liquids having different wettability by the photographic approach on the vapor

bubble and vapor film behavior on the cylinder surface. In the case of the highly wetting liquids, the vapor film behavior during transition to fully-developed nucleate boiling is just similar to that of the direct transition to film boiling. This vapor film behavior that is rapidly growing and covering the heater surface during initial boiling can never be seen in the water experiment with a quasi-steady state heat generation rate. It is confirmed that the initial boiling behavior is significantly affected by the property and the wettability of the liquid.

The final purpose of this work is to accumulate the CHF database to clarify generalized CHF phenomena in various liquids for wide range of subcoolings and pressures due to steady and transient heat inputs. This dissertation is concluded in Chapter 6, where the major contributions and results obtained in this work by analysis and experiment are represented.

2. Experimental apparatus and method

2.1 Pool boiling experimental apparatus

The schematic diagram of the experimental apparatus is shown in Fig. 2.1. It consists of a boiling vessel (main tank), an experimental heater, a pressurizer, auxiliary tank for degassing, coolant circulation device (cooler), a control device of heat generation rate, a data measurement and processing system, and a high-speed video camera. The boiling vessel with inspection windows is made of stainless steel having an inner diameter of 200 mm and a height of 600 mm. It is designed to use at pressure up to 2 MPa. Two current conductors and two potential conductors are mounted at the upper side of the vessel, which also are used to support the test heater. The liquid temperature in the boiling vessel is heated to the desired temperature by a sheathed heater installed at the downside of the vessel. The vessel is kept warm by micro heaters and thermally isolated with lagging materials. The liquid temperature is measured by K-type thermocouples. A pressure transducer measures the system pressure at position of the heater.

And a high subcooling is achieved by using pressurizer of self-steamy and coolant circulation device of -40^{o}C minimum in order to obtain the liquid temperature of around 0^{o}C, because the saturated temperature of highly wetting liquids such as ethanol, liquid nitrogen and FC-72 etc. is lower than that of water, and a high subcooling cannot be achieved at the room temperature level.

2.2 Experimental heater

Figure 2.2 shows the experimental heater (test heater) in detail. The heater is made of platinum wire having a diameter of 1.0 mm, which is horizontally mounted in the vessel.

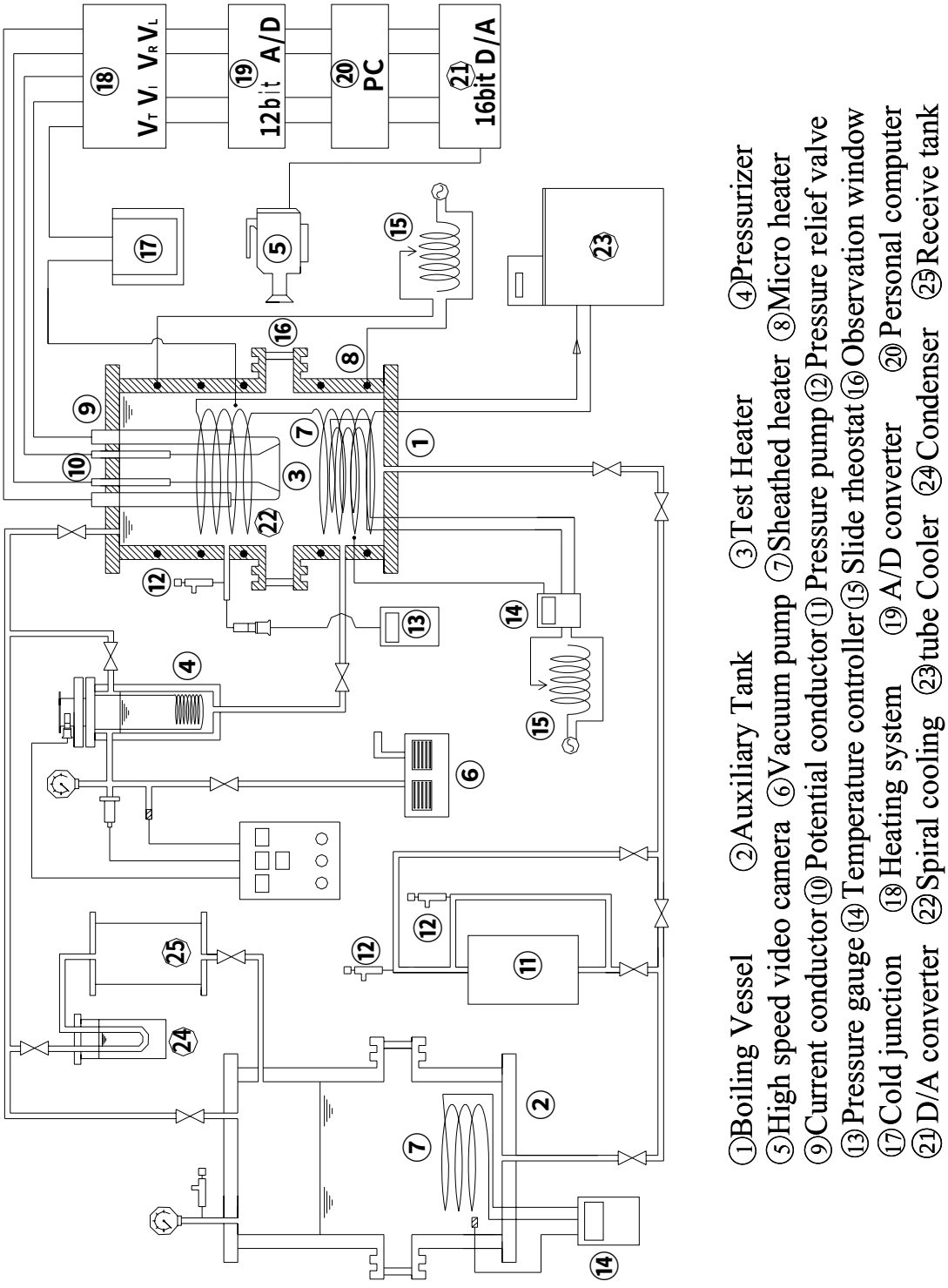

Fig. 2.1 Schematic diagram of experimental apparatus

2.2 Experimental heater

The heater diameter is from the reference paper reported by J. H. Lienhard et al. (1988, 1973) showing with the prediction curve for cylinder. As shown in the curve, non-dimensional length L' ($= L/[\sigma / g(\rho_l - \rho v)]^{1/2}$) becomes the diameter that is considered to be Zuber's infinite horizontal flat plate. Two fine-50 μm diameter platinum wires were spot-welded on each heater as potential taps at about 10 mm from each end of the heater. And the effect of surface condition on the same heater, which is investigated, for having different surface roughness one will be shown in Chapter 4 in detail.

The effective length of heater between the potential taps is 31 mm. The heater was annealed in order to maintain an even properties and its electrical resistance versus temperature relation was calibrated in water and glycerin baths using a precision double bridge circuit. The calibration accuracy was estimated to be within ±0.5 K.

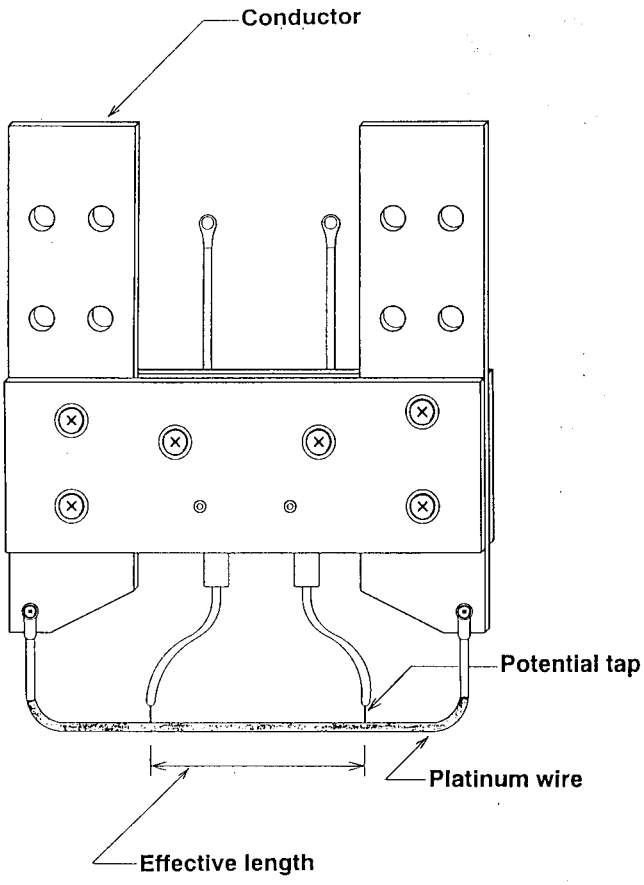

Fig. 2.2 Experimental heater and joint with conductor

2.3 Experimental method

In the case of a steady-state boiling phenomenon, and of course a transient boiling one, the heat generation rate will change simultaneously with resistance changes of the heater. Therefore, the method of controlling heat generation rate and temperature of heater while calculating with a high-speed analog computer is adopted in this experiment; an exponentially increasing heat is inputted regardless of the changes of heater temperature, and it is possible that heat generation rate is intercepted rapidly at a point which the heater temperature reached to the set-up value.

In this experiment, it was used a heat generation rate control system, which was improved on that of Sakurai et al. (1977). The diagram of the heating device for the test heater, and the measuring and data processing system are shown in Fig. 2.3. The test heater was heated electrically by a direct current source controlled by a computer so as to give increasing heat input with a time. The average temperature of the test heater was measured by resistance thermometry using the heater itself. A double bridge circuit with the heater as a branch was first balanced at the bulk liquid temperature. The output voltages of the bridge circuit, together with the voltage drops across the potential taps of the heater and across a standard resistance, were amplified and passed through analog-to-digital converters installed in computer. These voltages were simultaneously sampled at a constant time interval. The average temperature was obtained by using the previously calibrated resistance-temperature relation. The heat generation rate of the test heater was determined from the current to the heater and the voltage difference between potential taps on the test heater. The surface temperature was obtained by solving the conduction equation in the heater under the conditions of the average temperature and heat generation rate. The instantaneous surface heat flux was obtained from the heat balance equation for a given heat generation rate.

2.3 Experimental method

The electric current was supplied to the test heater directly with a constant voltage direct-current power supply (Max. current 700A) which an exponentially increasing heat input with time was given exactly regardless of resistance changes of heater due to temperature change of heater, so the heat generation rate increased with exponential function as follows;

$$Q = Q_0 \exp^{t/\tau} \tag{2.1}$$

where, Q is heat generation rate, W/m^3, Q_0 is initial heat generation rate, W/m^3, t is time, s. τ is period, s: the e-fold time corresponding to heat generation rate with the exponential increasing rates from quasi-steady to rapid ones. The heat generation rates of the heater were controlled and measured by a control device as shown in Fig. 2.3. The heat flux of the heater is calculated by the following equation for heat balance.

$$q = \frac{D}{4} Q - \rho_h c_h \frac{D}{4} \frac{dT_a}{dt} \tag{2.2}$$

where, D, ρ_h, c_h and T_a are the diameter, density, specific heat and the average temperature of the test heater, respectively. The test heater surface temperature can be calculated from unsteady heat conduction equation of the next expression by assuming the surface temperature around the test heater to be uniform.

For the cylindrical test heater, we have,

$$\frac{\partial T}{\partial t} = a\left[\frac{\partial^2 T}{\partial r^2} + \frac{1}{r}\frac{\partial T}{\partial r}\right] + \frac{Q}{\rho c} \tag{2.3}$$

Boundary conditions are as follows,

$$\left.\frac{\partial T}{\partial t}\right|_{r=0} = 0, \qquad -\lambda \left.\frac{\partial T}{\partial r}\right|_{r=R} = q$$

$$T_a = \frac{\int_0^R T(2\pi r)dr}{\int_0^R (2\pi r)dr} = \frac{2}{R^2}\int_0^R Trdr$$

where, Q (W/m^3) is the internal heat generation rate, T (K) is the temperature inside the test heater, $a = k/\rho c$ (m^2/s) is thermal diffusivity, and k (W/mK) is thermal conductivity.

The unbalanced voltage of the double bridge circuit including the heater, and the voltage differences between the potential taps of the heater and across the standard resistance were fed to the personal computer through an analog-to-digital (A/D) converter. The fastest sampling speed of the A/D converter is 5 μs/channel. All these calculations were carried out by the personal computer. The experimental error was estimated to be about ±1 K in the heater surface temperature and ±2 % in the heat flux. A high-speed video camera system (1000 frames/s with a rotary shutter exposure of 1/10000 s) was used to observe the boiling phenomena and to confirm the start of boiling on the test heater surface.

The CHF was determined at a start point that the measured average temperature rapi-

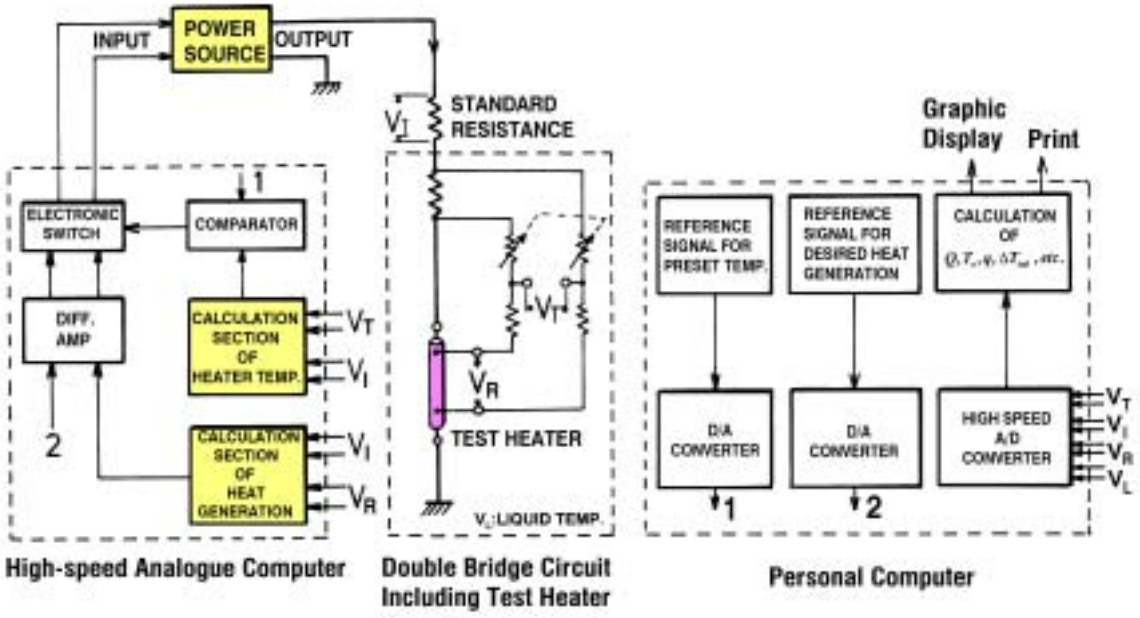

Fig. 2.3 Block diagram of the heating device for the test heater, and the measuring and data processing system.

dly increased up to the preset temperature lower than the actual burnout temperature of a test heater by using the burnout detector.

2.4 Experimental procedure

The experiment was carried out as follows. First, the liquids used in the experiment were degassed by keeping it boiling for 30 minutes at least in the auxiliary tank. Vapor was recovered to the pool with a water-cooled condenser. The liquid was fully filled in the boiling vessel with the free surface only in the pressurizer and sub tank. Liquid temperatures in the boiling vessel and in the pressurizer were separately controlled to realize the desired saturated and subcooled conditions. The heat input was raised with exponential function, $Q=Q_0 exp^{t/\tau}$. τ is period of heat generation rate, s, and a shorter period means a higher increasing rate of heat generation. Heat flux and surface temperature of the heater was measured by the data processing system with time.

3. CHFs for wide range of subcoolings and pressures in various liquids

3.1 Introduction

It is important to understand the mechanism and corresponding correlation of the boiling heat transfer for the effective use of existing energy conversion technology, so we need to accumulate a fundamental database of critical heat fluxes (CHFs) for energy conversion. Also, the detailed understanding of generalized saturated and subcooled pool boiling CHF mechanisms and corresponding correlations in water and highly wetting liquids such as FC fluids (Fluorinert liquid), ethanol, liquid nitrogen and liquid helium I, etc. are becoming increasingly important as the fundamental database for the design such as the high heat flux cooling systems using subcooled water pool boiling, the super-conducting magnets cooled by liquid helium and liquid nitrogen, the thermal control of microelectronic assemblies cooled by FC liquids for future super-computers. The present work is to make clear the generalized CHF mechanisms that can be applied in wide range of liquids. In this Chapter, it is confirmed that boiling heat transfer processes from non-boiling to film boiling or to fully-developed nucleate boiling are completely different from each other depending on the experimental liquids. Also it is recognized that they depend on the heat generation rates shown with period.

3.2 Experimental conditions

The boiling heat transfer processes on an experimental heater in a pool of water, ethanol or FC-72 due to exponential heat generation rate, $Q=Q_0 exp^{t/\tau}$, ranging from quasi-steadily increasing one to rapidly increasing one with periods, τ, ranging from

around 5 ms to 50 s were measured at pressures ranging from 101.3 to 1572 kPa for liquid subcoolings over the range from 0 to 160 K at pressures.

Table 1 presents several properties at normal condition in water, ethanol and FC-72. As seen in the table, when the physical-properties of liquids are compared with each other, it is shown the value becomes small with the order of water, ethanol and FC-72. Generally, highly wetting liquid means that it has lower surface tension than that of water, and it is easy to be originally flooded cavities with liquid, for example, ethanol, liquid nitrogen and FC liquids, etc. Among three liquids below, water has highest value of surface tension and FC-72 has lowest one, 1/6 of water. In the case of ethanol and FC-72 except for water, it is assumed that the transitions occurred due to the explosive-like heterogeneous spontaneous nucleation (HSN) in originally flooded cavities without the contribution of the active cavities entraining vapors for boiling incipience as mentioned before. The vapor behavior at initial boiling due to the HSN is shown later: it is considerably different from that due to active cavities.

Table 1 Comparison of properties in water, ethanol and FC-72

Properties		water	ethanol	FC-72
Boiling Point (1 atm)	[°C]	100	78	56
Liquid Specific Heat	[kJ/(kg·K)	4.19	2.42	1.05
Latent Heat of Vaporization	[J/g]	2257	855	88
Liquid Thermal Conductivity	[W/(m·k)]	0.61	0.17	0.06
Surface Tension	[$\times 10^{-3}$N/m]	72	21	12
Critical Temperature	[°C]	374	243	176
Critical Pressure	[MPa]	22	6.4	1.8

3.3 Time-dependence of heat generation rate, surface temperature and heat flux in ethanol

Figure 3.1 shows typical changes in the heater surface temperature, T_s, and heat flux, q, with time for an exponential heat generation rate, Q, (a) with a period of 1450 ms at a pressure of 494 kPa and (b) 32 ms at a pressure of 101.3 kPa under saturated conditions respectively. The heat generation rate, Q, increases exponentially regardless of the changes in surface temperature. The heat flux, q, increases with Q. In the case of (a) first, the surface temperature of heater increases with an increase in heat input. Incipient boiling starts at a point where corresponds to the q_{in} beyond saturation temperature, T_{sat}. The heater temperature continues to increase up to T_{ov} (called overshot point), then rapidly decreases and again gradually increases with an increase in heat input. Since the heat flux reaches the critical heat flux point, q_{cr} (=CHF), the heater surface temperature rapidly increases with time. In the case of (b), the surface temperature of heater increases with an increase in heat input without temperature overshot and at the incipient boiling point the heat flux rapidly decreases in a short time.

3.4 Typical boiling curve with transition to film boiling under saturated condition in ethanol

Figure 3.2 shows the transient phenomenon on a graph of heat flux, q, versus surface superheat, ΔT_{sat}, for the same conditions with (a) and (b) in Fig. 3.1. The surface superheat ΔT_{sat} is defined by the difference between the surface temperature of the heater and the saturation temperature of liquid corresponding to the system pressure. The steady-state natural convection (h_n) curve, the heat conduction (h_c) curve and the steady-state film boiling curve are also shown in the figure for comparison. Here, h_c is

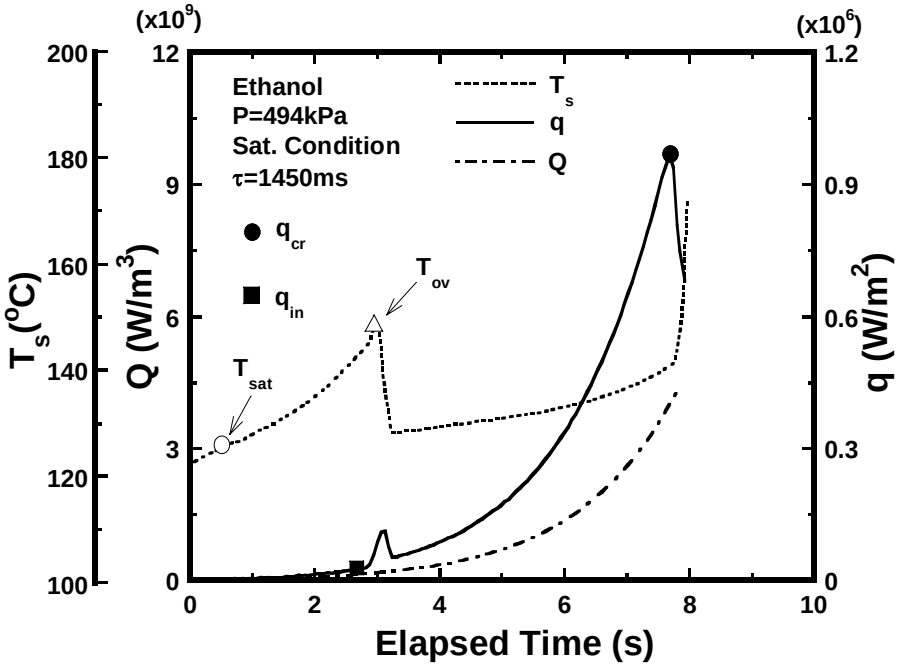

(a) P=494kPa, τ=1450ms

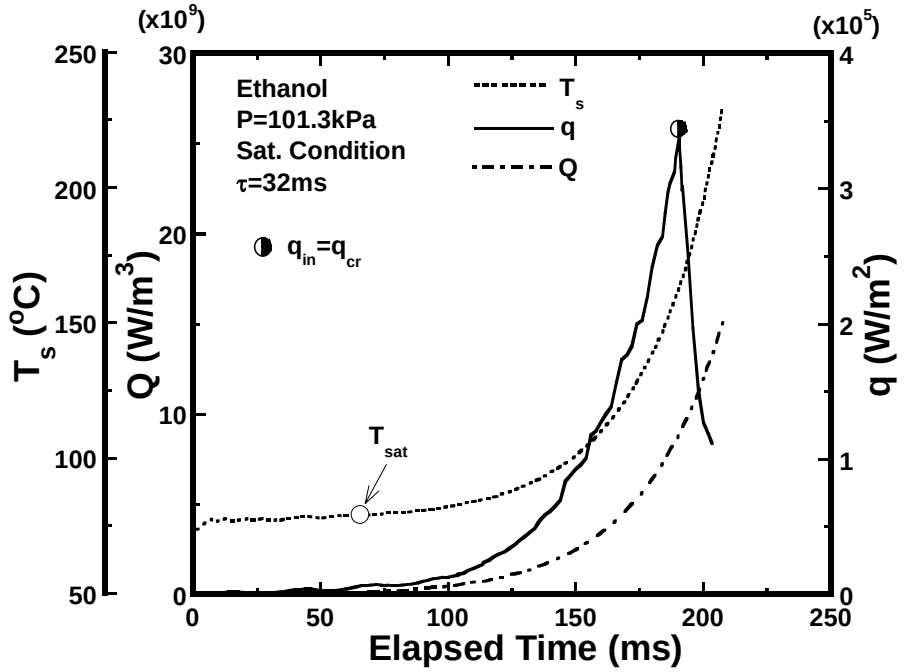

(b) P=101.3kPa, τ=32ms

Fig. 3.1 Illustrative time traces of heat generation rate, Q, heater surface temperature, T_s and heat flux, q.

calculated by the expression of Sakurai et al. (1977), and h_n is obtained using the correlation for laminar natural convection heat transfer derived by Takeuchi et al. (1995).

$$h = \left(h_c^{\,4} + h_n^{\,4}\right)^{1/4} \tag{3.1}$$

where,

$$h_c = (k_l \rho_l c_{pl} / \tau)^{1/2} K_{1st}(\mu D/2) / K_0(\mu D/2) \tag{3.2}$$

and $\mu = [\rho_l c_{pl} / k_l \tau]^{1/2}$; K_o and K_{1th} are the modified Bessel functions of the second kind of zero- and first-orders. k_l is the thermal conductivity of liquid (W/mk). ρ_l, c_{pl} are the density, specific heat of the liquid. τ is the period, and D is the diameter of heater.

$$h_n = N_u \, k / D \tag{3.3}$$

where,

$$N_u = 10^{\,z}$$

$$z = 0.193385 + 0.145037A + 0.664323\times10^{-2}A^2 - 0.232432\times10^{-3}A^3 - 0.238613\times10^{-4}A^4$$

$$A = \log R_f, \quad R_f = \frac{G_r^{\,*} P_r^{\,2}}{4 + 9P_r^{\,1/2} + 10\,P_r}, \quad G_r^{\,*} = N_u G_r$$

It should be noted that the physical properties of the fluid are calculated based on the following film temperature, which is used as a temperature of the representative.

$$T_f = \frac{T_s + T_l}{2}$$

Where, T_s and T_l are the test heater surface temperature, and the liquid temperature, respectively.

The boiling process caused by a steadily increasing heat input with a period of 1450 ms is as follows: heat flux, q, increases along slightly above the natural convection curve at first and after the occurrence of initial boiling, the surface superheat rapidly

decreases, and q increases along the steady-state nucleate boiling curve and reaches the CHF point, q_{cr}, near the extension of the curve and then the transition to film boiling occurs. The rising curve of non-boiling regime up to the initial boiling occurrence lies on the left hand side of the steady-state natural convection curve. It means the effect of heat conduction exists. This is described in the next paragraph. On the other hand, the boiling process caused by an exponentially increasing heat input with a period of 32 ms, shows that the *q* value increases along the transient conduction heat transfer curve, and a transition to film boiling directly without nucleate boiling occurs. The transition

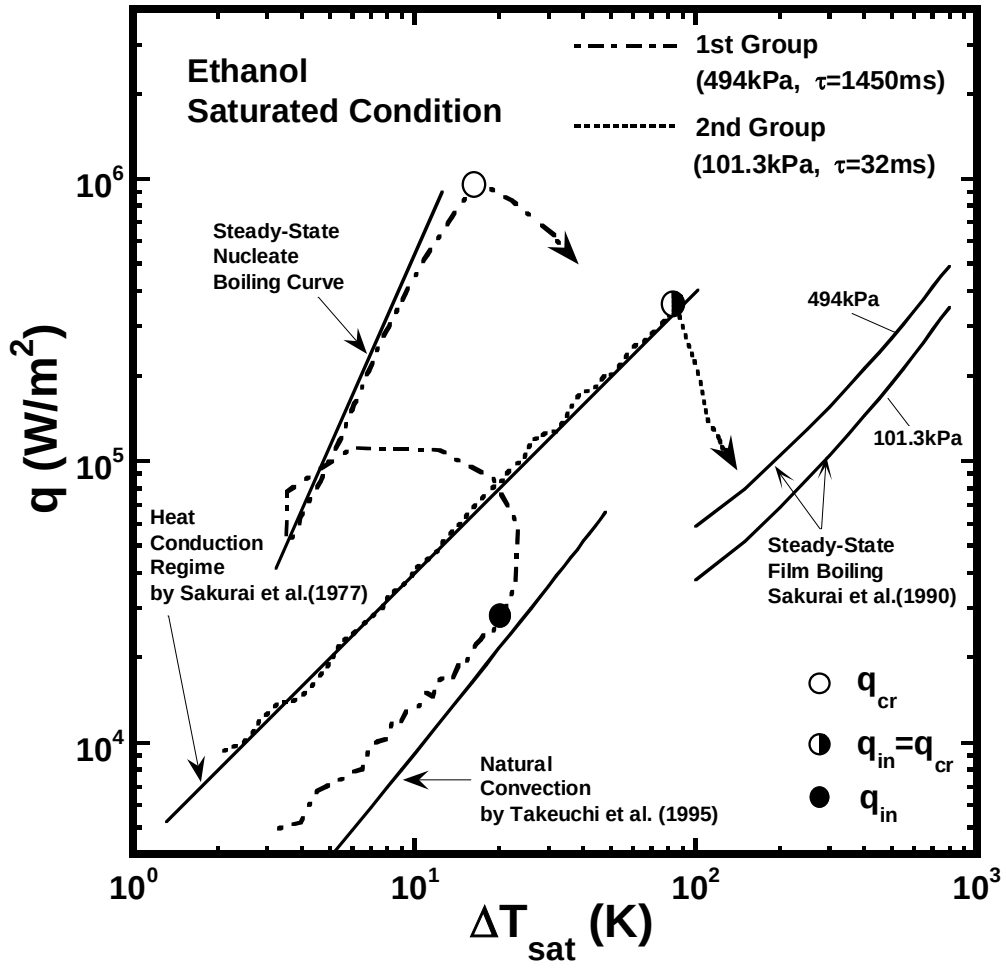

Fig. 3.2 Boiling heat transfer processes from non-boiling to film boiling or to fully-developed nucleate boiling under saturated condition in ethanol.

processes to film boiling are completely different from each other. In the case of boiling process with a period of 32 ms, it is considered that the direct boiling transition on the heater surface from non-boiling to film boiling is due to the heterogeneous spontaneous nucleation (HSN) in previously flooded cavities on heater surface as suggested by Sakurai et al. (1995).

3.5 The heat transfer in non-boiling state

Figure 3.3 shows typical experimental results of the heat transfer coefficient, h, before the initiation of boiling for ethanol as a function of period, τ. For a reference, the transient heat conduction correlation (h_c), the steady-state natural convection heat transfer correlation (h_n), and the combined heat transfer correlation (h_m) were also shown in the figure. As shown in the figure, heat transfer processes from the heater su-

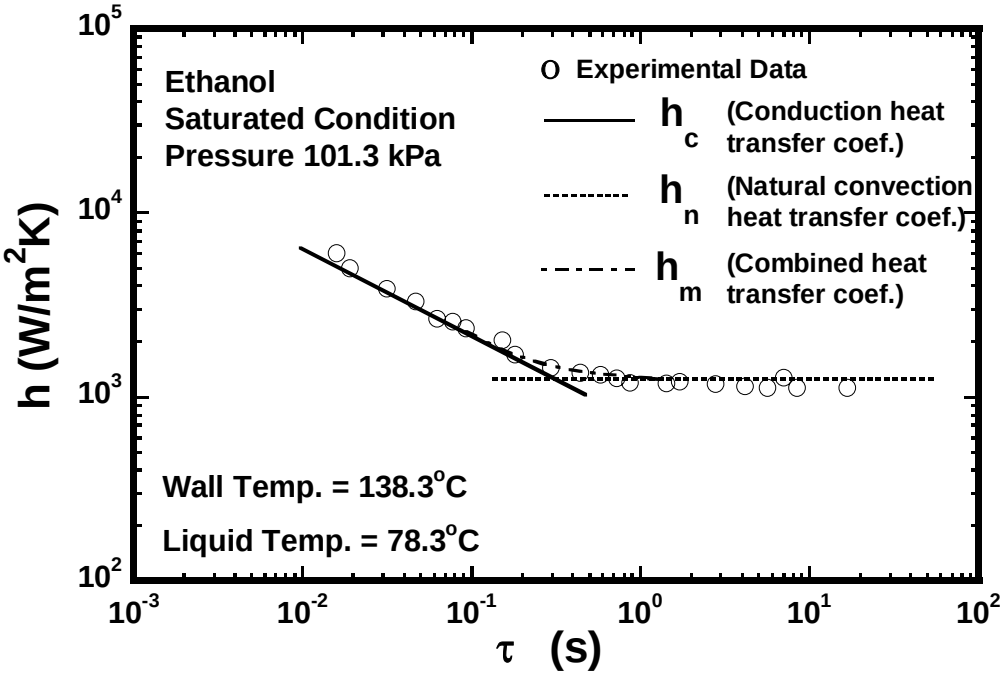

Fig. 3.3 Heat transfer coefficient before the initiation of boiling as a function of exponential period.

rface when the heat generation rate increased with exponential function under non-boiling state are as follows; as the period shortens, heat transfer due to the heat conduction becomes predominant from natural convection heat transfer, and in the region of the period over a second ($\tau > 1$ s), the heat transfer is considered to be quasi-steady-state heat transfer. In this study, heat transfer processes for the periods longer than 10 s are considered as quasi-steady-state one because the non-boiling region agreed with natural convection heat transfer, and all CHFs measured for the heat inputs with periods longer than 10 s are almost the same. Figure 3.4 certifies also that the steady-state natural convection (h_n) heat transfer becomes predominant in non-boiling regime for period of 20 s in the case of water and ethanol.

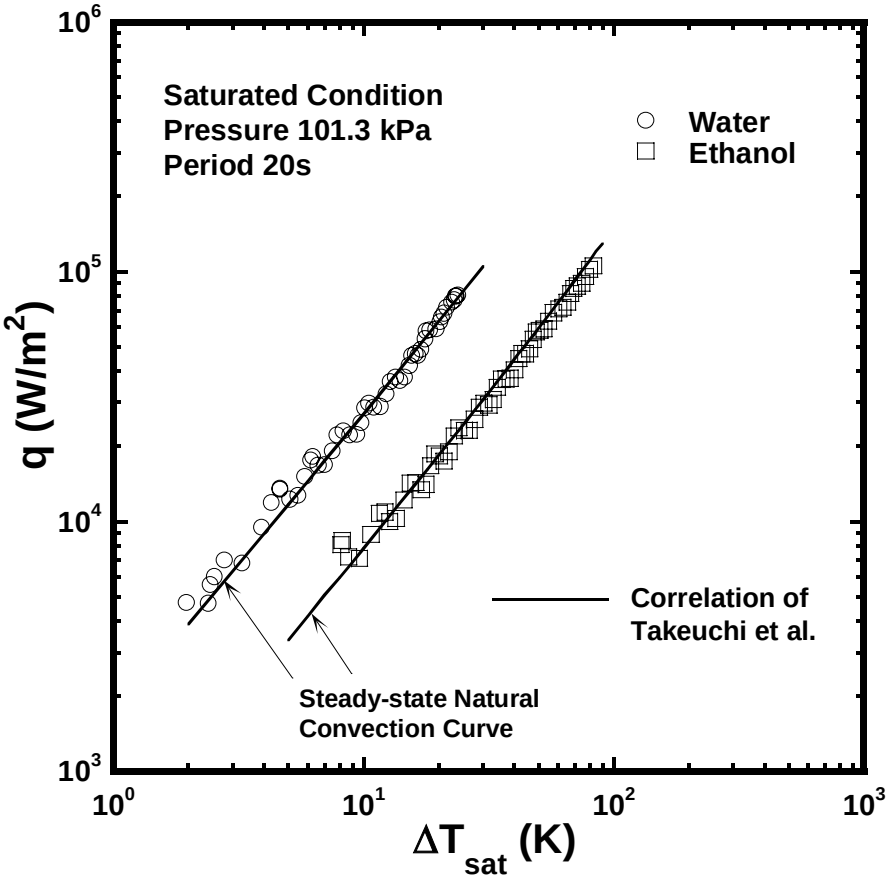

Fig. 3.4 The relation of q with ΔT_{sat} for quasi-steady state natural convection heat transfer.

3.6 Typical mechanism of heat transfer crisis at CHFs due to HSN

Figure 3.5 shows the transient phenomenon on a graph of heat flux, q, versus surface superheat, ΔT_{sat}, at a pressure of 101.3 kPa and a period of 10 s in ethanol. The surface superheat ΔT_{sat} is defined by the difference between the surface temperature, T_w, of the heater and the saturation temperature, T_{sat}, of liquid corresponding to the system pressure. The steady-state natural convection curve derived by Takeuchi et al. (1995) and the steady-state film boiling curve derived by Sakurai et al. (1990), are also shown in the figure for comparison. The boiling process caused by an exponentially increasing heat input with a period of 10 s at atmospheric pressure, shows that the q value increases along the natural convection heat transfer curve, and the boiling occurs at a surface superheat point of 100 K. Then it shows a transition directly to film boiling without passing the nucleate boiling. It was confirmed that the surface superheat of initial boiling gradually decreased with an increase in system pressure. It is considered that the direct boiling transition on the heater surface from non-boiling to film boiling is due to the heterogeneous spontaneous nucleation (HSN) in previously flooded cavities on heater surface without the contribution of active cavities in general as mentioned before.

As seen in the table 1 of the Section 3.2, wetting liquid such as ethanol means that it has lower surface tension than that of water, and it is easy to be originally flooded cavities with liquid. Therefore, it is assumed that the transitions occurred due to the explosive-like heterogeneous spontaneous nucleation (HSN) in originally flooded cavities without the contribution of the active cavities entraining vapors for boiling incipience. Also the vapor behavior at initial boiling due to the HSN is considerably different from that due to active cavities. As shown in the subsequent experimental results of the case of water, it will be confirmed that the superheat temperature of initial boiling is much lower than that of the wetting liquid due to flooded cavities.

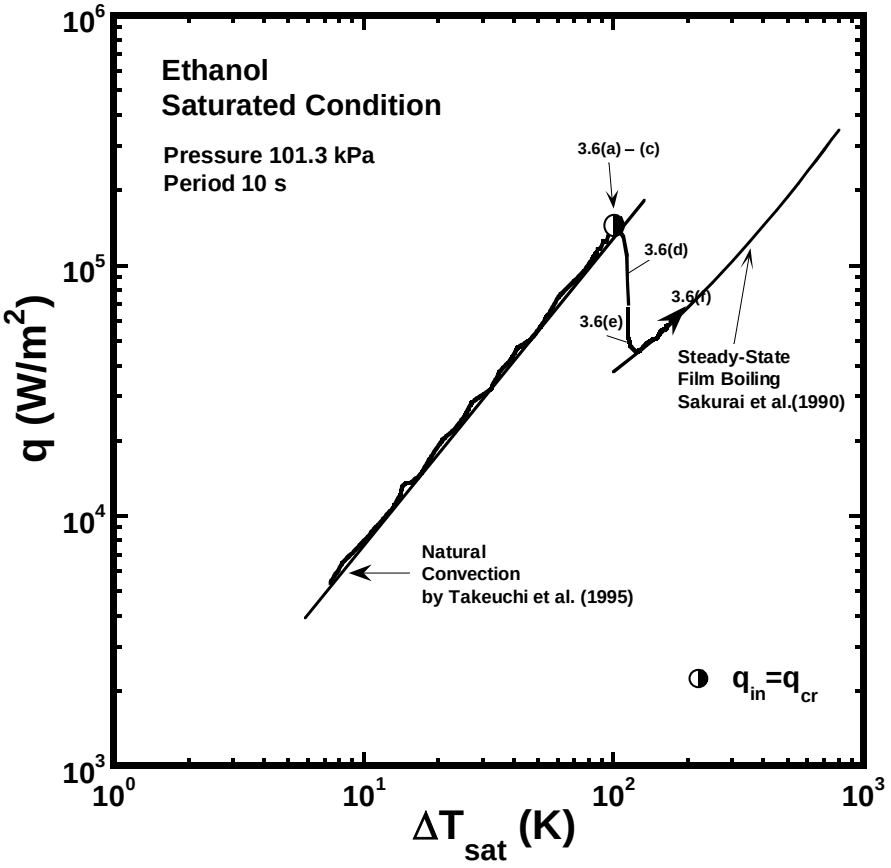

Fig. 3.5 Boiling heat transfer processes from non-boiling to film boiling under saturated condition in ethanol. Photographs shown in Fig. 3.6 were taken at points of 3.6(a) to (f) on the graph.

Figure 3.6 gives a series of subsequent photographs from the moment of onset of a vapor phase to film boiling on a surface at a pressure of 101.3 kPa in saturated ethanol. Figure 3.6(a) is the onset of boiling on the cylinder. The figure 3.6(b) taken at 1 ms after the first one shows a vapor tube due to the explosive-like HSN in flooded cavities, and it covers the whole cylinder surface by the large vapor tube. Figure 3.6(c) taken at 2 ms after the first one shows thick vapor film concentrically covering the cylinder. The vapor bubbles rapidly grow and completely cover the surface of the cylinder within just a few milliseconds. The temperature difference of the surface superheat between corre-

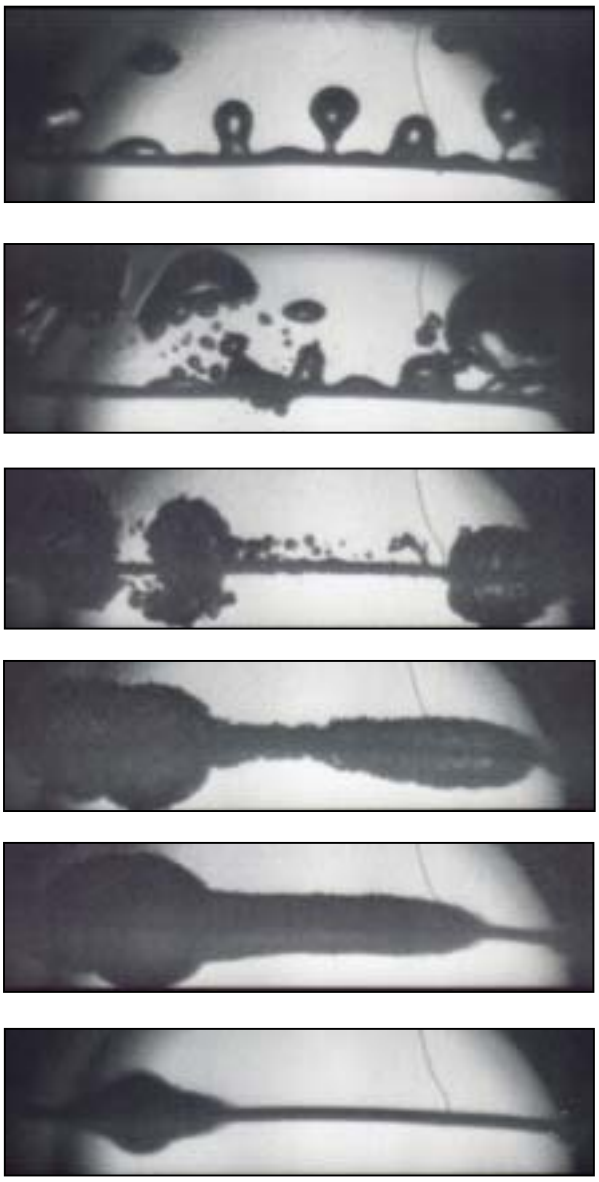

Fig. 3.6 Vapor film behavior during direct transition to film boiling for a period of 10 s at a pressure of 101.3kPa in saturated ethanol.

sponding to Figs. 3.6(a) to 3.6(c) is almost the same. Figure 3.6(d) taken at 7 ms after the first one shows that the vapor bubbles collapse from the boiling initiation bubbles. Then, large vapor bubbles are broken away from the large vapor film by buoyancy force and move upward as shown in Fig. 3.6(e). After detachment of the large vapor bubbles,

solid-liquid contacts occurs, and then new thin vapor film with the Taylor unstable wave on the upper part of the vapor-liquid interface covering the cylinder is formed by the explosive-like HSN on the places of solid-liquid contact and thin film boiling. At this moment the surface temperature starts increasing rapidly as a result of heat transfer deterioration. As shown in Fig. 3.6(f), the behavior of vapor-liquid interface in film boiling on the cylinder similar to that for steady-state film boiling on the cylinder is clearly observed after the detachment of large vapor bubbles. It will be shown in Chapter 5 in detail about the behavior of vapor bubbles and vapor film.

3.7 Transient boiling processes under saturated condition in water

The typical boiling heat transfer processes due to exponential heat generation rates in water are shown in Fig. 3.7 on a graph of heat flux, q, versus surface superheat, ΔT_{sat}. The steady-state natural convection curve, the heat conduction curve and the steady-state film boiling curve are also shown in the figure for comparison. The heat transfer processes for periods of 10 s, 1 s, 100 ms and 10 ms at a pressure of 101.3 kPa are shown in the figure. The processes from non-boiling to film boiling are completely different from each other depending on the periods. It can be found that the processes up to initial boiling heat fluxes, q_{in}, are the natural convection regime for periods from 10 s down to around 1 s, and the heat conduction regime for periods from 100 ms down to 10 ms as shown in the figure. It is recognized that the values of initial boiling heat flux, q_{in}, increase with a decrease in period, that is, they depend on the increasing rates of heat inputs, respectively. The CHF values are almost equal to each other for the periods tested here. When an exponentially increasing heat input is applied to the heater immersed in the pool of water, the heater surface temperature and the heat flux increased. As shown in the figure, the heat transfer processes up to, q_{in}, show that heat

flux, q, for the period of 1 s increases along the natural convection curve together with period of 10 s and natural convection heat transfer becomes predominant. As the period shortens, the heat conduction becomes predominant in heat transfer compared with the natural convection.

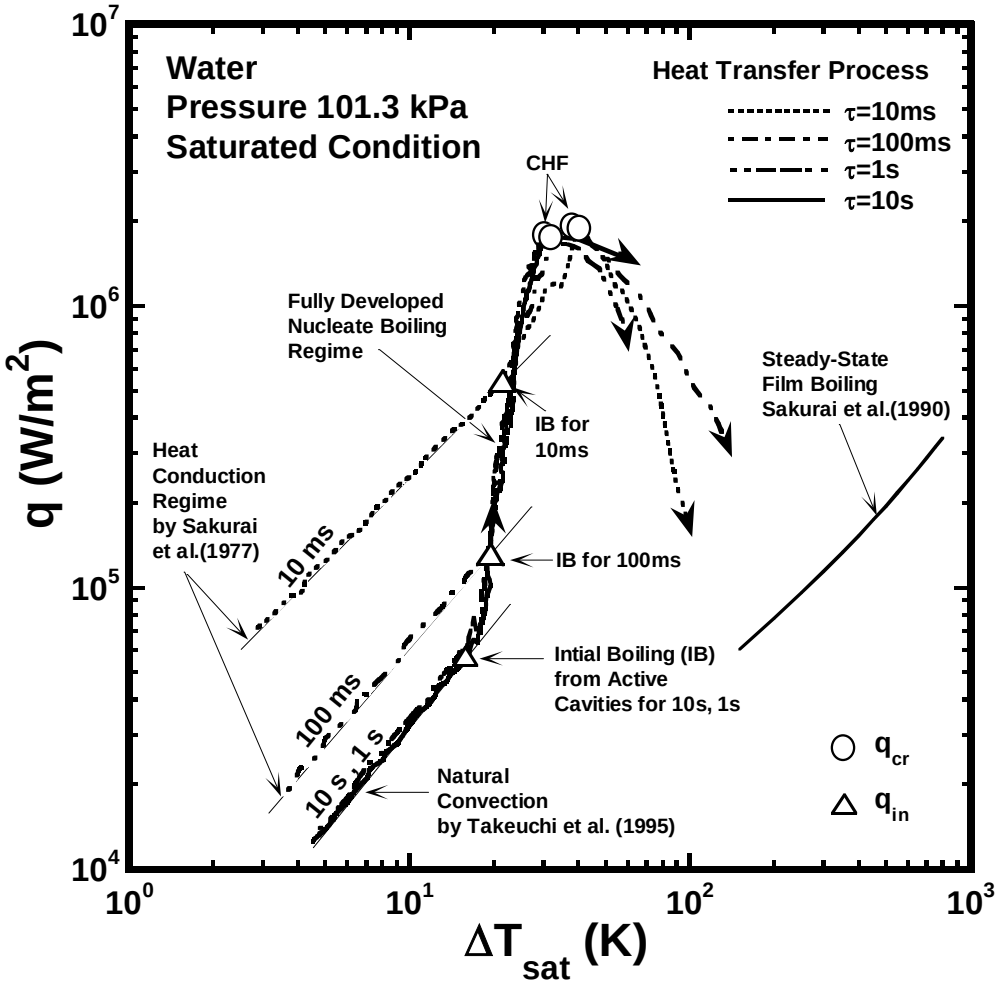

Fig. 3.7 Heat transfer process for periods of 10 s, 1 s, 100 ms and 10 ms saturated condition at atmospheric pressure in water.

It is considered that the initial boiling occurs from active cavities entraining vapor, and the initial boiling occurs at a surface superheat, ΔT_{sat}, of around 20 K. The active cavities entrain vapor bubbles so that it causes the rapid increase of heat flux. After

incipient boiling at a point which corresponds to the q_{in}, the surface superheat does not change so much with an increase in heat input. Then, the heat fluxes reach the CHF point, q_{cr}.

The heat transfer processes for periods of 10 s and 180 ms at a pressure of 494 kPa are shown in the Fig. 3.8. It is assumed that the initial boiling occurs from active cavities entraining vapor that cause the increase of heat flux. The superheat temperature of initial boiling is lower and the CHF values are higher than that in the case of 101.3 kPa.

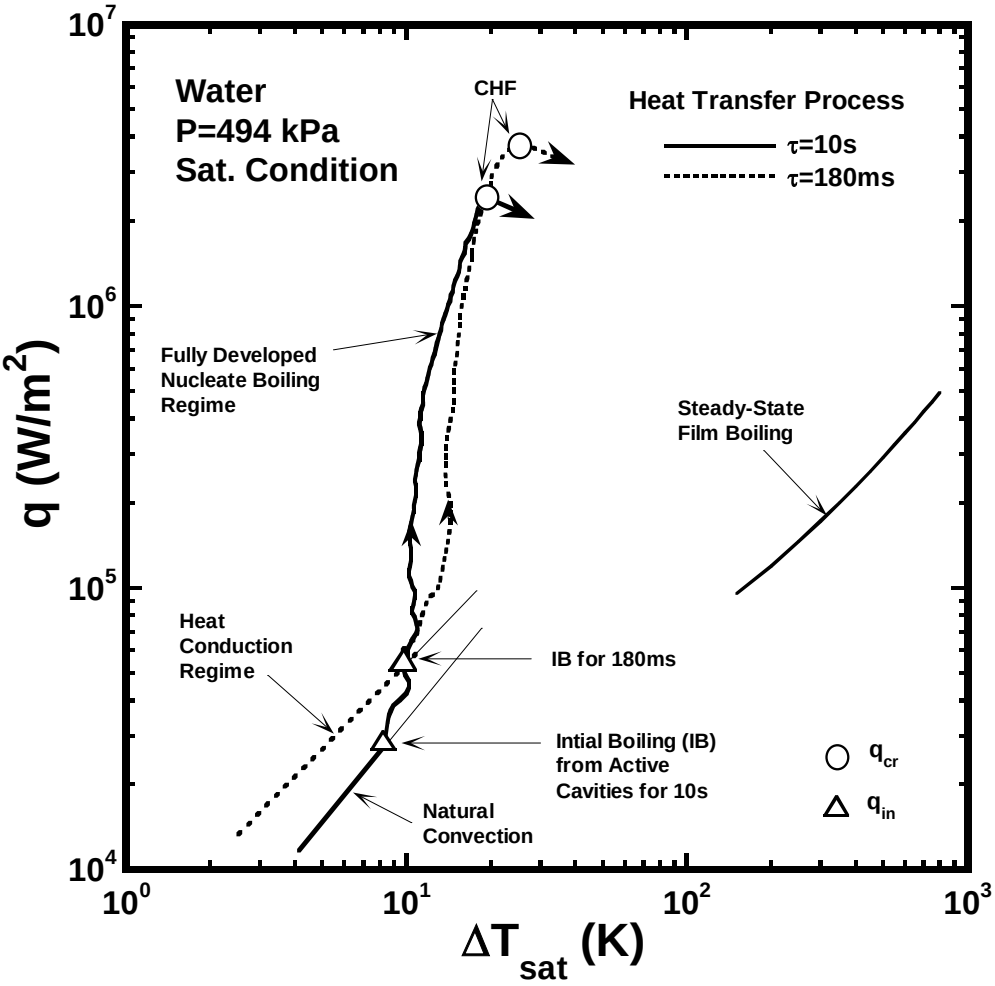

Fig. 3.8 Heat transfer process for periods of 180 ms and 10 s saturated condition at pressure of 494 kPa in water.

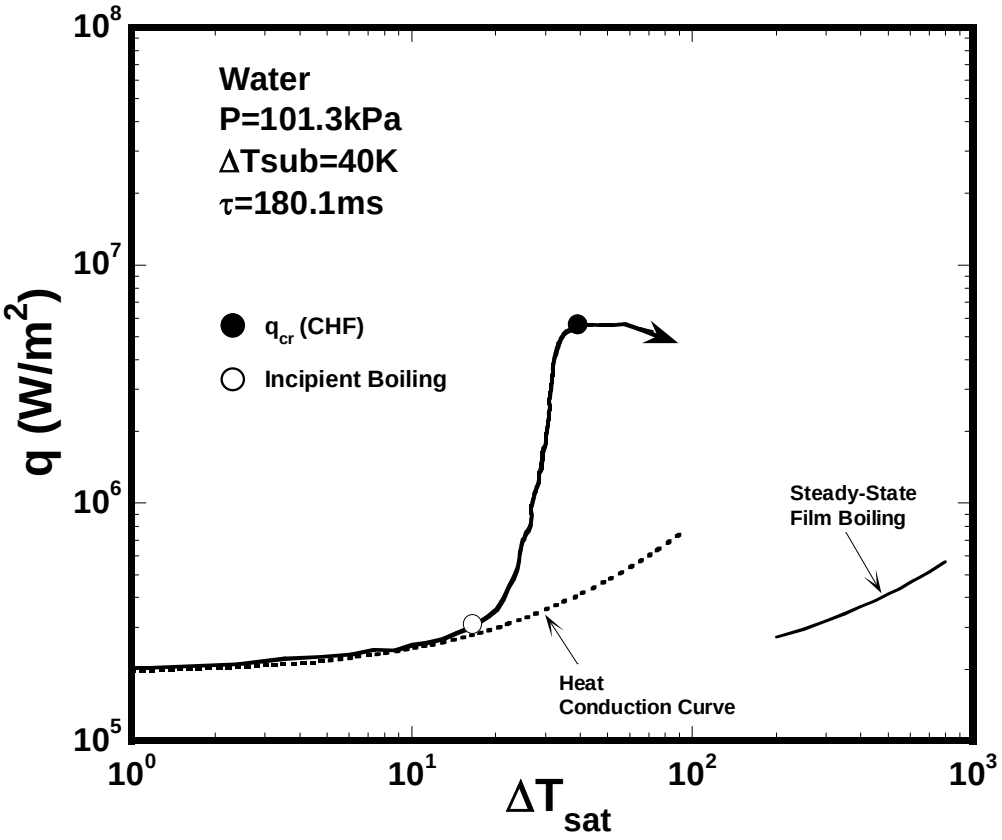

Fig. 3.9 Heat transfer process for period of 180.1 ms for subcooling of 40 K at atmospheric pressure in water.

In addition, figure 3.9 shows the heat transfer process under subcooled condition in water, subcooling temperature of 40 K. The process up to incipient boiling agrees well with the heat conduction curve derived by Sakurai et al. (1977) in the case of the subcooled condition also. As the period shortens, the heat conduction becomes pre-dominant in the heat transfer as mentioned before. And the CHF value is much higher than that of saturated condition at the same pressure shown in Fig. 3.7.

3.8 Heat transfer processes during transitions to fully-developed nucleate boiling or to film boiling in ethanol

Figure 3.10 shows the transient phenomenon on a graph of heat flux, q, versus surface superheat, ΔT_{sat}, for the periods of 50 s and 100 ms at an atmospheric pressure in ethanol. The heat transfer process for the periods of 50 s is shown with a solid line: heat flux, q, increases along the natural convection curve at first and after the occurrence of initial boiling at a surface superheat of 80 K, the surface superheat rapidly decreases, and the transition to fully-developed nucleate boiling occurs and reaches the CHF point, q_{cr}. On the other hand, the process for the periods of 100 ms is shown with a dashed

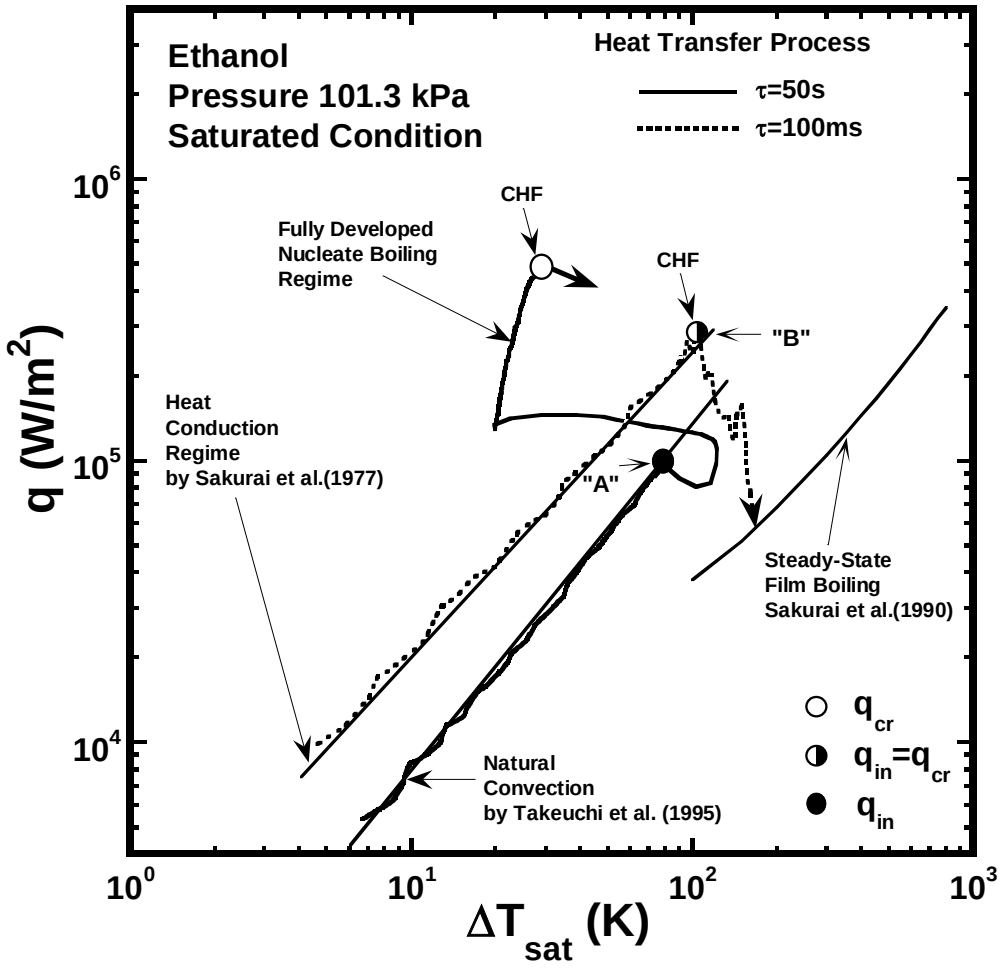

Fig.3.10 Boiling heat transfer processes from non-boiling to film boiling or to fully-developed nucleate boiling for periods of 50 s and 100 ms under saturated ethanol at pressure of 101.3 kPa.

line: the curve shows that the q increases along the natural convection curve, and the boiling occurs at a surface superheat point of 100 K, which is a little bit higher than that in the case of the period of 50 s, and then shows a transition directly to film boiling without passing the nucleate boiling. In the case of the boiling process shown with a dashed line, it is considered that the direct boiling transition on the heater surface from non-boiling to film boiling is due to the heterogeneous spontaneous nucleation (HSN) in previously flooded cavities on heater surface.

It is confirmed that the initial boiling in highly wetting liquid such as ethanol occurs in previously flooded cavities on heater surface, because the superheat temperature of initial boiling is much higher than that of water. At the point of ″A″, a large vapor tube

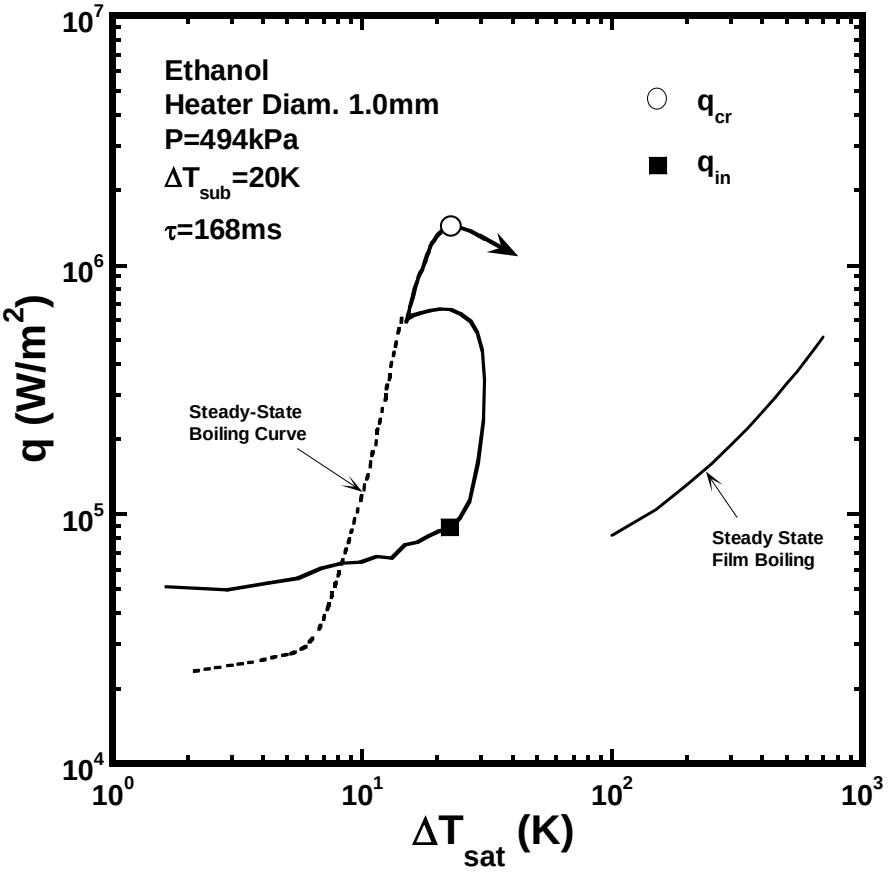

Fig. 3.11 Boiling heat transfer process for period of 168 ms at pressure of 494 kPa for the subcooling of 20 K.

is rapidly formed around each cylinder similar to that at point ″B″ due to the HSN. The vapor tubes then collapse rapidly, and large vapor bubbles break away from the heater surface. After the detachment of the vapor bubbles, nucleate boiling from the cavities entraining vapor occurs with a decrease in surface superheat down to that of the fully-developed nucleate boiling regime.

Figure 3.11 shows boiling heat transfer process for period of 168 ms at pressure of 494 kPa for the subcooling of 20 K in ethanol. The steady-state boiling curve for the same heater is also shown in the figure by a dashed line for comparison. It is assumed that the direct transitions occur for the periods shorter than this one. And it is confirmed that the incipient boiling point, q_{in}, in this case lies on the right-hand side of the steady boiling curve.

3.9 Heat transfer processes during transitions to fully-developed nucleate boiling or to film boiling at atmospheric pressure in saturated FC-72

As shown in the Fig. 3.12, the heat transfer process for a period of 10 s at a pressure of 101.3 kPa is shown with a dashed chain line, and the steady-state natural convection curve and the steady-state film boiling curve are shown in the same figure for comparison. On the other hand, the heat transfer process including direct transition point for a period of 100 ms at the same pressure is also shown with a dashed line and with the heat conduction curve. As shown in the figure, the transition processes to film boiling are completely different from each other due to the period: the e-fold time corresponding to heat generation rate with the exponential increasing rates from quasi-steady to rapid ones. And the boiling occurs at higher surface superheat point than that of water. In the case of the boiling process with a period of 100 ms, it is considered that the direct boiling transition from non-boiling to film boiling is due to the heterogeneous sponta-

neous nucleation (HSN) as mentioned before. And it can be seen that the incipient surface superheat at which direct transition occurs, becomes a little higher with a decrease in period.

In the case of a period of 10 s, after the occurrence of initial boiling, the nucleate boiling occurs from the cavities of entrained vapor that are formed after detachment of vapor bubbles with a slight decrease in surface superheat which prevents the growth of the HSN. If the detachment of vapor bubbles without decreasing in average surface superheat is realized, the direct or semi-direct transition occurs as in the case of rapidly increasing in heat input mentioned before.

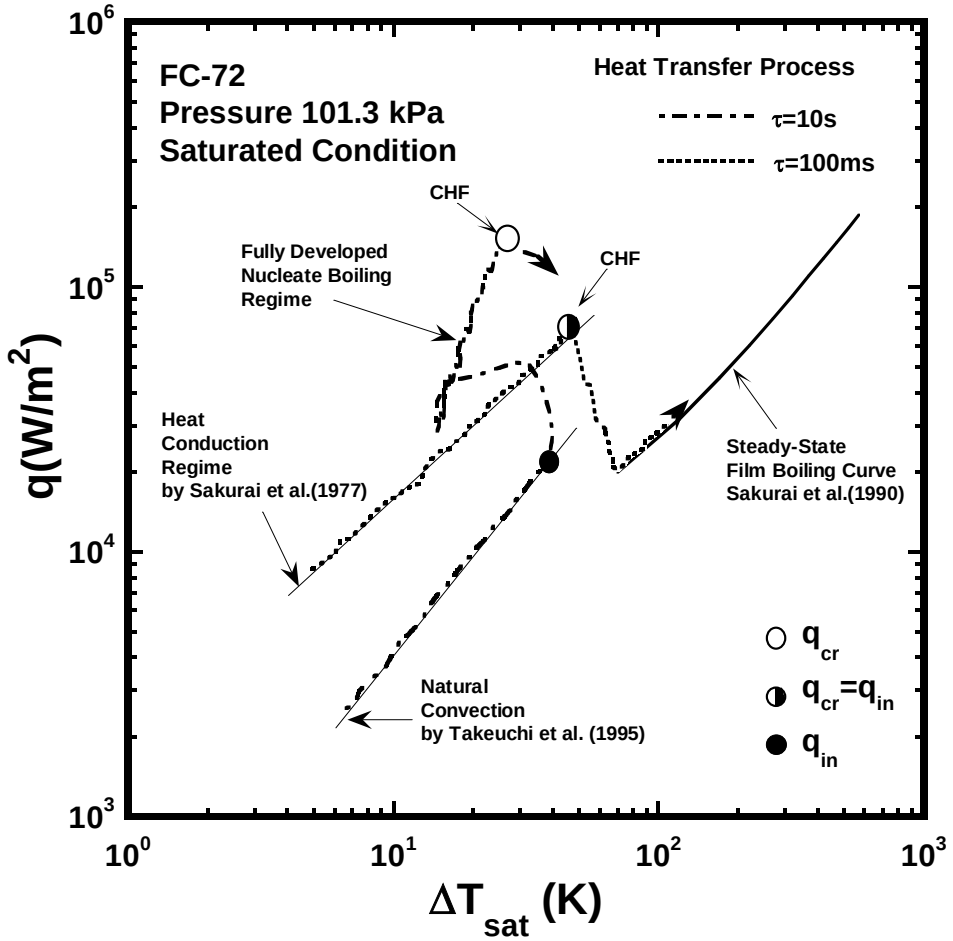

Fig. 3.12 Boiling heat transfer processes from non-boiling to film boiling or to fully-developed nucleate boiling under saturated condition in FC-72.

3.10 Steady-state critical heat fluxes (CHFs) under saturated and subcooled condition

In this experiments, heat transfer processes for the periods longer than 10 s were considered as quasi-steady-state ones because the non-boiling region agreed with natural convection heat transfer, and all CHFs measured for the heat inputs with periods longer than 10 s were almost the same.

3.10.1 CHFs for wide range of subcoolings and pressures in water

As described before, Sakurai et al. (1993) assumes that CHFs are explained by the transition mechanism based on hydrodynamic instability (HI) or heterogeneous spontaneous nucleation (HSN). From this opinion, he considered that there exist the non-linear effect of subcoolings in the CHF based on hydrodynamic instability (HI) from experimental results for wide range of subcoolings and pressures in various liquids. Eq. (3.4) is derived by modifying the Kutateladze's correlation taking into account the non-linear effect of high liquid subcoolings on the q_{cr}, and shown in Figs. 3.13-3.15 by solid line.

The CHFs, q_{cr}, on horizontal cylinder in water for various pressures and subcoolings due to quasi-steadily increasing heat input given by exponential time function were measured. The obtained $q_{cr,sub}$ values are shown in Fig. 3.13 for subcoolings with pressure as a parameter. The predicted values of CHF by Eq. (3.4), Kutateladze's correlation and Sakurai's data are also shown in comparison with the experimental data in Fig. 3.13. The CHFs for the subcoolings lower than near 40K at the pressures and the subcoolings up to 80K at pressures lower than 199kPa almost agree with the values derived from Eq. (3.4). But in the case of pressures higher than 297kPa, most of the data

does not agree with the values when subcoolings become higher than 60K. That is to say, the CHFs for high subcoolings at high pressures cannot be expressed by the correlation, Eq. (3.4). This fact means that there exists another mechanism of heat transfer crisis at the CHFs different from that based on the HI model as mentioned before. Sakurai et al. conducted an experiment on the same heater in water for more wide range of subcoolings and pressures, and they derived the empirical equation of CHF for high subcoolings at high pressures as shown Eq. (3.6). The measured $q_{cr,sub}$ without having the effect of pressure existed almost within ±5% around the $q_{cr,sub}$ curve for subcooling derived from Eq. (3.6) with the K_3 value of 3.81×10^5. It was previously assumed that the heat transfer crisis at the CHFs expressed by Eq. (3.6) occurred due to the heterogeneous spontaneous nucleation, HSN, in originally flooded cavities on the cylinder surface with liquid.

Consequently, it was clarified that the CHFs measured were mainly divided into two mechanisms for lower and higher subcooling at a pressure in water. It can be confirmed the original Sakurai et al.'s data in the several papers (1995, 1996, 2000, 2002).

$$q_{cr,sub} = q_{cr,sat}\left[1 + K_2(\rho_l / \rho_v)^{0.69}(C_{pl}\Delta T_{sub} / L)^{1.5}\right] \tag{3.4}$$

$$q_{cr,sat} = K_1 L \rho_v \left[\sigma g(\rho_l - \rho_v) / \rho_v^2\right]^{0.25} \tag{3.5}$$

$$K_1 = 0.17, \qquad K_2 = 0.40(L')^{-0.6}$$

$$L' = \frac{D/2}{\sqrt{\sigma / g(\rho_l - \rho_v)}}$$

$$q_{cr,sub} = K_3 \Delta T_{sub}^{\ 0.73} \tag{3.6}$$

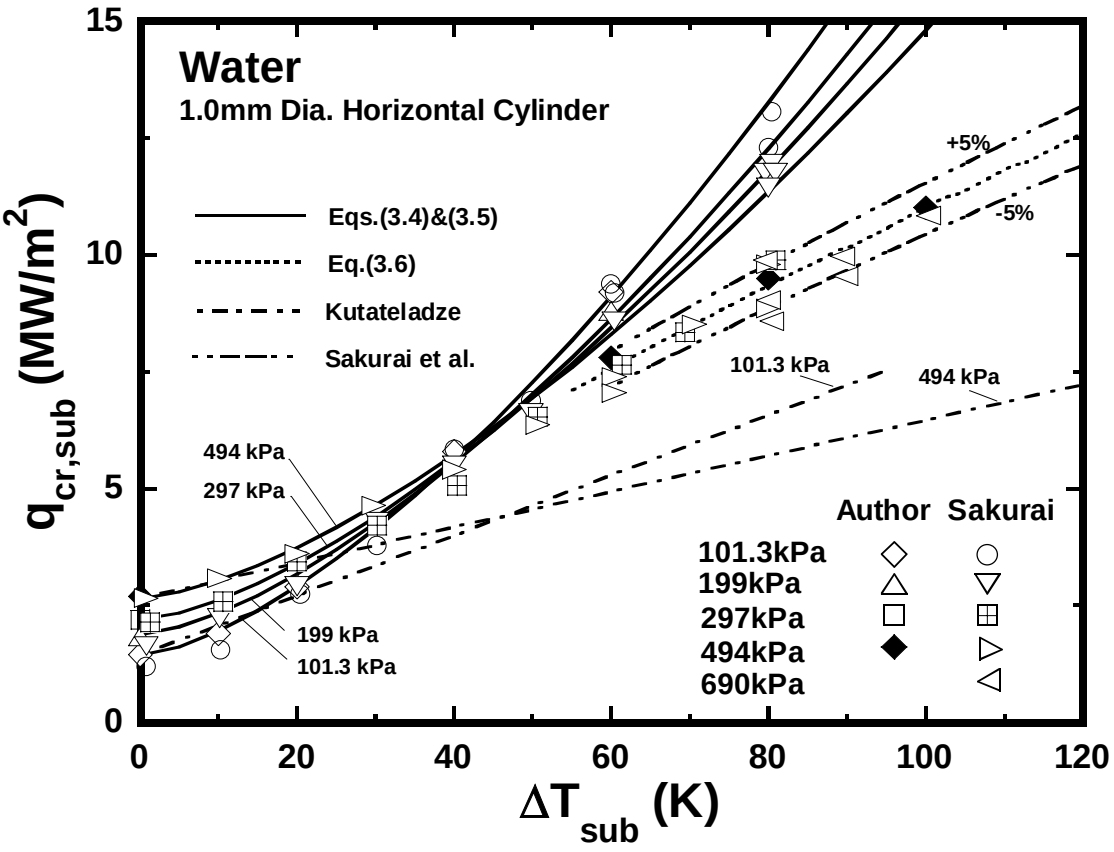

Fig. 3.13 Comparison of prediction with $q_{cr,sub}$ for subcooling with pressure as a parameter in water using Eqs.(3.4), (3.6), Kutateladze's correlation and Sakurai's data.

3.10.2 CHFs in wetting liquids such as ethanol and FC-72

Figure 3.14 shows steady-state CHF data related to subcoolings with pressure as a parameter in a pool of ethanol with corresponding CHF curves obtained by empirical equations, Eq. (3.4) and (3.7) for comparison. The following Eq. (3.7) representing $q_{cr,sub}$ resulting from the HSN is derived instead of Eq. (3.6) to express the subcoolings including the $q^*_{cr,sat}$ resulting from the HSN for zero subcooling.

$$q_{cr,sub} = q^*_{cr,sat}(1 + K_4 \Delta T_{sub}{}^{0.73}) \tag{3.7}$$

The $q^*_{cr,sat}$ value measured or extrapolated is used. The obtained K_1, K_2, $q^*_{cr,sat}$ and K_4 are shown in the table on the figure. As shown in the figure, the CHFs dependent on pressure exist in a very narrow range of low subcoolings near saturated condition, and they gradually increase with an increase in subcooling. It also seems that they are almost independent of the pressures for the subcooling higher than around 40 K. As mentioned before, Sakurai et al. (1996) has reported that CHF data obtained for high subcoolings at high pressures in a pool of water were due to the HSN. In the case of CHF data in a pool of ethanol which is highly wetting liquid, the surface tension is lower than that of water and its contact angle between liquid and heater surface is smaller than that of water, so that it may be easy for a wetting liquid such as ethanol to flood cavities on a heater surface. Therefore, it can be seen on the figure that the CHFs

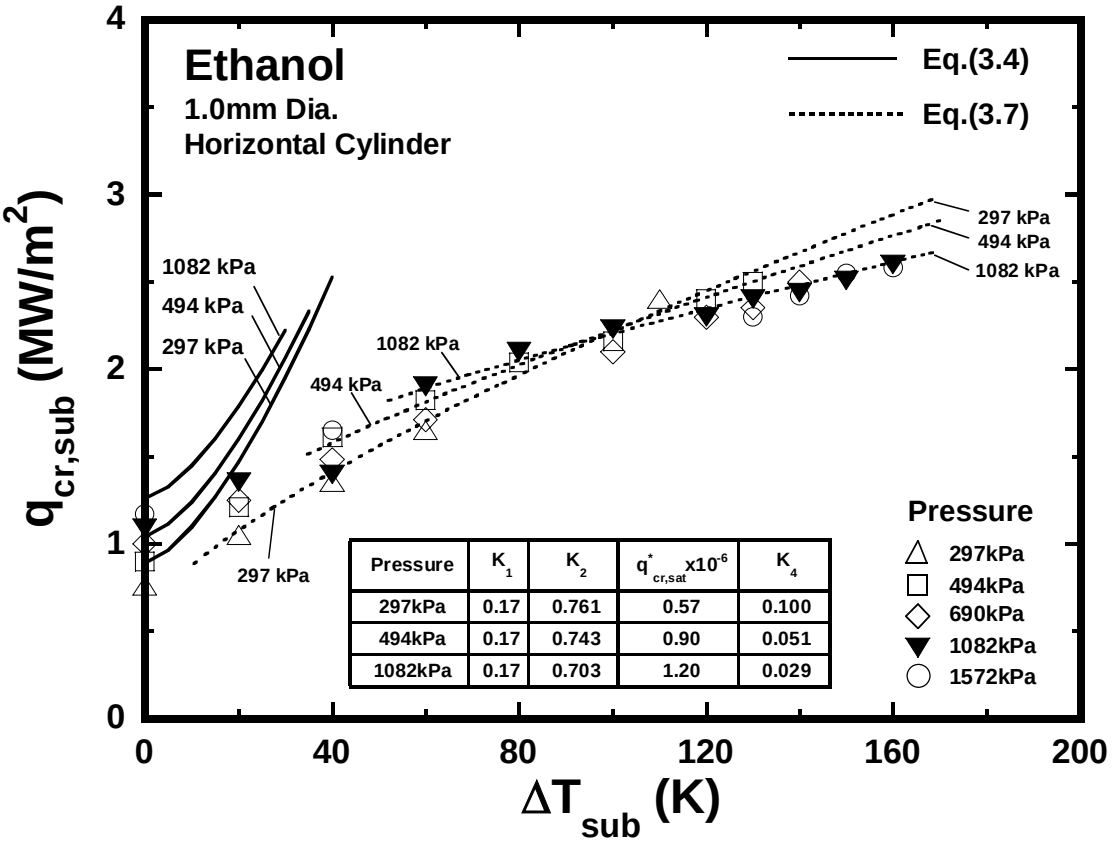

Fig. 3.14 Comparison of prediction representing $q_{cr,sub}$ related to subcooling at pressure as a parameter in ethanol using Eqs. (3.4) and (3.7).

from lower subcooling near saturated condition than that of water is due to HSN. As shown in the regime for the subcoolings higher than about 100 K with the corresponding CHF curves obtained from Eq. (3.7), the experimental data slightly depending on the pressures agree with the corresponding predicted values. In the case of FC-72, the dependability of pressure in the high subcooling regime becomes more certain. Figure 3.15 describes this.

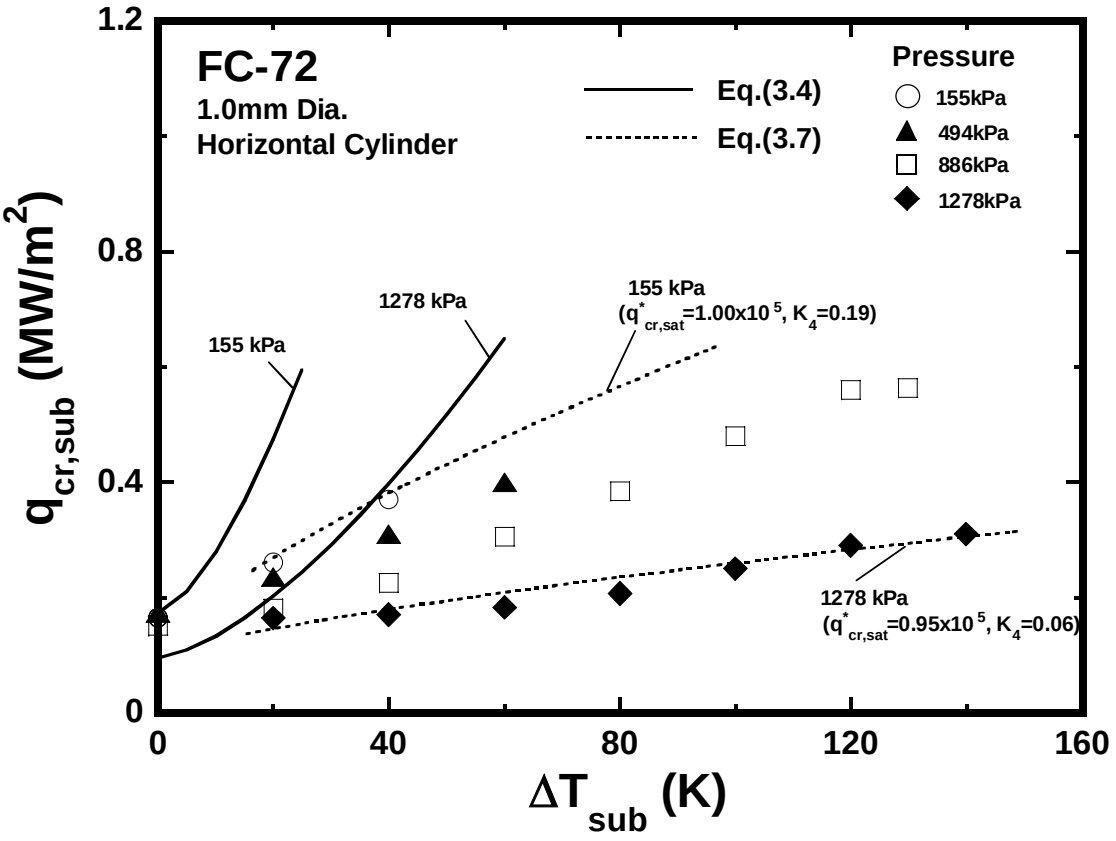

Fig. 3.15 Comparison of prediction representing $q_{cr,sub}$ related to subcooling at pressure as a parameter in FC-72 using Eqs. (3.4) and (3.7).

Figure 3.15 shows the $q_{cr,sub}$ data in FC-72 for the subcoolings ranging from zero to 140 K at the pressure of 155, 494, 886 and 1278 kPa with corresponding HI curves derived from Eq. (3.4), and the corresponding HSN curves derived from Eq. (3.7). In the case of FC-72 with having lower values of property in critical pressure or surface

tension etc. than that of ethanol, the dependability of pressure in the high subcooling regime becomes more remarkable than ethanol. And the CHFs depend on pressure for the subcooling over the range from 140 K to 20 K except the saturated condition because of the properties different with ethanol and water. The $q_{cr,sub}$ data at the pressure of 155 kPa are divided into two groups for the subcoolings: the former $q_{cr,sub}$ data agreed with the corresponding HI curve representing the CHF resulting from the HI at the saturated condition. The latter $q_{cr,sub}$ for the pressures of 155 and 1278 kPa for the subcoolings are well expressed the corresponding HSN curves derived from Eq. (3.7). The $q^*_{cr,sat}$ and K_4 are supposed by extrapolation. It should be noted that each HSN curve representing the CHF resulting from the HSN measured exist depending on pressure. In conclusion, it can be assumed that the similar trends of $q_{cr,sub}$ for higher subcooling at higher pressures will be obtained for water also as shown in ethanol, when it goes further into higher subcooling. As shown in Fig. 3.16, most of the data do not agree with the values derived from Eqs. (3.4) and (3.5).

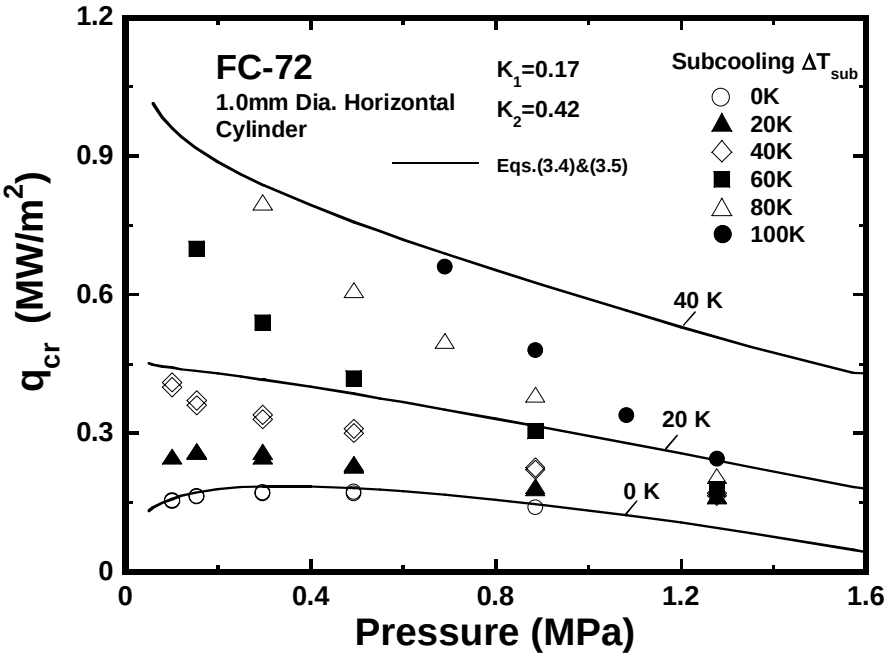

Fig. 3.16 Comparison of CHF data for FC-72 with the corresponding CHF curves obtained from Eqs. (3.4) and (3.5).

3.10.3 Saturated CHFs for various pressures in the liquids

The CHFs measured under saturated conditions at the pressures tested here are shown in Fig. 3.17 with the curve obtained from the saturated CHF correlation by Eq. (3.5) with K_1 value of 0.17. As shown in the figure, the CHF curves correlation by Eq. (3.5) increase with increasing in pressure up to the maximum CHF value, and then the curves decrease from the value. That is why the mechanism of heat transfer crisis at CHF and the properties, i.e., latent heat of vaporization, surface tension, density of saturation liquid etc. are affected in CHF correlation by Eq. (3.5). And they take a maximum at around 1/3 regime of the critical pressure, $P_{cr,l}$. Sakurai et al. (1992, 1996) have carried out the experiments of the CHFs in cryogenic liquids such as liquid helium and liquid nitrogen, and it is confirmed that the curves derived from Eq. (3.5) well agree with the

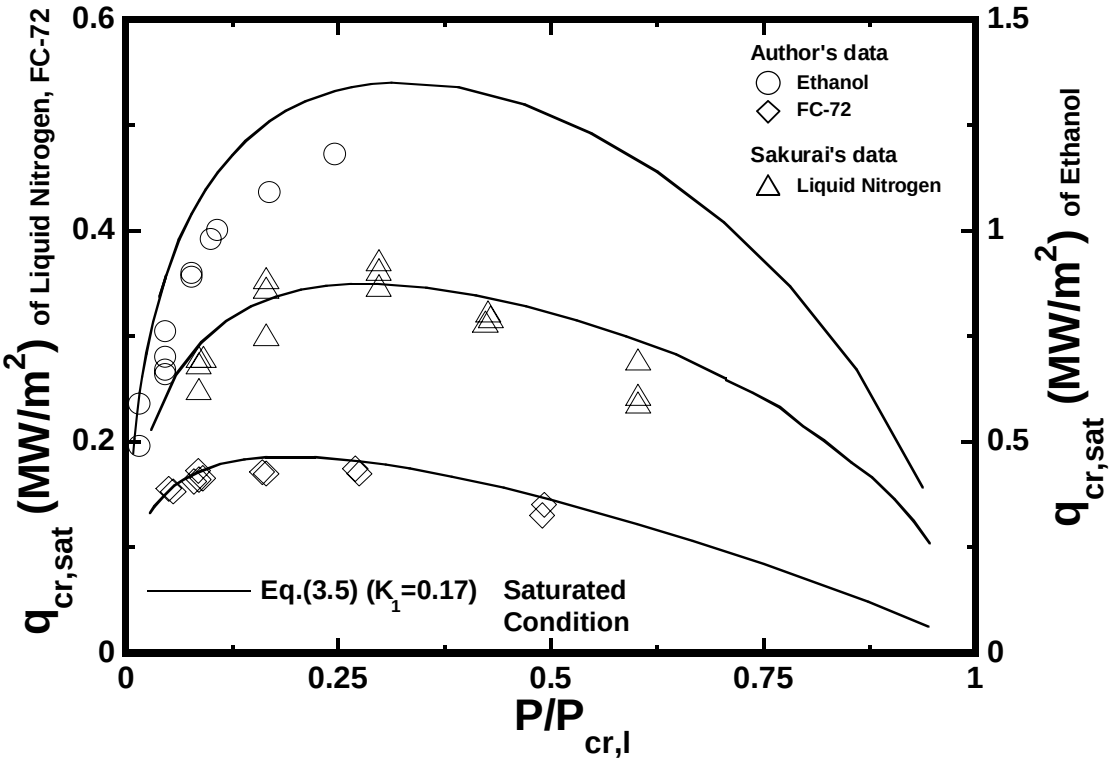

Fig. 3.17 Critical heat fluxes under saturated conditions at elevated pressures.

CHF values at lower pressure regime, though the CHFs at higher pressure regime are significantly lower than those estimated from Eq. (3.5) based on the HI model for $q_{cr,sat}$. From this result, they have suggested another mechanism assumed that the transition occurs due to the HSN. This experiment also brought a similar result.

3.11 Transient heat transfer up to heat transfer crisis

There exist two types of boiling incipience on the cylinder surface in a liquid due to an increasing heat input; one is that from originally unflooded active cavities entraining vapor and the other is that from another mechanism without contribution of the active cavities. The former is observed in water and the latter is in ethanol and FC-72. The latter boiling mechanism was suggested by Sakurai et al. (1993) to be due to the HSN from originally flooded cavities on the cylinder surface in the liquids. The heat transfer processes including the transition from the non-boiling regime to film boiling or to fully-developed nucleate boiling (FDNB) on a horizontal cylinder due to the exponentially increasing heat inputs at pressure was classified into three groups.

The heat transfer processes in response to the exponential heat inputs with the periods of 1 s and 20 ms at pressures of 101.3 and 494 kPa in ethanol are shown on the graph of heat flux q versus surface superheat ΔT_{sat} in Fig. 3.18. First, the transitions from non-boiling regime to fully-developed nucleate boiling (FDNB) occur in the natural convection regime for periods longer than a certain value dependent upon the pressure at pressures higher than atmospheric. In the case of a period of 1 s at a pressure of 494 kPa, the heat transfer process shows the typical case like this transition shown with a dashed chain line. At the transition point ◊ (q_{in} for 494 kPa), the wall superheat and the heat flux rapidly change through the process to FDNB heat transfer. The decrease of wall superheat is due to the activation of originally flooded cavities. The heat flux then

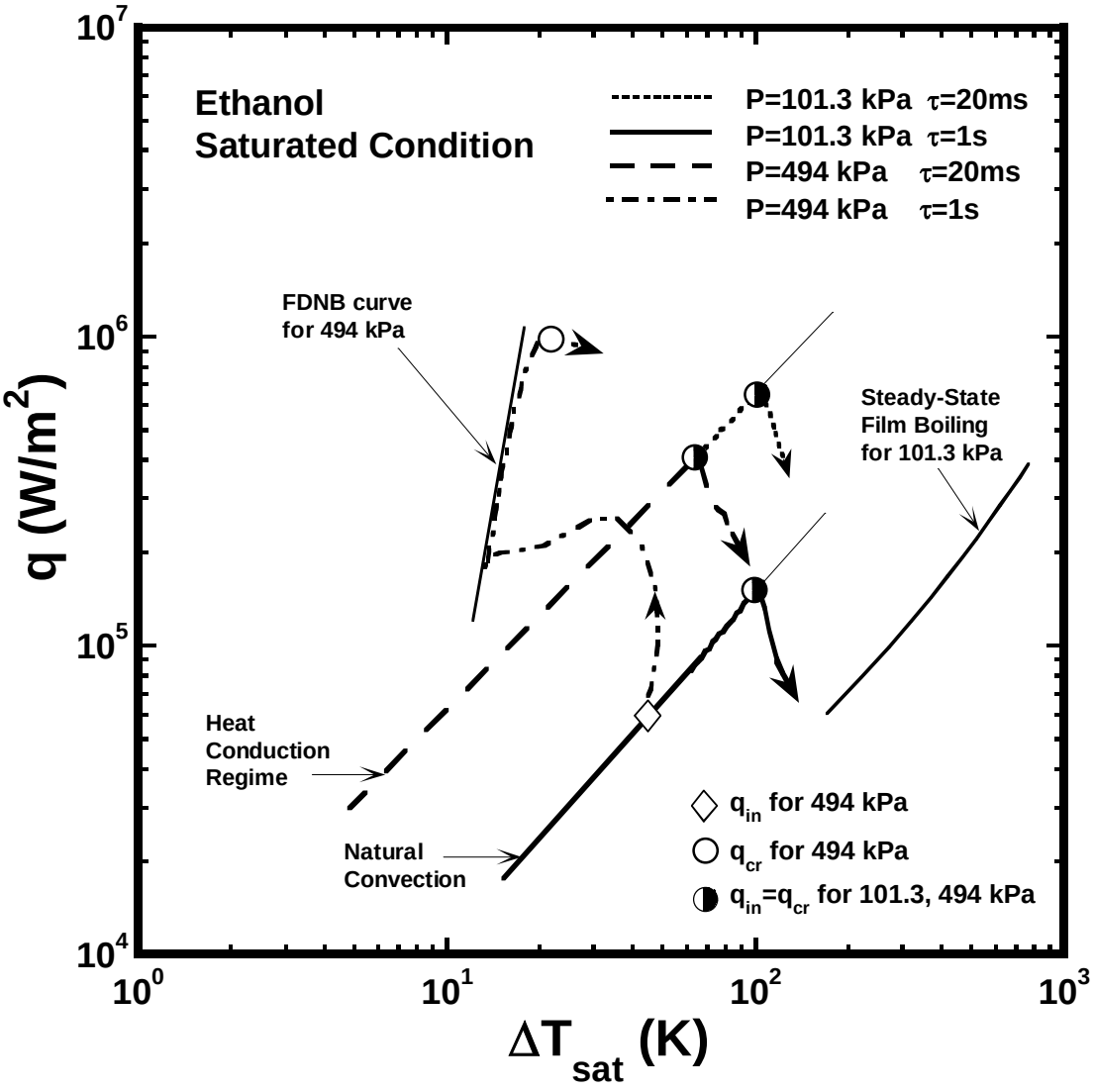

Fig. 3.18 Transitions from non-boiling to film boiling or to fully-developed nucleate boiling caused by exponential heat inputs in saturated ethanol at pressures of 101.3 and 494 kPa.

increases gradually with an increase in wall superheat up to critical heat flux q_{cr} point, where the transition from FDNB to film boiling occurs due to the HI (Kutateladze, 1959; Zuber, 1959) in the two-phase region near the heater surface. The process from the non-boiling regime to film boiling thorough FDNB is divided into the first group.

On the other hand, the direct transitions occur for almost of all the periods at pressures lower than around atmospheric and for shorter periods at pressures higher than atmospheric. Direct transitions show the heat transfer processes at pressure of 101.3 kPa and for the period of 20 ms at pressure of 494 kPa. At the direct transition points, a thick vapor film formed on the whole heater surface. And the heat transfer processes approach the steady-state film boiling curve on the graph: the steady-state film boiling curve can be evaluated by using the correlation (Sakurai et al., 1992). The critical heat flux, q_{cr}, at the direct transition which is equal to the initial boiling heat flux, q_{in}, is due to HSN as mentioned before. This process is divided into the second group. According to the experiment here, the direct transitions occurred for periods ranging from 5 ms to 20 s at atmospheric pressure and for periods ranging from 5 ms to 400 ms at pressure of 494 kPa.

In addition, although it is not shown in this figure, it could be also observed the third group with an intermediate period between first and second group. The q_{cr} of the third group between the first and second one occurs by HSN before reaching the critical heat flux in FDNB.

Fig. 3.19 shows transient CHFs, q_{cr}, and initial boiling heat fluxes, q_{in}, versus periods, τ, ranging from 5 ms to 20 s in saturated ethanol at pressures of 101.3 kPa and 494 kPa. The q_{cr} for the periods can be separated into two principal groups as shown in the figure; the first group is shown with a solid line at pressure of 494 kPa, and the second groups are shown with a dashed line at both pressures and with a dashed chain line at pressure of 101.3 kPa, respectively.

It can be assumed that the q_{cr} values for the first group at pressure of 494 kPa are on the extension of FDNB curve on q versus ΔT_{sat} as shown in Fig. 3.18. These values are considerably higher than the corresponding boiling initiation heat fluxes q_{in}. And the value of q_{cr} increases gradually with a decrease in the period from 20 s down to around

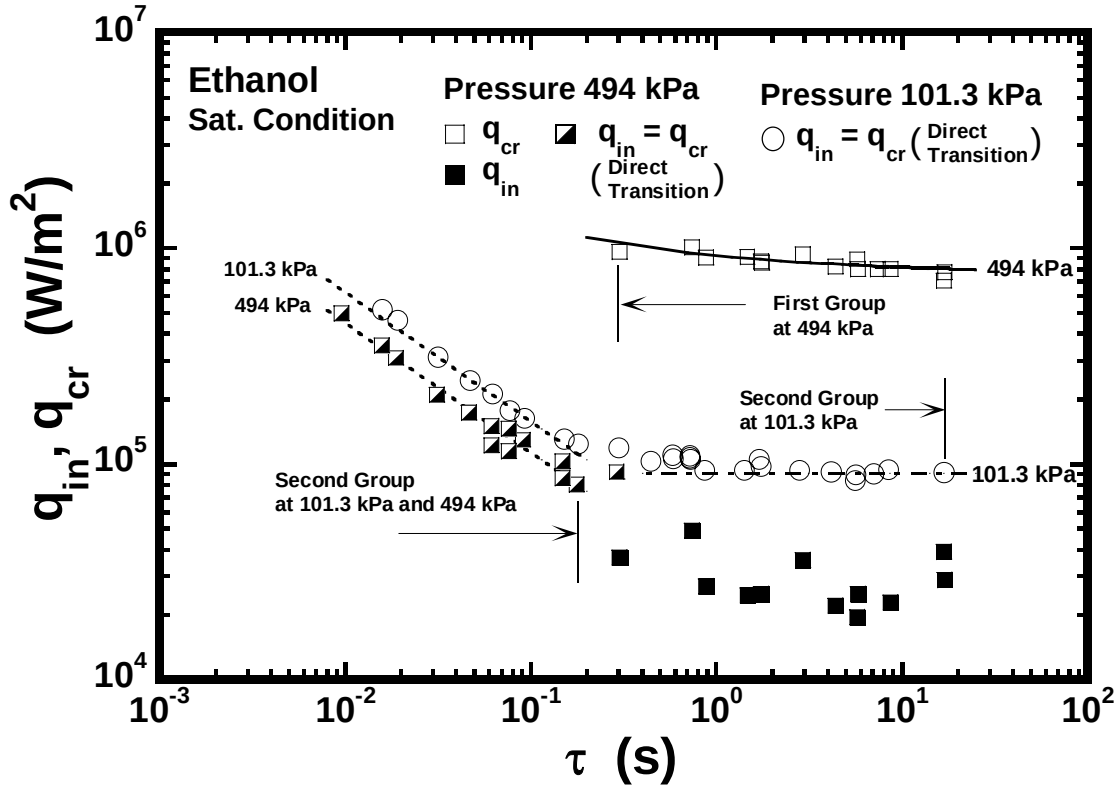

Fig. 3.19 The relation between boiling initiation heat flux q_{in}, critical heat flux q_{cr} and exponential period τ in saturated ethanol at pressures of 101.3 and 494 kPa.

400 ms. The increasing trend of q_{cr} is explained by the time lag of the HI which starts at the steady-state critical heat flux, q_{st} (Sakurai et al., 1993). The q_{cr} of the second group ($\tau \leq 400$ ms) at pressure of 494 kPa is due to the direct transition from single phase conduction regime to film boiling; the value q_{cr} is equal to q_{in}. In addition, the direct transition at pressure of 101.3 kPa for a period ranging from 5 ms to 20 s is also shown in Fig. 3.19: direct transitions occur for all the periods tested here.

The relationship between q_{cr} and τ for a pressure of 494 kPa in saturated water is shown in Fig. 3.20. The relationship is similar to that for the pressure of 494 kPa in ethanol shown in Fig. 3.19 except that the values of q_{cr} for periods shorter than 40 ms are not equal to q_{in}. The reason is that the boiling incipience on the heater surface in water causes an increasing heat input from originally unflooded active cavities entrain-

ing vapor bubbles.

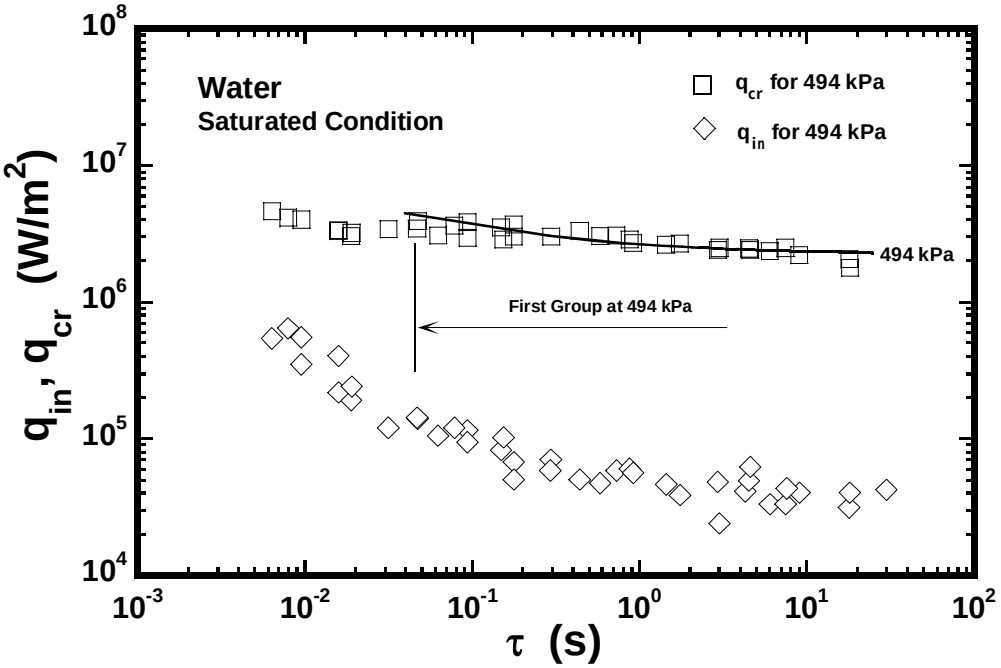

Fig. 3.20 The relation between boiling initiation heat flux q_{in}, critical heat flux q_{cr} and exponential period τ in saturated water at pressure of 494 kPa.

3.12 Typical trend of the CHF values in relation to the periods

The results of the CHF values, q_{cr}, for $Q_0 exp^{t/\tau}$ with the periods, τ, ranging from 20 s down to 5 ms for saturated water at the pressures of 101.3 and 494 kPa, and for the subcooling, ΔT_{sub}, of 60 K at same pressure obtained for the horizontal cylinder are shown in Fig. 3.21. The q_{cr} values for all periods at pressure of 101.3 kPa increase up to the maximum q_{cr} first, then decrease down to the minimum q_{cr} and again increase with the decreases in exponential period; they are clearly classified into three groups for the period. First one is for the periods longer than 60 ms, second one is for the periods shorter than 20 ms, and third one is for the period between 20 and 60 ms. Fukuda et al. (1995) suggested the several empirical equations representing transient CHF values

versus periods belonging to the first and second group in a pool of water for wide range of subcoolings and pressures. The CHF belonging to the first group with longer periods occurs with a FDNB heat transfer process. At the second group with shorter periods, the direct or semi-direct transition to film boiling occurs with explosive-like boiling from non-boiling. The CHF belonging to the first group caused by the heat inputs with a long period under a lower subcooling condition and a higher subcooled one is expressed by the Eq. (3.8) and Eq. (3.9), respectively. The CHF belonging to the second group with a shorter period is expressed by the Eq. (3.10). As shown in the subsequent experimental results, the empirical equations (3.8), (3.9), and (3.10) are effective for not only water but also the highly wetting liquids such as ethanol and FC-72.

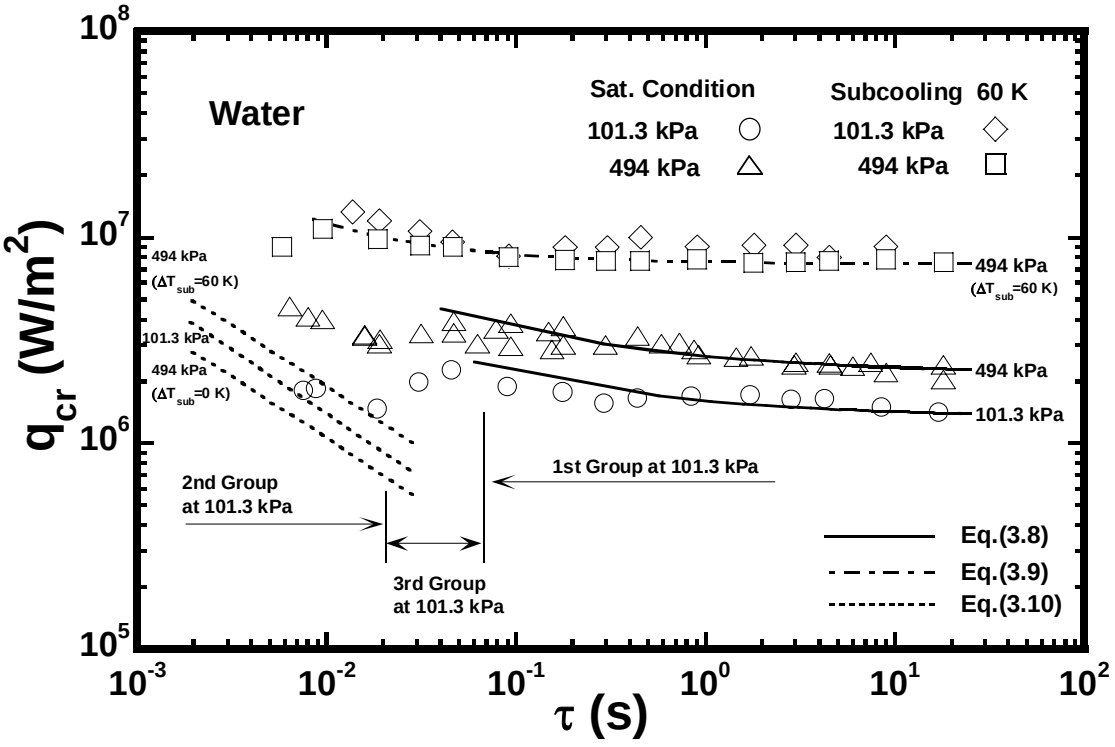

Fig. 3.21 The relation between q_{cr} and τ for saturated condition and subcooling of 60K at pressures of 101.3 and 494 kPa in water.

3.12 Typical trend of the CHF values in relation to the periods

$$q_{cr} = q_{st,sub}\left(1 + 0.21\tau^{-0.5}\right) \tag{3.8}$$

$$q_{cr} = q_{st,sub}\left(1 + 2.3\times10^{-2}\tau^{-0.7}\right) \tag{3.9}$$

where the $q_{st,sub}$ is given by the quasi-steady-state CHF data in each experiment.

$$q_{cr} = h_c\left(\Delta T_{in}(\tau) + \Delta T_{sub}\right) \tag{3.10}$$

where $h_c = (k_l\rho_l c_{pl}/\tau)^{1/2} K_{1th}(\mu D/2)/K_0(\mu D/2) \cong (k_l\rho_l c_{pl}/\tau)^{1/2}$, and $\mu = [\rho_l c_{pl}/k_l\tau]^{1/2}$. K_o and K_{1th} are the modified Bessel functions of the second kind of zero- and first-orders. h_c is the heat transfer coefficient resulting from transient heat conduction, $\Delta T_{in}(\tau)$ is the initial boiling surface superheat due to the HSN in conduction regime, and ΔT_{sub} is liquid subcooling.

The trend of q_{cr} expressed by the Eq. (3.8) is due to the hydrodynamic instability (HI) at which the transition from fully-developed nucleate boiling (FDNB) to film boiling occurs. The transition mechanism has been already pointed out by Kutateladze (1959) and Zuber (1959). The trend that the q_{cr} values gradually increases with a decrease in period for the group is explained by the time lag of the HI by which the transition to film boiling occurs at steady-state q_{cr} (Sakurai et al., 1995). On the other hand, in the case of water, the steady-state CHF, $q_{st,sub}$, values for the subcooling higher than around 60 K at the higher pressures except the pressures lower than around 300 kPa become lower than those expected by the correlation based on the HI. It was assumed by Sakurai et al. (1996) that the transition to film boiling at the steady-state CHF, $q_{st,sub}$, due to the heat input with the long period such as 20 s for subcoolings higher than around 60 K at pressures higher than around 400 kPa occurs due to the HSN at a lower limit of HSN temperature. Therefore, the trend of q_{cr} values related to periods, expressed by the Eq. (3.9), becomes different from the corresponding curve estimated by Eq. (3.8) due to the HI. The q_{cr} data in relation to the periods also gradually increases

with a decrease in period because the HSN surface superheat depends on an increasing rate of surface superheat as mentioned previously by Sakurai et al (1995).

The second group of q_{cr} for the periods shorter than the period corresponding the minimum q_{cr} is expressed by the Eq. (3.10). The q_{cr} values for the periods at each pressure are expressed by a linear asymptotic line on a log-log graph, and those are considered that the direct boiling transition on the heater surface from non-boiling to film boiling. The values of $\Delta T_{in}(\tau)$ in Eq. (3.10) are experimentally measured for periods at pressures. Those depend on the increasing rates of surface superheat, pressures and liquid subcoolings (Fukuda et al., 1995) (Sakurai et al., 1995).

As shown in the Fig. 3.21, the q_{cr} values at pressure of 101.3 kPa are classified clearly into three groups for the period tested here. On the other hand, the second groups of q_{cr} for the saturated and subcooled conditions at the pressure of 494 kPa were not observed. It can be supposed from Fig. 3.21 that the direct transitions occur for the periods shorter than about 1 ms at the pressure of 494 kPa in water. The q_{cr} values for the periods belonging to the first group at the saturated pressures of 101.3 and 494 kPa are well expressed by Eq. (3.8) that represents the CHF due to the HI. The q_{cr} values for the subcooling of 60 K at the pressure of 494 kPa are well expressed by Eq. (3.9) that represents the CHF due to the HSN as mentioned above, so those occur due to the explosive-like HSN at the lower limit of HSN surface superheat though the nucleate boiling due to active cavities on fully-developed nucleate boiling (FDNB) coexist.

3.13 Transient critical heat flux (CHF) in ethanol

3.13.1 The q_{cr} for period under saturated condition

Figure 3.22 shows transient CHFs, q_{cr} versus the periods, τ, ranging from around 50 s down to 5 ms under saturated condition at various pressures in ethanol. As shown in the

figure, the q_{cr} values for all periods gradually increase with a decrease in period up to the maximum CHF from the steady state one corresponding to the CHF for a period of 20 s or more, and then decrease down to the minimum one and again increase with a decrease in period. Also the CHF values in relation to the periods can be divided into three principal groups as shown in the figure; the first groups are shown with a solid line, and the second groups are shown with a dashed line. The q_{cr} values for the periods belonging to the first group at the saturated pressures are well expressed by Eq. (3.8), also the q_{cr} values for short periods belonging to the second group for each pressure are approximately expressed by Eq. (3.10).

In the case of the saturated condition at various pressures, the q_{cr} values for periods belonging to the first group are well dependent on pressure similar to water. The increasing trend of q_{cr} is explained by the time lag of heat transfer crisis at steady-state critical heat flux, q_{st}. As for the second group shown with a dashed line at each pressure,

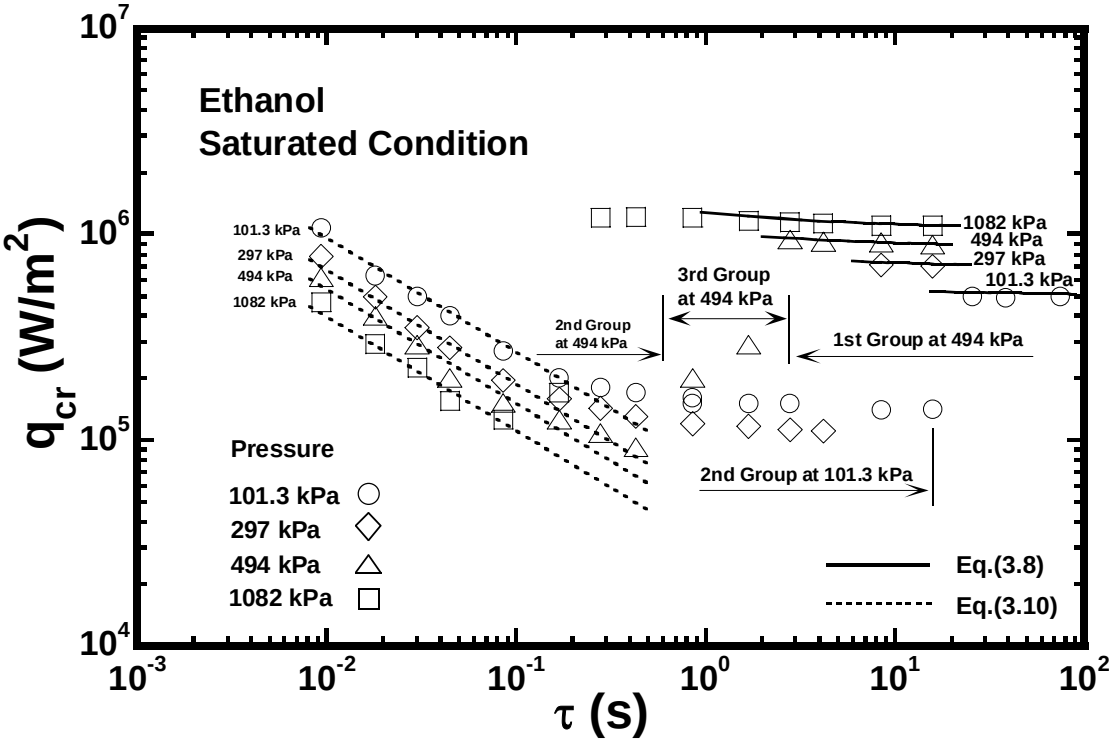

Fig. 3.22 The relation between q_{cr} and τ for saturated condition in ethanol.

the q_{cr} decreases with an increase in pressure with a constant period because the lower limit of HSN surface superheat decreases with an increase in pressure. As seen in the figure, the shortest period for the q_{cr} belonging to the third group becomes shorter with an increase in pressure. Therefore, the q_{cr} at the longest period which belongs to the second group could not be observed at higher pressures by the heat input with the shortest period tested here. The minimum q_{cr} for the period under the pressure of 494 kPa for the saturated condition is observed at around 400 ms. It should be noted that the value is about 14% of steady-state one corresponding to the CHF for the period of 20 s. As a result from the experimental data, the minimum q_{cr} values within the second group at each pressure were much lower than the corresponding steady state CHF. This fact means that conduction heat transfer becomes more predominant as the period becomes shorter than natural convection heat transfer. Therefore, the heat transfer coefficient becomes higher due to heat conduction and a direct or semi-direct transition to film boiling occurs at the heat flux point that is higher than that of natural convection.

3.13.2 The q_{cr} for period under subcooled condition

The experimental data obtained for the pressure of 690 kPa for the subcoolings over range of 0 to 100 K in ethanol are shown in Fig. 3.23 versus exponential period as a typical. The curves representing the q_{cr} for τ for the subcooling of 0 K, namely the saturated condition, derived form Eq. (3.8) is shown in the figure with a solid line. The values of q_{cr} increase gradually with a decrease in period up to those at the periods around 2 s for the subcooling of 0 K. As mentioned before, the trend of q_{cr} for τ was explained as the time lag of heat transfer crisis which occurs at steady-state q_{cr}. On the other hand, the values of q_{cr} for periods for subcoolings higher than 20 K are expressed by the Eq. (3.9) with a dashed chain line, and those are lower than the values predicted

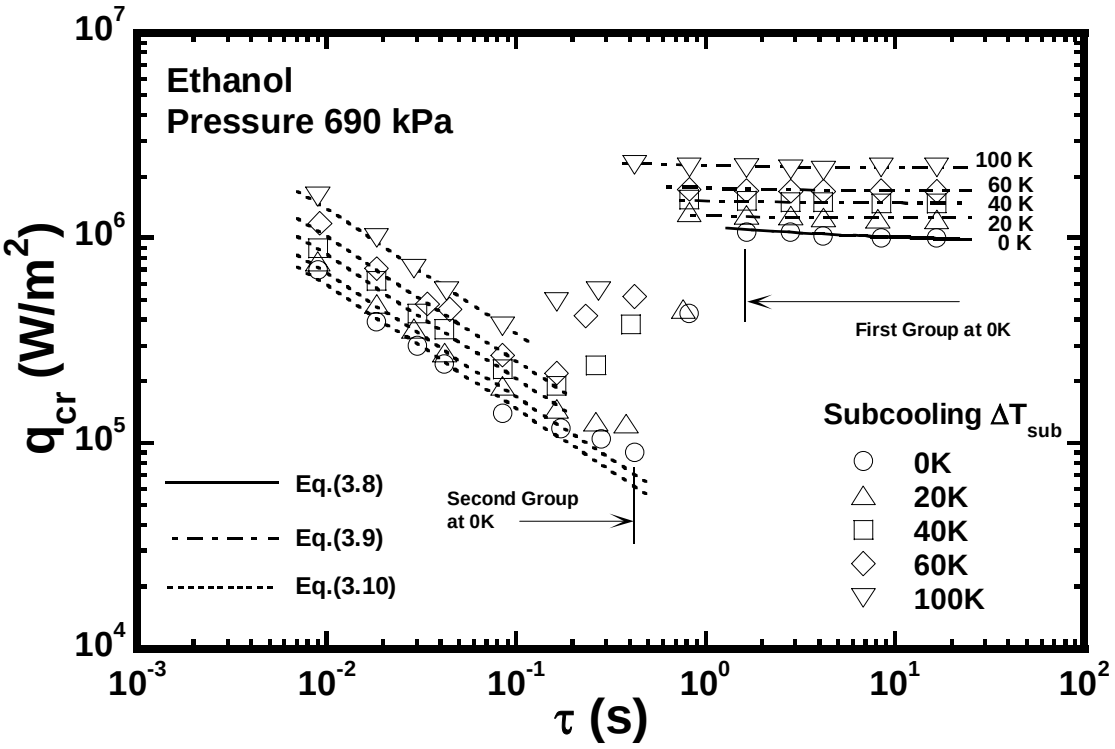

Fig. 3.23 The relation between q_{cr} anḍ τ for various subcoolings at pressure of 690 kPa in ethanol.

by the Eq. (3.8). The values of q_{cr} for the liquid subcoolig of 100 K increase more gradually with a decrease in period up to those at the period around 0.4 s. The trend of q_{cr} for period is explained due to the effect of increase in HSN surface superheat dependent on the increasing rate of surface superheat at the incipience of HSN.

The value of q_{cr} for the period of 20 s, namely steady-state critical heat flux, for subcooling of 0 K is a little bit lower than that described by Eq. (3.4) based on HI, so the $q_{st,sub}$ value measured in the experiment was used and expressed by Eq. (3.8). And the values for the subcoolings higher than 20 K are due to the HSN and described by Eq. (3.7) as mentioned in Section 3.10.2 and can be seen in Fig. 3.14.

As for the second group shown with a dashed line at each subcooling, the q_{cr} increases with an increase in subcooling and well dependent on liquid subcooling. As

seen in the figure also, the longest period for the q_{cr} belonging to the second group becomes shorter with an increase in subcooling. It can be assumed that the q_{cr} at the longest period which belongs to the second group won't be observed at higher subcoolings for the exponential heat input with the shortest period.

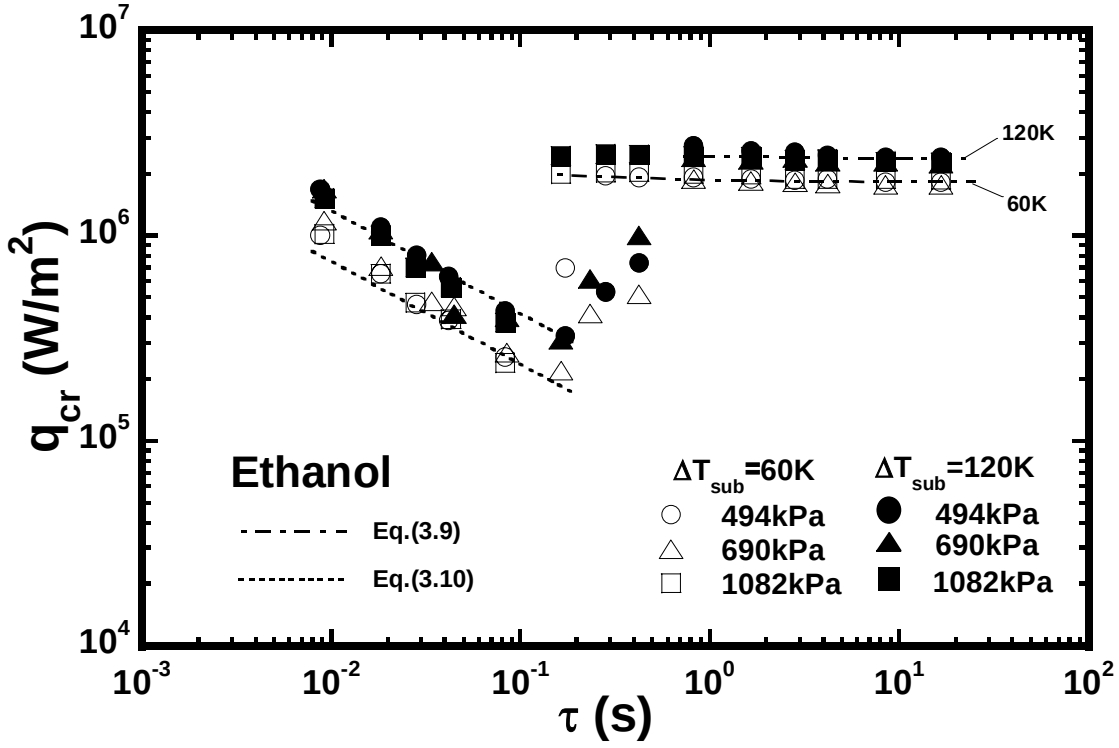

Fig. 3.24 The relation between q_{cr} and τ for subcoolings of 60 and 120 K at various pressures in ethanol.

Figure 3.24 shows transient CHFs, q_{cr} versus periods, τ, for the subcooling of 60K and 120 K at each pressure in ethanol. The q_{cr} values are clearly divided into three principal groups depending on the periods. The first group with a period longer than around 1 s is shown with a dashed chain line expressed by Eq. (3.9), and the second group with a period shorter than around 0.1 s is shown with a dashed line expressed by Eq. (3.10). As seen in the figure, q_{cr} values clearly increase with an increase in subcooling. However they are almost independent of pressure. The steady-state CHFs for high

subcooling at the pressures are also independent of the pressures. Sakurai et al. (1995) have explained this fact by assuming that the transition to film boiling at the steady-state CHFs occurs due to the explosive-like HSN in FDNB regime. The minimum CHFs for the period of around 200 ms are observed. The trend of q_{cr} for periods belonging to the first and second groups are well expressed because the CHFs at which the transitions to film boiling occur due to the HSN instead of the hydrodynamic instability as mentioned before.

3.14 Transient critical heat flux (CHF) in FC-72

3.14.1 The q_{cr} for period under saturated condition

The q_{cr} versus periods ranged from 20 s down to 5 ms at several pressures for saturated condition in a pool of FC-72 are shown in Fig. 3.25. The q_{cr} values for all periods gradually increase up to the maximum q_{cr} first, then decrease down to the minimum q_{cr} and again increase with the decreases in exponential period. The trend of q_{cr} values versus periods is clearly divided into three groups similar to ethanol. The first group with a period longer than 1 s at pressures is shown with a solid line, and the second group with a period shorter than around 0.1 s is shown with a dashed line.

Here, it should be observed that the trend of q_{cr} values belonging to the first group with a period longer than about 1 s in FC-72 is quite different with ethanol and water as shown in the figure. The q_{cr} values belonging to the first group are almost independent of pressure, and there is no large difference among the q_{cr} values at all the pressures expressed by Eq. (3.8) shown with a solid line. The steady-state CHFs under saturated condition are also almost independent of pressure. The steady-state critical heat fluxes for the subcooling of 0 K were well described by Eqs. (3.4) & (3.5) based on HI as

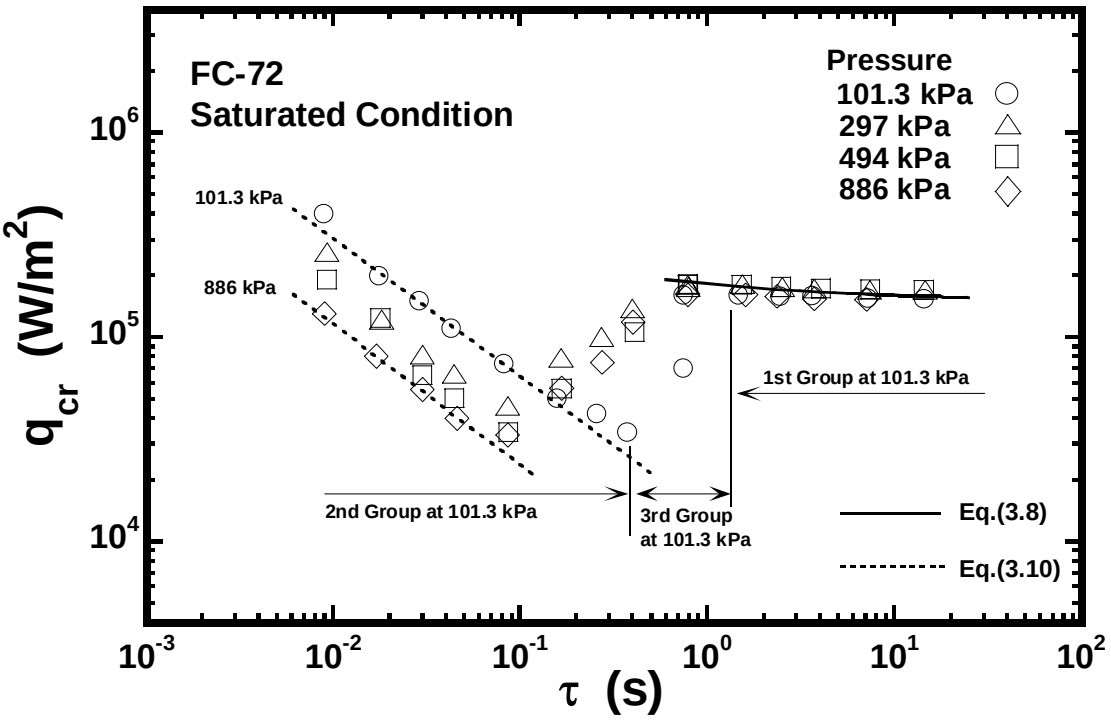

Fig. 3.25 The relation between q_{cr} and τ for saturated condition at various pressures in FC-72.

mentioned in Section 3.10.2 and can be seen in Fig. 3.16. On the other hand, the q_{cr} values for short periods belonging to the second group are approximately expressed by Eq. (3.10) shown with a dashed line. The trend of q_{cr} values for the second group is almost the same with those for the ethanol under saturated condition.

3.14.2 The q_{cr} for period under subcooled condition at a fixed pressure

The q_{cr} versus periods ranged from 20 s down to 5 ms at a pressure of 494 kPa for subcoolings of 20, 40 and 60 K in a pool of FC-72 are shown in Fig. 3.26. The trend of q_{cr} values versus periods is clearly divided into three groups similar to ethanol. The q_{cr} values are well dependent on subcooling. Those belonging to the first group are

expressed by Eq. (3.9), and the q_{cr} values for short periods belonging to the second group are approximately expressed by Eq. (3.10).

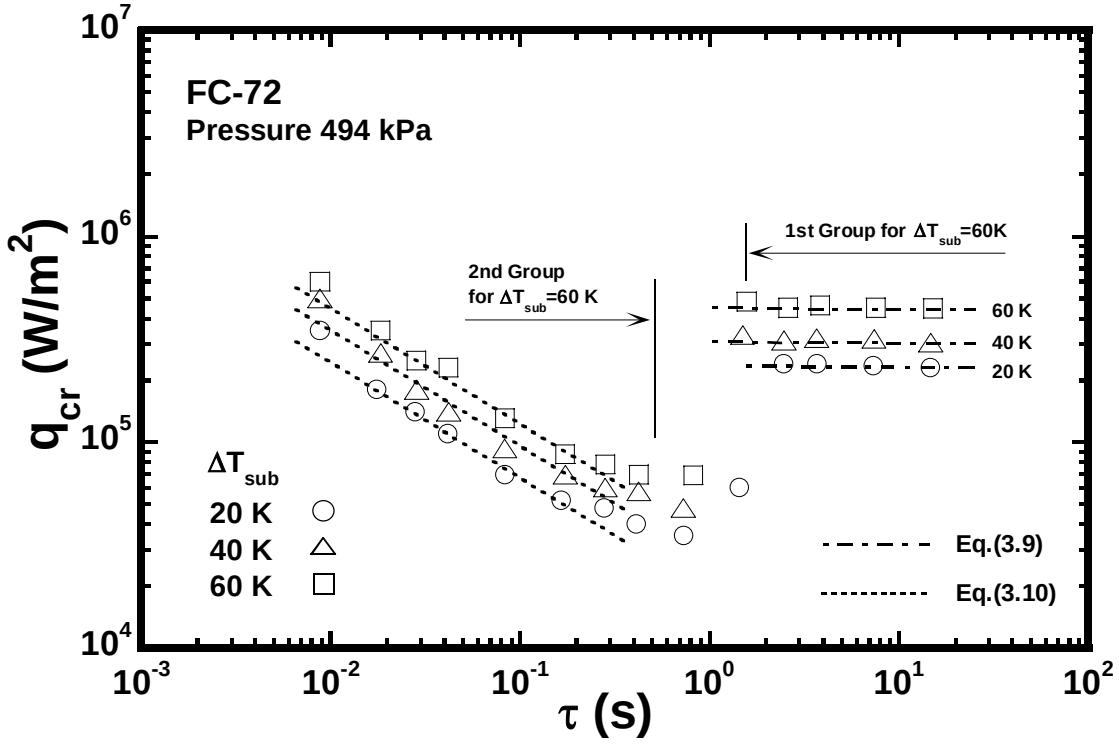

Fig. 3.26 The relation between q_{cr} and τ at pressure of 494 kPa for various subcoolings in FC-72.

3.14.3 The q_{cr} for period at subcoolings of 60 and 80 K at pressures

As shown in Fig. 3.16, the steady-state q_{cr} values for the subcoolings are well dependent on pressures except the values around low subcooling near saturated condition, besides there is a rapid inclination in the values with an increase in pressure as it becomes higher in subcooling.

The q_{cr} for τ at the pressures for the subcoolings of 60 and 80 K in a pool of FC-72 are shown in Fig. 3.27 and Fig. 3.28, respectively. The trend of q_{cr} values belonging to the first group with a period longer than about 1 s is quite different with ethanol and

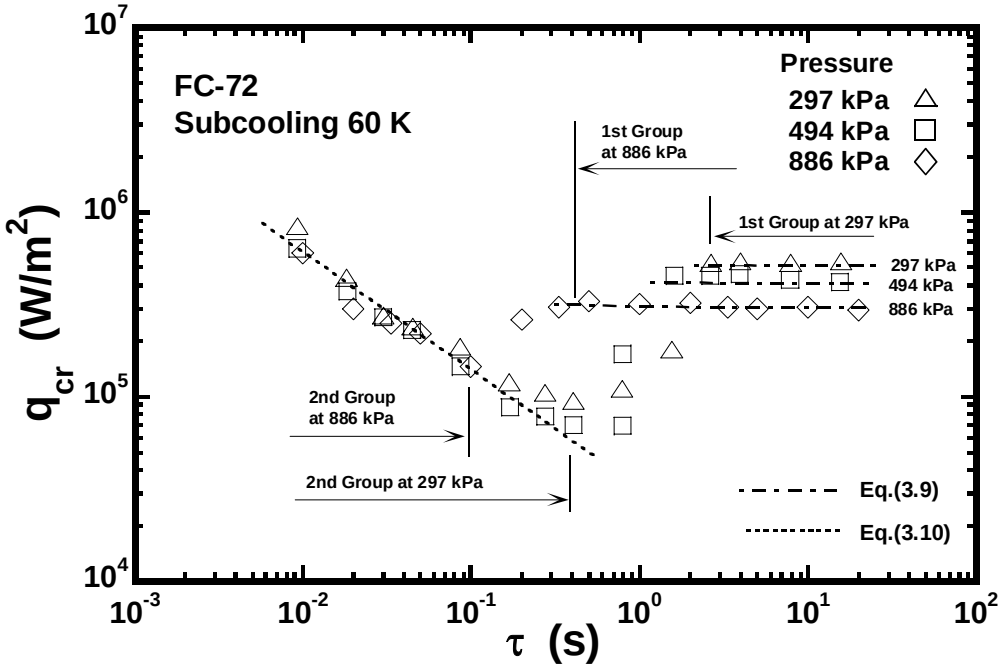

Fig. 3.27 The relation between q_{cr} and τ for subcooling of 60 K at various pressures in FC-72.

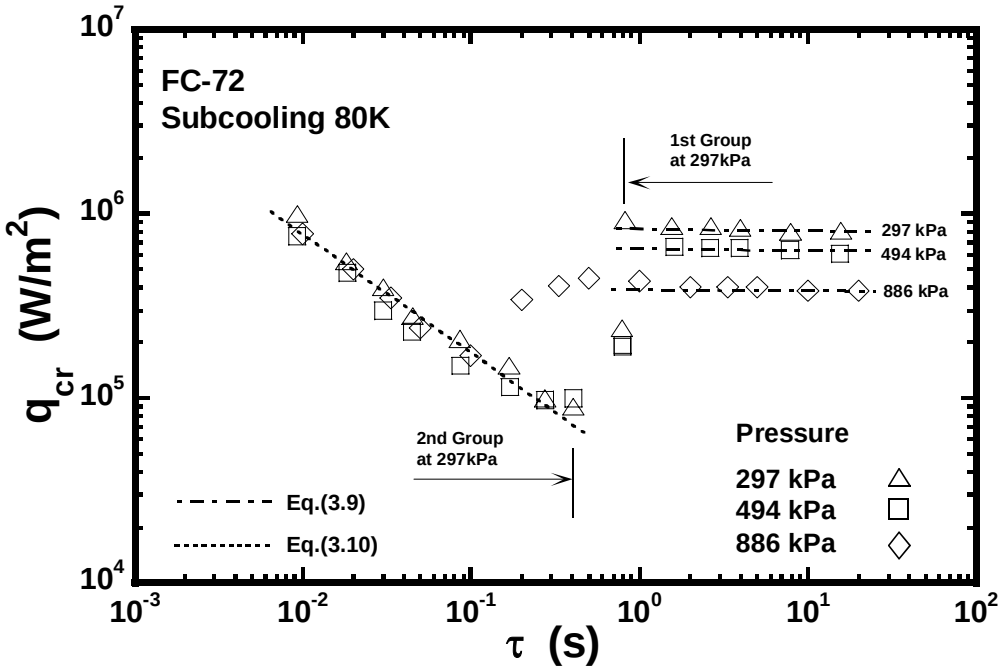

Fig. 3.28 The relation between q_{cr} and τ for subcooling of 80 K at various pressures in FC-72.

water as shown in the figure. In the case of the subcooled condition at the pressures, those are well dependent on pressure; those become lower as it becomes higher in pressure that are expressed by Eq. (3.9) shown with a dashed chain line. The values of the first group are gradually increasing with a decrease in period. The increase of surface temperature increasing rate due to the decrease of period causes the slight increase of initial boiling superheat by the HSN; the increase of HSN surface superheat induces the slight increase of the q_{cr} with the decrease in period. On the other hand, the q_{cr} values for short periods belonging to the second group are expressed by Eq. (3.10) shown with a dashed line. Those are also almost independent of pressure as same as ethanol under high subcooled condition.

Consequently, it should be noted that the trend of the transient q_{cr} values belonging to the first group different with ethanol and water is due to steady-state CHF data. As known well, the CHFs are considerably affected by the properties of boiling liquids that are changeable due to a temperature and pressure. Therefore, the properties of boiling liquid, i.e., latent heat of vaporization, surface tension, density of saturation liquid etc. are affected in CHF as well as the mechanism of heat transfer crisis at CHF.

3.15 Summary

(1) The processes from non-boiling to film boiling were completely different from each other depending on the period. The values of initial boiling heat flux increased with a decrease in period, namely, as the period shortens, the heat conduction became predominant in heat transfer compared with the natural convection.

(2) The vapor behavior at initial boiling due to the HSN was considerably different from that due to active cavities; it covered the whole cylinder surface by the large vapor tube in a short time. It is considered that the direct boiling transition on the

heater surface from non-boiling to film boiling is due to the HSN in previously flooded cavities on heater surface without the contribution of active cavities in general.

(3) The quasi-steady-state CHFs measured were mainly divided into two mechanisms for lower and higher subcooling at a pressure; the former and latter CHFs occurred due to hydrodynamic instability (HI) and explosive-like heterogeneous spontaneous nucleation (HSN) on the cylinder surface respectively. The dependability of pressure in the high subcooling regime became different depending on the boiling liquids.

(4) The transient CHFs were clearly classified into three principal groups for the periods: first group for the longer period, second group for the shorter and third group for the intermediate. And those were dependent on subcooling whichever groups in the case of a constant pressure.

4. Subcooled pool boiling CHFs for different surface condition of heater in various liquids

4.1 Introduction

The development of knowledge for generalized pool boiling CHF mechanisms and those correlations for cylinder surface conditions in water and wetting liquids are becoming increasingly important as the fundamental database for not only the design of high heat flux cooling system recently needed but also the derivation of subcooled flow boiling CHF correlations based on the pool boiling ones. Boiling CHF was assumed to happen based on hydrodynamic instability (HI), and the value was thought to be unaffected by the surface condition of heater so far. However, it has been understood that the CHF value changes systematically depending on experimental conditions according to a series of experiment of our research group. Then it has presented that there exists a new physical model due to explosive-like heterogeneous spontaneous nucleation (HSN) on the cylinder surface. Especially, the HSN appears remarkably in transient boil CHF. HI model hardly depends on the heater surface condition. According to the new physical model, however, it is thought basically that HSN model depends on the surface energy and the cavity size distribution from a physical model on CHF, therefore it physically influences the surface condition. The research of the effect of cylinder surface conditions on CHF remained unresolved for a long time. Recently the experiment in a pool of water was conducted by Sakurai (2000, 2002) and Fukuda et al. (2000, 2002, 2004), and reviewed in detail. The present work is also in a series of the research process, which is changed into highly wetting liquids besides water to clarify the effect of surface condition in various wetting liquids. The purpose of the present work is to investigate the effect of the surface conditions such as the commer-

cially-available surface (CS) and the roughly-finished surface (RS) with the different cavity size distribution and surface energy for saturated and subcooled liquids at various pressures on the transient pool boiling CHFs caused by the exponential heat generation rate shown with the periods. Also, it is clarified that the trend of CHF for the shorter periods meaning of higher heat generation rate is significantly affected by the test cylinder surface conditions in the experimental liquids. It is suggested that more study on the diverse surface conditions with different liquid-solid contact angle on the CHF is necessary.

4.2 Experimental conditions

Boiling heat transfer processes on a test heater in a pool of water, ethanol or FC-72 with different mechanisms due to a heat generation rate increased by exponential function, $Q=Q_0 exp^{t/\tau}$, ranging from quasi-steadily increasing one to rapidly increasing one with periods, τ, ranging from around 50 s to 5 ms are measured for a 1.0-mm diameter horizontal cylinders at pressures ranging from 101.3 to 1867 kPa for liquid subcoolings over the ranges from 0 to 160 K at pressures.

Experiments were performed on the following test heaters: Two horizontal cylinder test heaters of 1.0 mm in diameter were used. One is no surface preparation as shown in Fig. 4.1a, and the other one is finished by Emery-4 paper as shown in Fig. 4.1b. They have the different surface conditions of CS and RS, respectively. The photographs of heater surfaces were taken by a Scanning Electron Microscope (SEM). The roughness profiles are also shown in the figures. Arithmetical mean roughness, Ra, is as follows:

CS = 0.11 μm

RS = 0.24 μm

Experimental apparatus and method were already shown in Chapter 2 in detail.

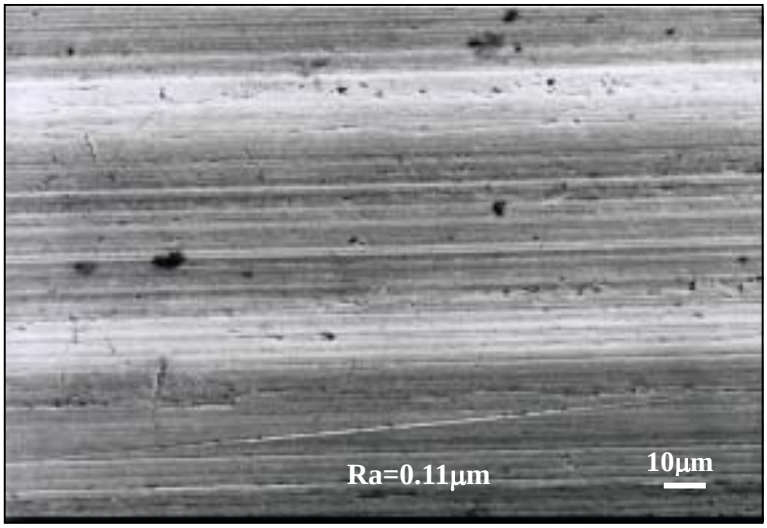

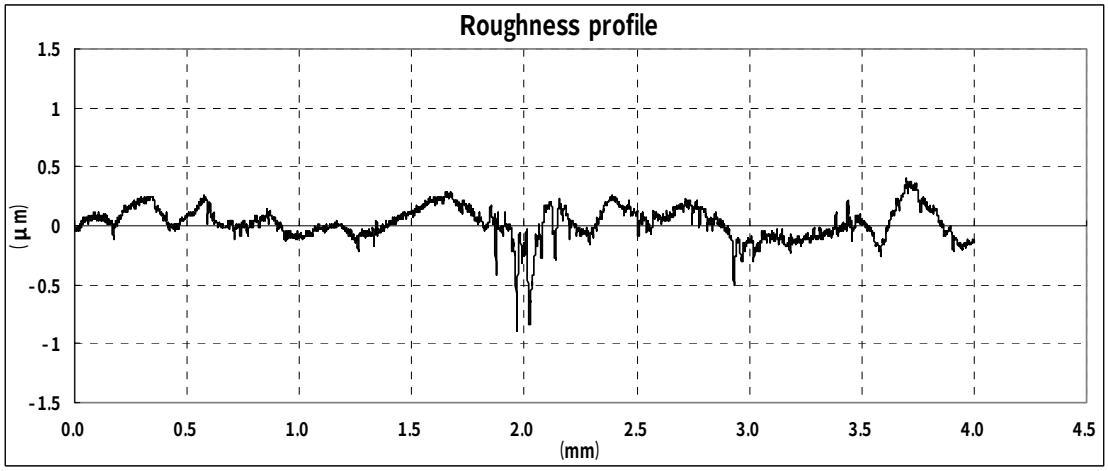

Fig. 4.1a CS photo and roughness profile

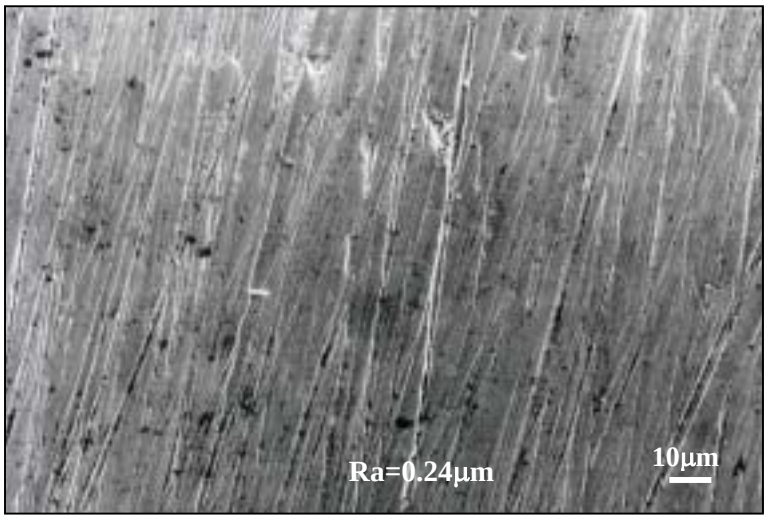

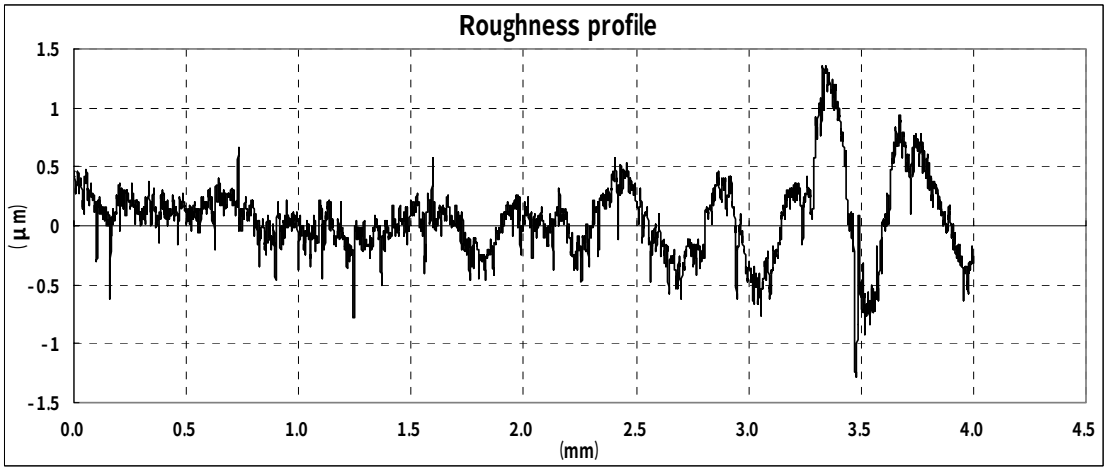

Fig. 4.1b RS photo and roughness profile

4.3 Previous work on CHF for the test cylinders with different surface condition in water

4.3.1 Steady-state CHF for the horizontal cylinders with different surface roughness

The CHF data measured using the roughly-finished surface (RS) and heater surface like mirror (MS) cylinders for subcoolings at pressures were compared with the corresponding CHFs using a horizontal cylinder with commercially-available surface (CS) by Sakurai and Fukuda (2002). It was concluded that the CHFs resulting from the HI and the HSN have the different effects of the surface condition. There existed the CHFs resulting from the HI measured for the horizontal cylinders with CS, RS and MS for lower subcoolings at lower pressures; the CHFs almost agree with one another at the same subcooling independently of the surface conditions. The CHFs resulting from the HSN for the MS cylinder were extremely lower than the corresponding CHFs for CS and RS cylinders at higher pressures. They also mentioned that the effect of the surface energy measured by contact angle which is the another aspect of surface condition different from surface roughness, on the CHFs resulting from the HI and HSN have got to be considered.

4.3.2 Effect of surface conditions on transient CHFs in water

The results of the CHF values, q_{cr}, for $Q=Q_0 exp^{t/\tau}$ with the periods, τ, ranging from 20 s down to 5 ms for saturated water at the pressures of 101.3 and 494 kPa, and for the subcooling, ΔT_{sub}, of 60 K at the pressure of 494 kPa obtained for the cylinder with CS are shown in Fig. 4.2. The q_{cr} values for saturated conditions at the pressure of 101.3

kPa for the cylinder with RS derived by Fukuda et al. (2000, 2004), are also shown in the figure for comparison. The q_{cr} values for all period at pressure of 101.3 kPa increase up to the maximum q_{cr} first, then decrease down to the minimum q_{cr} and again increase with the decreases in period. They are clearly separated into three groups; the first, second and third groups of q_{cr} are for the long periods, for the short and the intermediate tested here as shown in the figure. On the other hand, the second groups of q_{cr} for the saturated and subcooled conditions at the pressure of 494 kPa are not observed as shown in Fig. 4.2.

As mentioned before, Fukuda et al. (1995) suggested the several empirical equations representing transient CHF values versus periods belonging to the first and second groups in a pool of water for wide range of subcoolings and pressures. The CHF belonging to the first group caused by the heat inputs with a long period under a lower subcooled condition and a higher subcooled one is expressed by the Eq. (3.8) and Eq. (3.9), respectively. The CHF belonging to the second group with a short period is expressed by the Eq. (3.10). The q_{cr} values for the periods belonging to the first group at the saturated pressures of 101.3 and 494 kPa are well expressed by Eq. (3.8) which represents the CHF due to the HI, also those for the cylinder with CS and RS at the pressure of 101.3 kPa almost agreed with each other as shown in the figure. The q_{cr} values for the subcooling of 60 K at the pressure of 494 kPa are well expressed by Eq. (3.9) which represents the CHF due to the HSN as mentioned before, so they occur due to the explosive-like HSN at the lower limit of HSN surface superheat though the nucleate boiling due to active cavities on fully-developed nucleate boiling (FDNB) coexist.

According to Fukuda et al. (2000, 2004) research, the three groups of the CHFs for the periods in a pool of water were clearly observed for the cylinder with RS, though the CHFs for short periods belonging to the second group expressed by Eq. (3.10) were not

observed for the cylinder with CS except those for the saturated condition at around atmospheric pressure. And the CHFs for longer periods at low and high subcoolings belonging to the first group obtained for the cylinder with RS at pressures higher than around 400 kPa were expressed by Eq. (3.8) representing the CHF due to the HI and Eq. (3.9) representing the CHF due to the HSN respectively. Those agreed corresponding with those obtained for the cylinder with CS. As shown in the Fig. 4.2, the second group does not appear for CS cylinder at the pressure of 494 kPa even during a shortest period test here. The reason is assumed that cavity contribution to vapor forming are more than RS cylinder, so that the heat flux slight increases with insufficient nucleate boiling. It can be supposed that the direct transitions belonging to the second group occur for the periods shorter than about 1 ms at the pressure of 494 kPa in water.

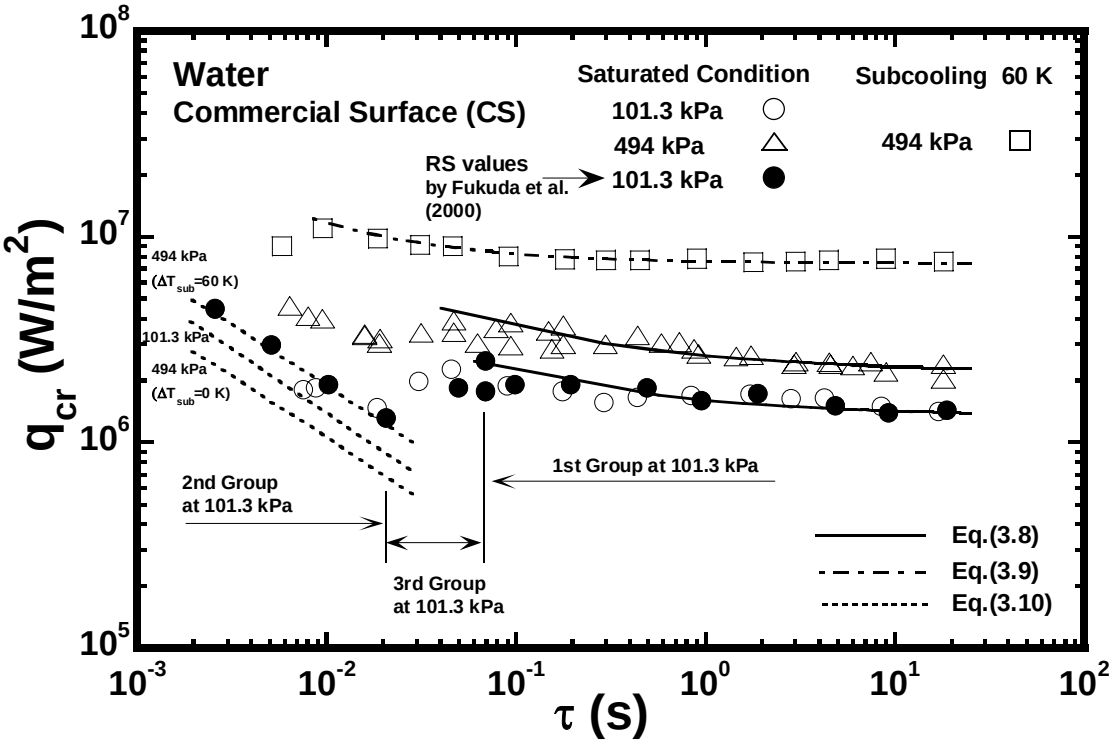

Fig. 4.2 The relation between q_{cr} and τ at pressures of 101.3 and 494 kPa for the cylinder with CS in water.

4.4 CHF for the test cylinders with different surface roughness in boiling liquids except water

4.4.1 Trend of heat transfer processes for different surface conditions in ethanol

Figures 4.3 and 4.4 show the transient phenomenon at a pressure of 494 kPa for subcoolings of 0 K and 40 K in ethanol on a graph of heat flux, q, versus surface superheat, ΔT_{sat}, defined by the difference between heater surface temperature and saturation temperature corresponding to the system pressure. The steady-state natural convection curve derived by Takeuchi et al. (1995), the heat conduction heat transfer curve derived by Sakurai et al. (1977) and the steady-state film boiling curve derived by Sakurai et al. (1990), are also shown in the figure for comparison.

The boiling processes caused by a steadily increasing heat input with a period of 8.1 s are as follows: heat flux, q, increases along the natural convection curve at first and after the occurrence of initial boiling, the surface superheat rapidly decreases, and q increases along the fully-developed nucleate boiling (FDNB) regime and reaches the CHF point, q_{cr}, and then the transition to film boiling occurs. On the other hand, the boiling processes caused by an exponentially increasing heat input with a period of 30 ms, show that the q value increases along the transient conduction heat transfer curve, and a directly transition to film boiling without nucleate boiling occurs. As suggested by Fukuda et al. (1995) and Sakurai et al. (1995), the transition processes are divided into several groups and the transient CHFs caused by increasing heat inputs in a pool of water depend on the periods, the processes are divided into two principal groups. The CHF belonging to the first group with longer periods occurs with a FDNB heat transfer process. At the second group with shorter periods, the direct transition to film boiling occurs with explosive-like boiling from non-boiling. As shown in the figure, the boiling

process with a period of 8.1 s belongs to the first group and the one with a period of 30 ms belongs to the second group. In addition, although it is not shown in this figure, it could be also observed the third group with an intermediate period between the first and the second group. In the case of the boiling process with a period of 30 ms, it is considered that the direct boiling transition on the heater surface from non-boiling to film boiling is due to the heterogeneous spontaneous nucleation (HSN) in previously flooded cavities on heater surface as suggested by Sakurai et al. (1995).

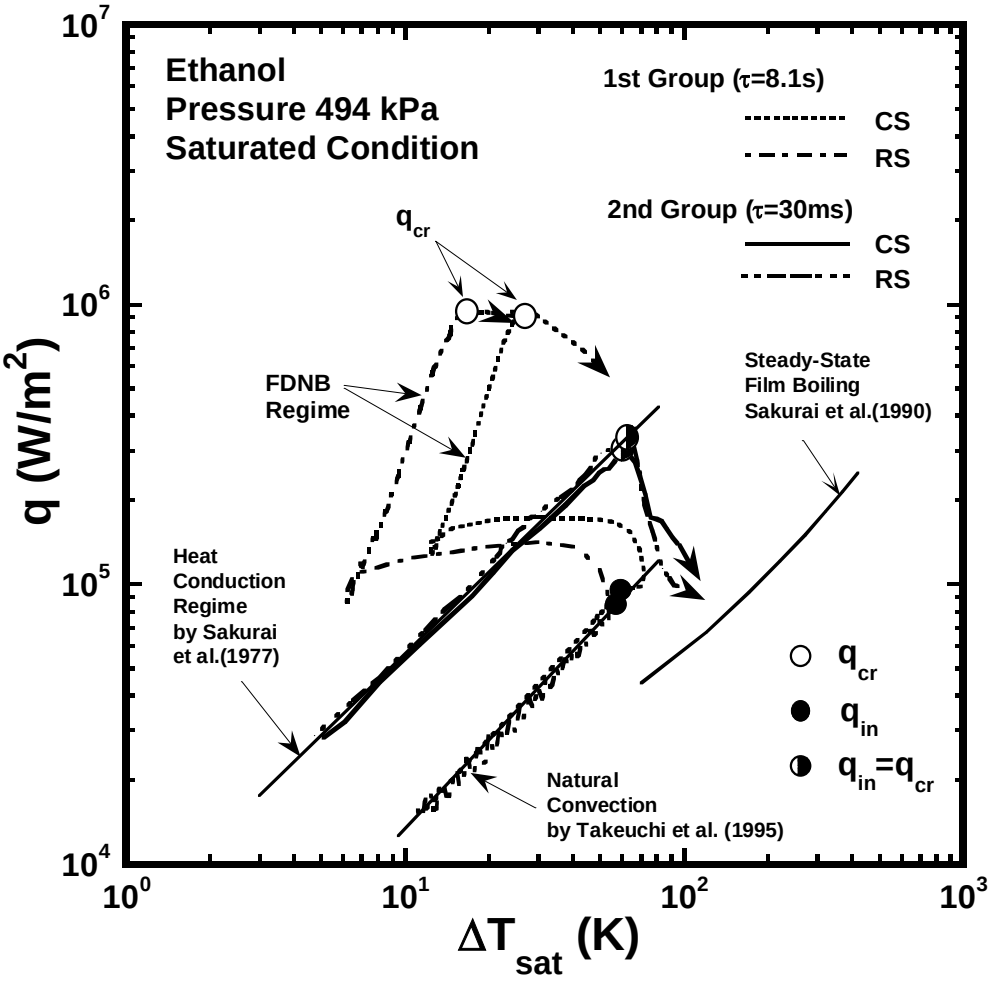

Fig. 4.3 Boiling heat transfer processes for various surface conditions from non-boiling to film boiling or to fully-developed nucleate boiling under saturated ethanol at a pressure of 494 kPa.

As shown in the figures, boiling initiation heat fluxes, q_{in}, are different according to the periods for an exponential heat input with time, but initial boiling surface superheat at that time doesn't so much affected by the surface conditions such as CS and RS of test cylinder. The critical heat fluxes, q_{cr}, belonging to the first group are almost same each other, and q_{cr}, belonging to the second group are almost same also though the values for the RS cylinder are slightly high compared with that for the cylinder with CS. Also in the case of the first group, it can be seen to that the curves for the test cylinder with RS

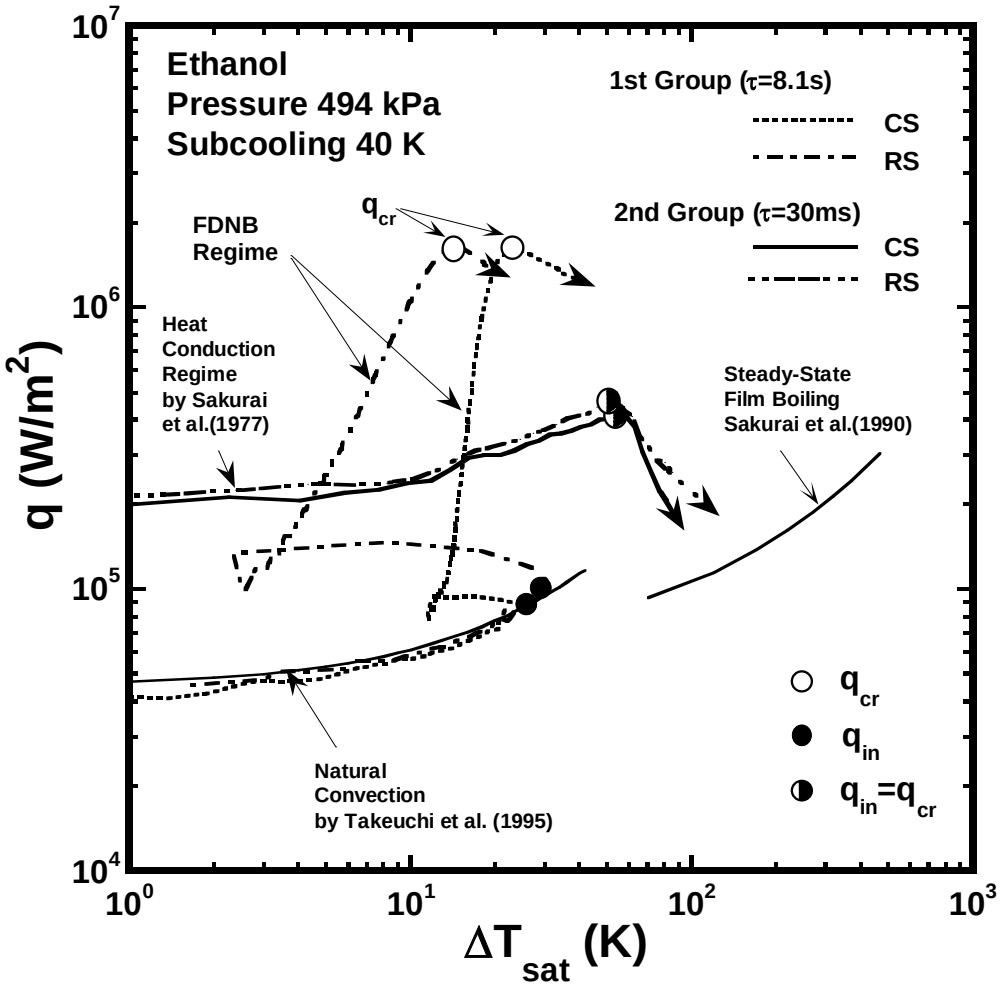

Fig. 4.4 Boiling heat transfer processes for various surface conditions from non-boiling to film boiling or to fully-developed nucleate boiling at a pressure of 494 kPa for subcooling of 40 K.

move to the lower surface superheat side than those for the cylinder with CS in the FDNB regime. At the points of boiling initiation belonging to the first group, a large vapor tube is rapidly formed around each cylinder similar to that of boiling initiation belonging to the second group, then the vapor tubes collapsed rapidly, and large vapor bubbles broke away from the cylinder surface. After the detachment of the vapor bubbles, nucleate boiling from the active cavities entraining vapor occurred with a decrease in surface superheat down to that of the FDNB regime.

After all, the critical heat fluxes, q_{cr}, and boiling initiation heat fluxes, q_{in}, obtained for the cylinder with CS are similar to those obtained for the cylinder with RS according to above test conditions, though the transition processes to film boiling becomes completely different due to the exponentially increasing heat inputs with the period.

4.4.2 Effect of surface condition on steady-state CHFs for wide range of subcoolings and pressures

The subcooled pool boiling CHFs in ethanol were measured using the horizontal cylinders with commercial and rough surfaces for the subcoolings up to about 160 K at the pressures from 0.1 to 2 MPa respectively. As shown in the Fig. 4.5, the CHF data measured for the RS cylinder were compared with the corresponding CHFs for the cylinder with CS. The CHFs measured using the RS and CS cylinders clearly agreed with each other for subcoolings from zero to 20 K at pressures. It is confirmed that the CHFs for low subcoolings at pressures have not the effect of cylinder surface condition. In the case of the subcooling higher than 40 K, the CHFs measured for the CS cylinder almost agree with that of RS one, though the CHF data for the rough cylinder at some pressures are slightly larger than that of the CS cylinder. Moreover, in the range of subcooling higher than 120 K, the CHF data become constant to an asymptotic value

with an increase in subcooling. The reason why the $q_{cr,sub}$ becomes constant for the subcoolings higher than a certain subcooling with an increase in subcooling for both cylinders needs further consideration in detail.

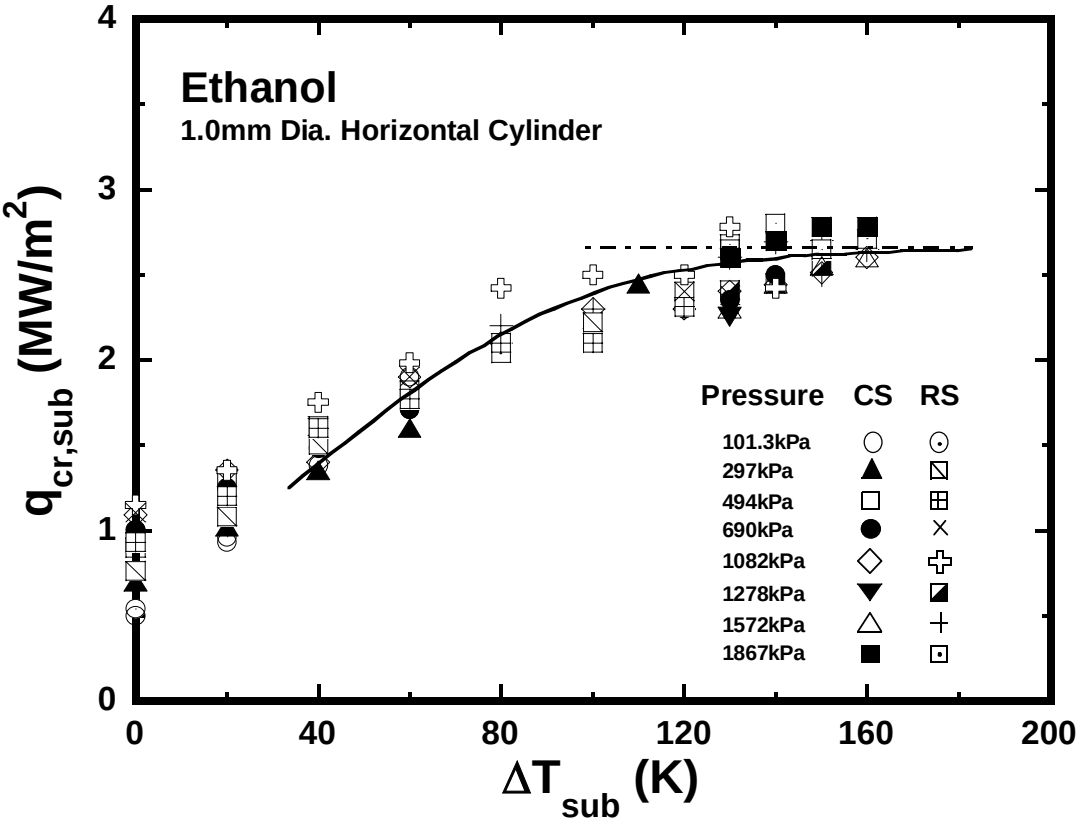

Fig. 4.5 The relation between steady-state $q_{cr,sub}$ and subcooling for surface conditions with RS and CS.

Figure 4.6 shows steady-state CHF versus subcooling measured using 1.0 mm diameter CS and RS at pressures of 886 and 1278 kPa in FC-72 with the corresponding HSN curves derived from Eq. (3.7). The CHF data gradually increase with an increase in subcooling, also they are dependent on pressure for the subcooling over the range from 20 to 140 K except the saturated condition. As shown at pressure of 1278 kPa with the corresponding HSN curves for the cylinders with CS and RS, the experimental data slightly depending on the cylinder surface conditions agree well with the corresponding

predicted values. The CHFs slightly depending on the cylinder surface conditions for the subcooling are shown at a pressure of 886 kPa also.

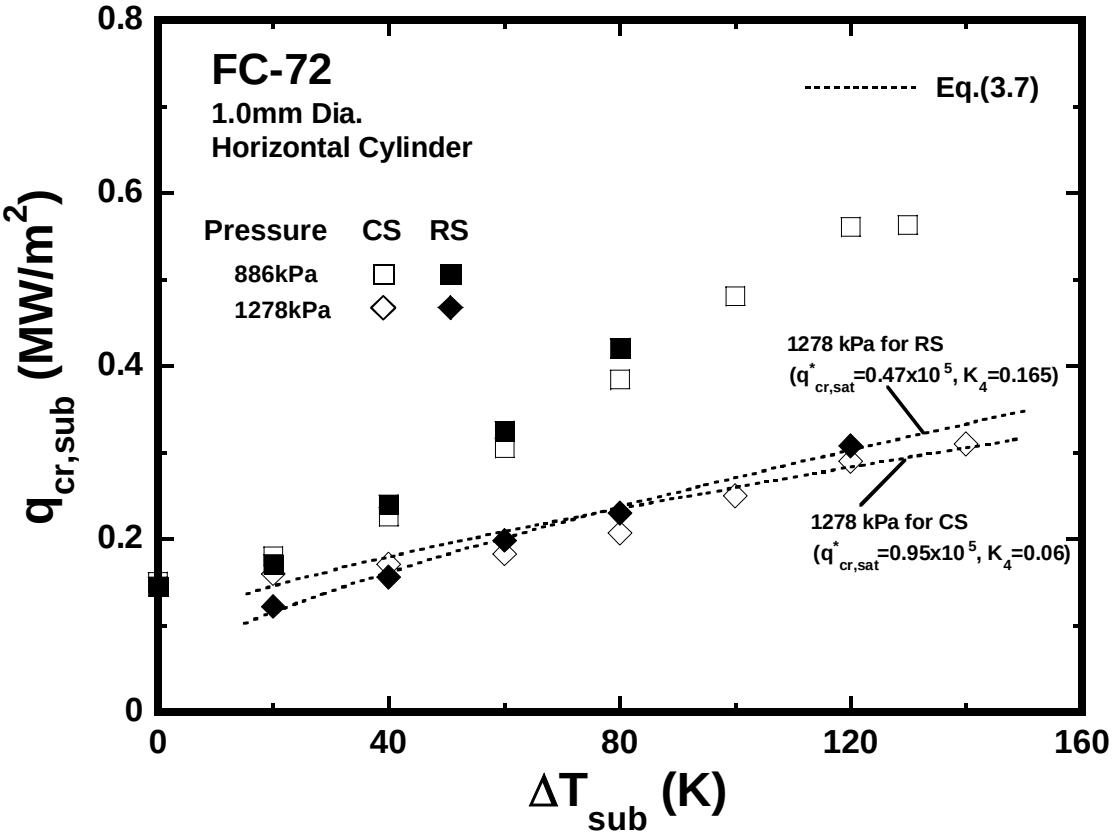

Fig. 4.6 The Comparison of prediction with $q_{cr,sub}$ for the subcooling measured by cylinders with CS and RS at pressures of 886 and 1278 kPa in FC-72 using Eq. (3.7).

4.4.3 Effect of surface condition on transient CHFs at various pressures in ethanol

Figures 4.7 and 4.8 show transient CHFs, q_{cr} versus periods, τ, ranging from around 50 s down to 5 ms under saturated ethanol at various pressures, and for the liquid subcooling of 60 K at the pressure of 494 kPa on the cylinders with CS and RS, respectively. The trend of q_{cr} values related to periods for the cylinder with CS and RS

are clearly divided into three groups as shown in the figures. The first group is shown with a solid and dashed chain lines, and the second group is shown with a dashed line. Besides this, the third group with an intermediate period between the first and second groups can be observed as shown in the figures. The q_{cr} values belonging to the first group for periods at saturated pressures for cylinders with CS and RS are expressed by Eq. (3.8) that represents the CHF due to the HI depending on pressures, and those at a pressure of 494 kPa for the subcooling of 60 K were expressed by Eq. (3.9) that represents the CHF due to the HSN mentioned before. The curves of the q_{cr} for the periods for the cylinder with CS and RS almost agree with each other.

On the other hand, the q_{cr} values for a shorter period of 100 ms belonging to the second group were approximately expressed by Eq. (3.10), though the q_{cr} values for RS

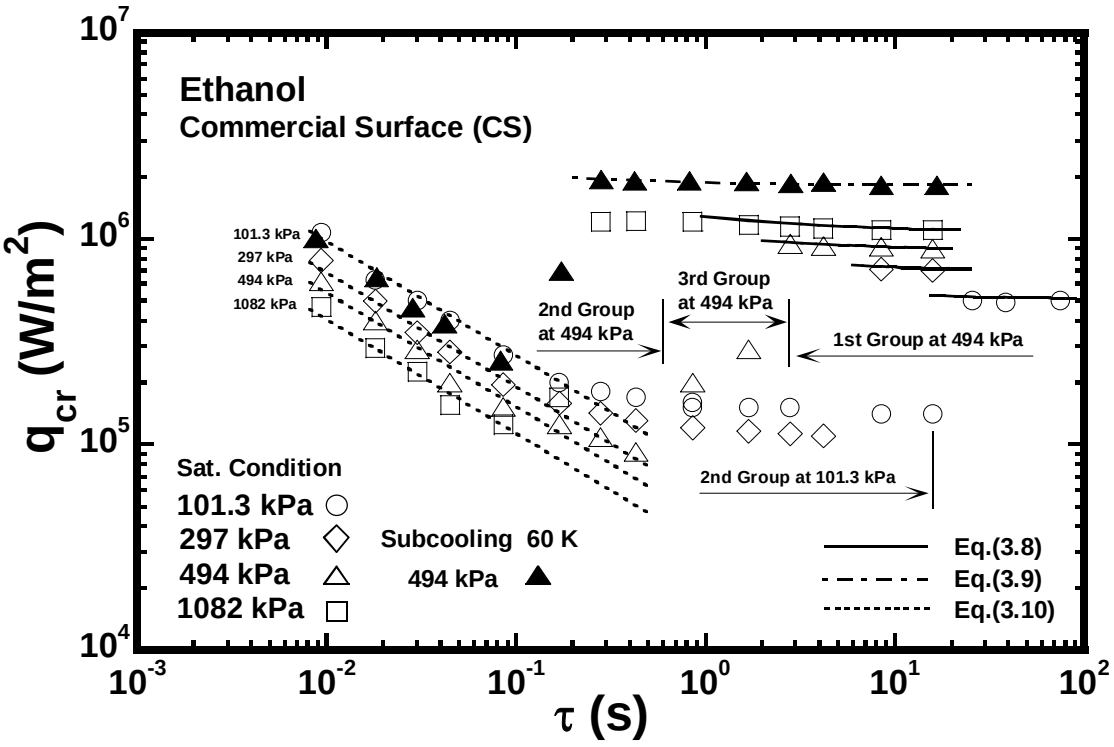

Fig. 4.7 The relation between q_{cr} and τ at pressures of 101.3, 297, 494 and 1082kPa for the cylinder with CS in ethanol.

cylinder existed at slightly higher than CS cylinder. In addition, the q_{cr} values decrease with an increase in pressure with a fixed period because the lower limit of HSN surface superheat decreases with an increase in pressure (Sakurai et al., 1995). The q_{cr} values also increase with a decrease in period. The direct or semi-direct transitions at the CHF occurs from non-boiling regime to film boiling without or with the heat flux increase for a short period of time, and the minimum q_{cr} values for the longest period for the second group at each pressure are much lower than the corresponding steady-state CHF. The minimum q_{cr} values obtained for CS cylinder disagree with those obtained for RS cylinder. A range of period for third group q_{cr} for the cylinder with RS becomes narrow in comparison with that for the cylinder with CS. As a result, a range of period for the second group q_{cr} becomes wider in a range of period. In the case of RS cylinder, a fini-

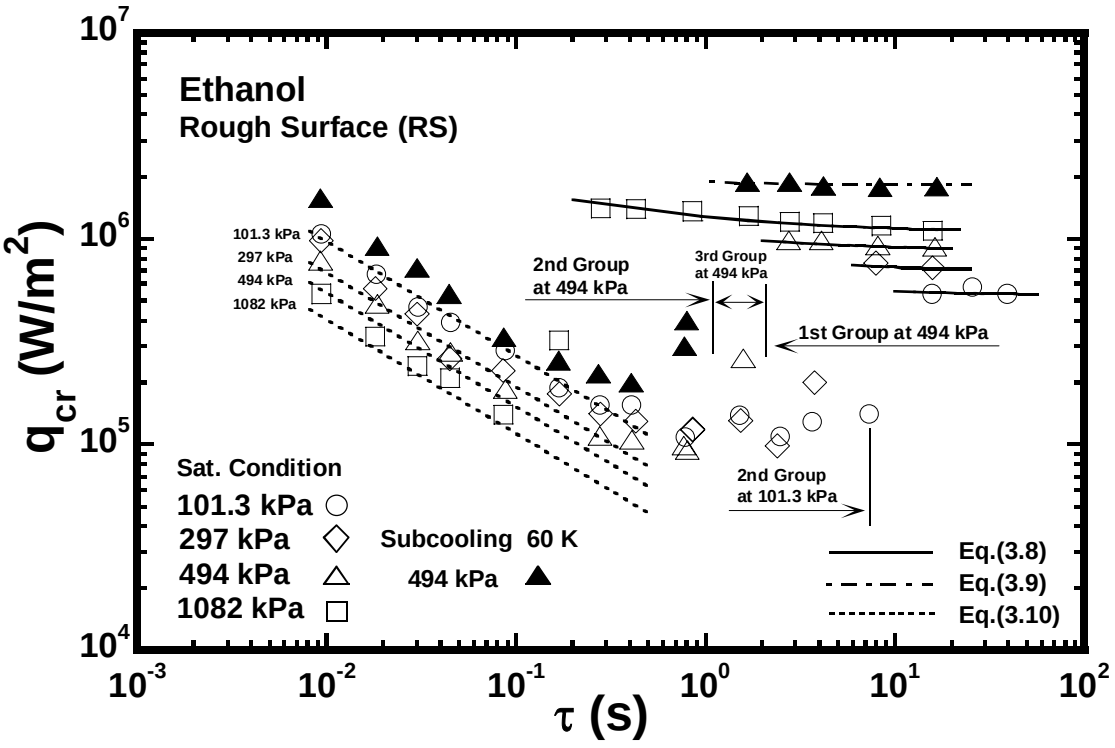

Fig. 4.8 The relation between q_{cr} and τ at pressures of 101.3, 297, 494 and 1082kPa for the cylinder with RS in ethanol.

shed treatment by emery paper was done to eliminate cavity contribution to vapor forming. Therefore it is difficult to occur the initial boiling then could result in the direct boiling transition from non-boiling to film boiling due to HSN. Consequently, the q_{cr} values belonging to the second and third group are considerably affected by the surface conditions.

4.4.4 Effect of surface conditions on the CHFs at various pressures for subcooled condition in ethanol

The q_{cr} values versus the periods for a subcoolings of 60 and 120 K at the pressures ranged from 494 to 1082 kPa for cylinders with CS and RS are shown in Figs. 4.9 and 4.10, respectively. As seen in the figures, the CHF values are clearly divided into three principal groups depending on the periods. The q_{cr} values belonging to the first group with a period longer than around 1 s were expressed by Eq. (3.9) representing the CHF due to HSN even for the steady-state one. The curves of the q_{cr} versus periods for cylinders with CS and RS almost agreed with each other. However, it is almost independent of pressure. The steady-state CHFs values for high subcooling at the pressures are also independent of the pressures. Sakurai et al. (1995) have explained this fact by assuming that the transition to film boiling at the steady-state CHF occurs due to explosive-like HSN in FDNB regime as mentioned before. On the other hand, the q_{cr} values belonging to the second group with a period shorter than around 0.1 s were approximately expressed by Eq. (3.10) as shown in the figure. They are also independent of pressure. In the case of the subcooling of 60 K at a pressure of 494 kPa in the Fig. 4.9, the minimum q_{cr} values for periods of around 100 ms for a cylinder with CS and around 400 ms for a cylinder with RS are observed, respectively. Therefore, a range in period for the second group CHF for RS cylinder becomes wide in comparison with that

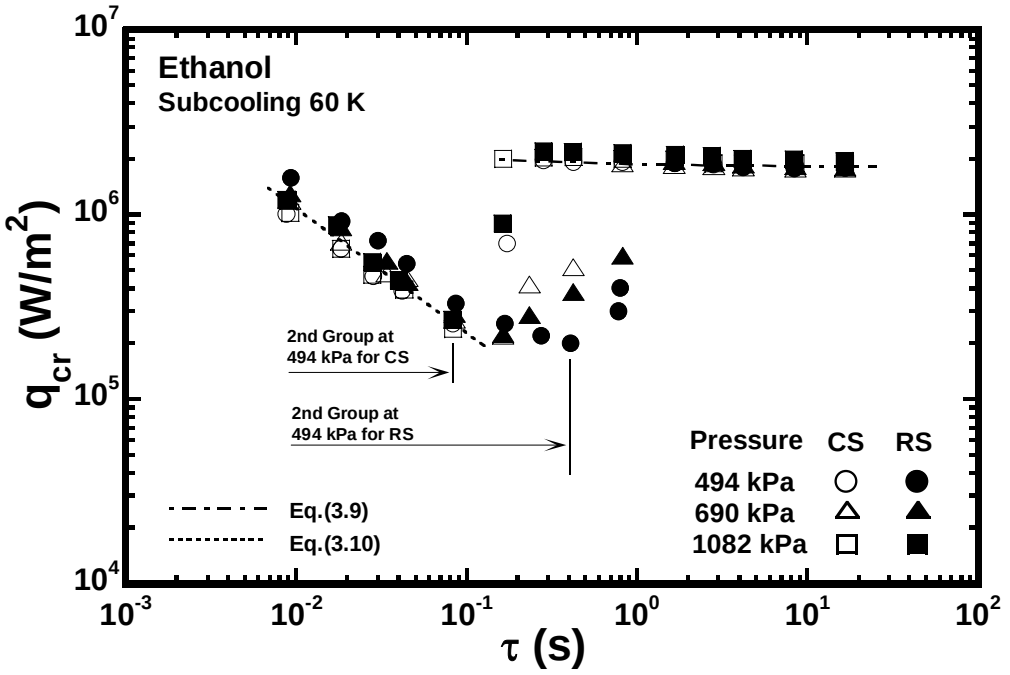

Fig. 4.9 The relation between q_{cr} and τ for subcooling of 60 K at various pressures for the cylinders with CS and RS in ethanol.

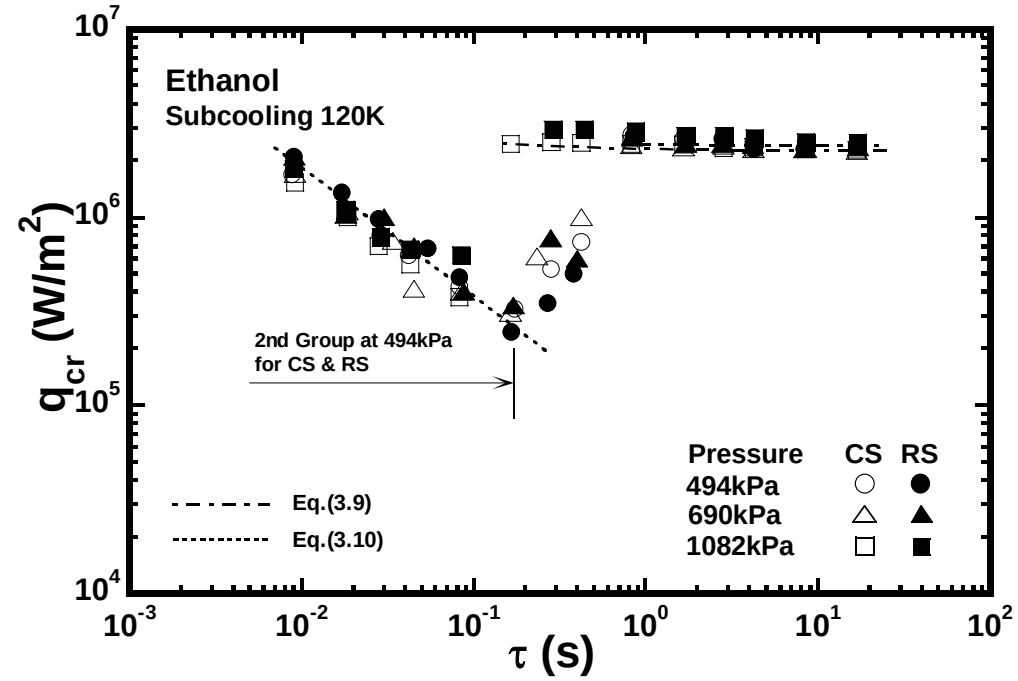

Fig. 4.10 The relation between q_{cr} and τ for subcooling of 120 K at various pressures for the cylinders with CS and RS in ethanol.

of a CS cylinder within range in period tested here. It should be noted that the minimum q_{cr} under the pressure of 494 kPa in the Fig. 4.9 is observed about 14% of the corresponding steady-state CHF for the cylinder with CS, and about 11% of the corresponding steady-state CHF for a cylinder with RS. In the case of the subcooling of 120 K in the Fig. 4.10, a range in period for the second group CHF for RS and RS cylinders are not different from each other tested here. The ratio of minimum CHF to steady state one for the CS cylinder is same with that of subcooling of 60 K as well as the RS cylinder. As a result, it is observed that the trend of CHFs for period belonging to the second group is affected by the cylinder surface conditions.

4.4.5 Effect of surface conditions on CHFs for various subcoolings at a pressure of 494 kPa in FC-72

The q_{cr} versus periods ranged from 20 s down to 5 ms for a cylinder with CS at a pressure of 494 kPa for subcoolings of 20, 40 and 60 K in a pool of FC-72 are shown in Fig. 4.11 in comparison with those for a cylinder with RS. The trend of q_{cr} values versus periods for each cylinder is clearly divided into three groups similar to ethanol. The q_{cr} values are well dependent on subcooling. Those belonging to the first group for cylinders with CS and RS become almost same with each other as it becomes longer in period, and are expressed by Eq. (3.9). On the other hand, the q_{cr} values for short periods belonging to the second group for each cylinder are approximately expressed by Eq. (3.10), though the q_{cr} values for cylinders with RS become slightly higher with a decrease in period compared with that for a cylinder with CS.

The q_{cr} values in relation to periods gradually increase with a decrease in period up to a maximum q_{cr} from a corresponding steady-state q_{cr} for a period of 20 s, then decreases down to a minimum q_{cr}. Here, q_{cr} of CS cylinder for a range in period of the first group

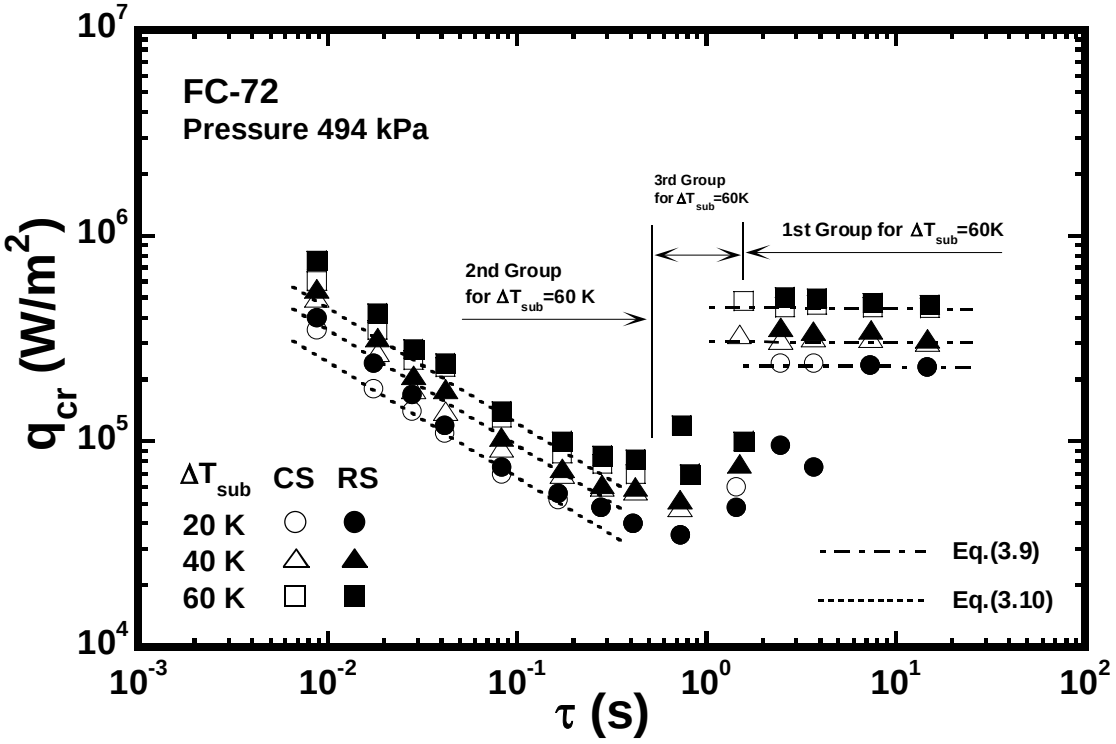

Fig. 4.11 The relation between q_{cr} and τ for various subcoolings at a pressure of 494 kPa for the cylinders with CS and RS in FC-72.

becomes wider in comparison with that for RS cylinder. In other words, the transition from the first group to the second group for RS cylinder occurs at longer period than that for CS cylinder. It means that a range in period for q_{cr} of the second group becomes wider. Consequently, it should be noted that there exists an effect of surface condition on the CHF belonging to the second and third groups similar to ethanol.

Figure 4.12 shows the q_{cr} versus τ for a cylinder with CS at pressures of 101.3, 297, 494 and 886 kPa in saturated FC-72 in comparison with those for a cylinder with RS represented by (a), (b), (c) and (d), respectively. In the case of the Fig. 4.12 (a), the pressure of 101.3 kPa, it should considered that the q_{cr} values for the periods longer than 1 s show completely different from each other depending on the surface condition: the values for the CS cylinder is the one from occurrence of FDNB in the natural convection regime, therefore they are considerably higher than that for the RS cylinder which

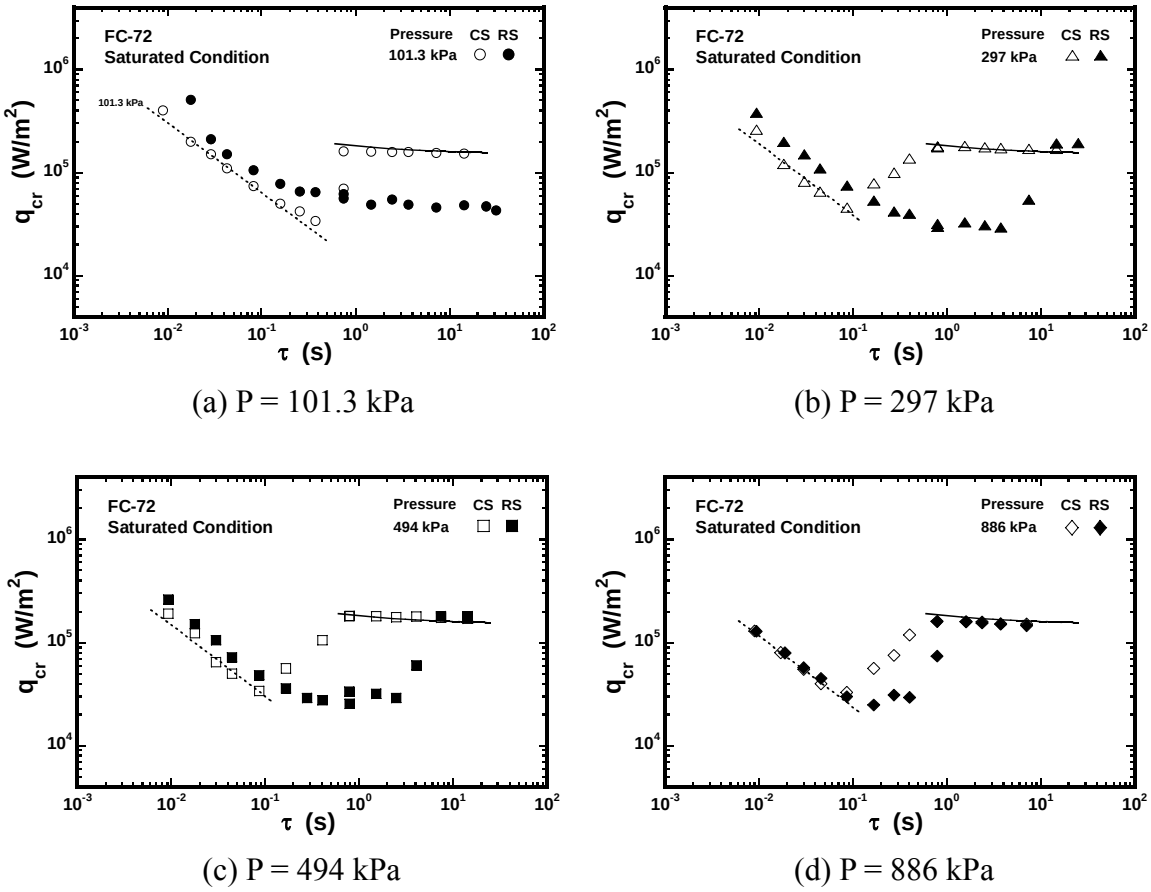

(a) P = 101.3 kPa (b) P = 297 kPa

(c) P = 494 kPa (d) P = 886 kPa

Fig. 4.12 The relation between q_{cr} and τ at various pressures for the cylinders with CS and RS in saturated FC-72.

direct transition occurs for all the periods. It can be supposed for the RS cylinder that the transitions to FDNB occur for the periods much longer than around 30 s. In the case of the pressures of 297, 494 and 886 kPa shown with Fig. 4.12 (b), (c) and (d), the q_{cr} values for longer period belonging to the first group for cylinders with CS and RS are almost same with each other as it becomes longer in period. On the other hand, the q_{cr} values for short periods belonging to the second group for the cylinder with RS are same or slightly higher compared with that for the cylinder with CS. It should be noted that the transition from the first group to the second group for RS cylinder occurs at longer period than that for CS cylinder. It means that a range in period for q_{cr} of the

second group becomes wider. The periods at the minimum q_{cr} within the second group for the RS cylinder are as follows: 30 s at (a), 4 s at (b), 0.8 s at (c) and 0.2 s at (d). It means those are considerably affected by the surface condition on the CHF belonging to the second and third groups. It is suggested that more study on the effects of surface conditions such as the cavity size distribution and surface energy on the CHF is necessary.

4.5 Summary

This work is to find the mechanism in the transient boiling CHF, which is confirmed that it depends on the HI and HSN. It is clarified that there exist two different CHF mechanisms related to the period, and the CHF for the shorter periods is affected by the cylinder surface conditions in highly wetting liquids such as ethanol and FC-72. And of course this, the CHFs belonging to the first group with the longer period are also classified into two mechanisms depending on the lower and higher subcooling, and it is assumed that the CHFs measured are not affected with the surface roughness tested here. It is suggested that more study on the diverse surface conditions such as the cavity size distribution and surface energy on the CHF is necessary for a wider range of subcoolings and pressures. The results are as follows.

(1) The effect of surface condition on steady-state CHFs for wide range of subcoolings and pressures was investigated. The CHFs measured for the CS cylinder almost agreed with that of RS one though the data for the rough cylinder at some pressures were slightly larger than that of the CS cylinder.

(2) The transient CHFs are clearly existed into three groups in ethanol and FC-72 for the cylinders with CS and RS, though the values for the shorter periods belonging to the second group for the cylinder with CS were not observed in the case of water

tested here except those for the saturated condition at around atmospheric pressure.

(3) The transient CHFs belonging to the first group for longer periods at lower and higher subcoolings at the pressure tested obtained for the cylinder with RS, expressed by Eq. (3.8) representing CHF due to the HI, and Eq. (3.9) representing CHF due to the HSN, respectively, are similar to those obtained for the cylinder with CS. On the other hand, the second groups of CHFs for the shorter periods for each cylinder are approximately expressed by Eq. (3.10) which gives the theoretical conduction heat flux corresponding to a short period at the corresponding HSN surface superheat depending on the period, though the CHF values for RS cylinder existed at slightly higher than the CS cylinder.

(4) The period range of the third group CHF for the cylinder with RS became narrow in comparison with that for the cylinder with CS. As a result, the period range of the second group CHF became wide in the range of the periods. The minimum CHF values for the longest period for the second group at each pressure were much lower than the corresponding steady-state CHF, and the minimum CHF values obtained for CS cylinder disagreed with those obtained for RS cylinder. Consequently, the CHF values belonging to the second and third group were considerably affected by the surface conditions.

5. Photographic Study on Transient Phenomena in Pool Boiling CHF for Various Liquids

5.1 Introduction

The correct understanding and prediction of the transient critical heat fluxes (CHFs) for various test heater configurations and surface conditions in water and wetting liquids such as FC fluids (Fluorinert liquid), liquid nitrogen and liquid helium I, etc. are becoming increasingly important as the fundamental database for the design such as the high heat flux cooling systems using subcooled water pool boiling and for the safety assessment of nuclear reactor accidents caused by a power burst, and so on. Furthermore, the evaluation of the pool boiling CHF becomes an essential problem when the liquid flow in the cooling equipment stops due to accidents.

The anomalous trend of CHFs caused by an exponential heat inputs, $Q_0 exp^{t/\tau}$, for period, τ, that the CHF up to a maximum one, and then it decreases down to a minimum CHF and finally again increases with a decrease in period, has been observed many years ago by Sakurai and Shiotsu (1974, 1977) in a pool a water. The CHFs for the shorter periods at which direct or semi-direct transitions to film boiling occurred in transient conduction regime due to a quasi-steadily increasing or increasing heat input for the liquids including water. A direct transition from non-boiling convective regime to film boiling one was reported by Avksentyuk and Mamontova (1973) and Kutateladze et al. (1973) in liquid metals and wetting liquids as some peculiarities of CHF. However, the CHF mechanism of CHFs for the heat inputs with shorter periods remained unresolved for a long time.

The direct transition from a non-boiling regime such as natural convection and transient conduction regimes to film boiling without nucleate boiling was observed by

Sakurai et al. (1992, 1993). They carried out the experiments of the CHFs for the heat inputs with various periods on a platinum horizontal cylinder in liquid nitrogen at various pressures, and found that direct transition to film boiling occurred in transient conduction regime. It was assumed that the transitions occurred due to the levitation of liquid on the cylinder surface by the explosive-like heterogeneous spontaneous nucleation (HSN) in originally flooded cavities without the contribution of the active cavities entraining vapors for boiling incipience. All the cavities on the surface that could serve as nucleation sites would initially be flooded since the liquid surface tension is so low that vapor are not entrained in surface cavities and there is no dissolved gas in liquid nitrogen except for possible trace amounts of helium, hydrogen and neon. The explosive-like HSN assumed in originally flooded cavities on a horizontal cylinder in the wetting liquid of liquid nitrogen at which heat transfer crisis occurs was first observed without nucleate boiling under natural convection regime at atmospheric pressure due to steadily increasing heat input at a certain HSN surface superheat which is considerably lower than the corresponding the HSN on a flat surface and the homogeneous spontaneous nucleation at surface superheats theoretically obtained. They carried out the water experiment at wide range of pressures and subcoolings. They assumed that the heat transfer crisis at CHF for the short periods also occur mainly due to the HSN in initially flooded cavities though the vapor bubbles from the active cavities coexist with those due to the HSN; the bubbles from active cavities lead to the occurrence of the HSN at lower surface superheat because of the decrease of surface superheat increasing rate due to the increase of heat transfer by the bubbles growing in the liquid on the surface at near CHF due to the HSN.

It was confirmed the transition mechanism to film boiling by a photographic study on the vapor bubble and vapor film behavior on the cylinder surface by Sakurai et al. (2000). They concluded by the photographs that the semi-direct transition from

conduction regime to film boiling with nucleate boiling due to the rapidly increasing heat inputs in water occurs due to Heterogeneous Spontaneous Nucleation (HSN) in originally flooded cavities with or without nucleate boiling at around the lower limit of HSN surface superheat. Fukuda et al. (2004) investigated the effect of the surface conditions of the platinum horizontal test cylinders with two different surface conditions in a pool of saturated and subcooled water at various pressures. As the result, it was confirmed that the photographs of vapor bubbles and film behavior during transitions to film boiling in water for the cylinders with various surfaces were not different with each other not only for quasi-steadily increasing heat input but also for rapidly increasing one. However, the boiling heat transfer phenomenon is significantly affected by the surface tension of the liquid and the wettability on the heater surface but the mechanism has not been clarified yet.

The purpose of this work is to make clear the transition phenomena to film boiling in several liquids having different wettability by the photographic approach on the vapor bubble and vapor film behavior on the cylinder surface by using a high-speed video camera.

5.2 Experimental conditions

Boiling heat transfer processes on a test heater in a pool of water, ethanol or FC-72 with different mechanisms due to exponentially increasing heat generation rate, $Q=Q_0 exp^{t/\tau}$, ranging from quasi-steadily increasing one to rapidly increasing one with periods, τ, ranging from around 50 s to 5 ms were measured for a 1.0-mm diameter horizontal cylinder made of platinum wire at pressures ranging from 101.3 to 1867 kPa for liquid subcoolings over the ranges from 0 to 160 K at pressures. A high-speed video camera system (1000 frames/s with a rotary shutter exposure of 1/10000 s) was used to

observe the boiling phenomena and to confirm the start of simultaneous boiling on the test heater surface. Experimental apparatus and method were already shown in Chapter 2 in detail.

5.3 Previous work on boiling heat transfer processes and critical heat fluxes

The CHFs, q_{cr}, for $Q_0 exp^{t/\tau}$ versus the exponential periods, τ, ranging from around 20 s down to 5 ms on a 1.0-mm diameter platinum horizontal cylinder in saturated ethanol at pressures of 101.3 and 494 kPa are shown in Fig. 5.1. At the CHFs for periods tested here at the pressure of 101.3 kPa, direct transitions from non-boiling regime such at natural convection or transient conduction to film boiling occur. The CHF, q_{crD}, at the direct transition agrees with corresponding heat flux of initial boiling, q_{in}. On the other hand, the CHF for the period at the pressure of 494 kPa first gradually increase with a decrease in period up to the maximum CHF from the steady state one corresponding to the CHF for a period of 20 s, and then decrease down to the minimum one at around period of 0.2 s and again increase with a decrease in period. The CHFs measured are separated into the three groups for the periods; first group for the longer period, second group for the shorter and third group for the intermediate. At the CHFs for the short periods belonging to the second group, the direct transitions to film boiling occur: the CHF agrees with the initial heat flux, q_{in}, at the short period. The CHFs for the periods belonging to the first and second groups are well expressed by the following equations, respectively. They are same ones with the Eqs. (3.8) and (3.10).

$$q_{cr} = q_{st,sub}\left(1+0.21\tau^{-0.5}\right), \text{ for first group} \tag{5.1}$$

where the $q_{st,sub}$ is given by the quasi-steady-state CHF data in each experiment.

$$q_{crD} = h_c\left(\Delta T_{in}(\tau)+\Delta T_{sub}\right), \text{ for second group} \tag{5.2}$$

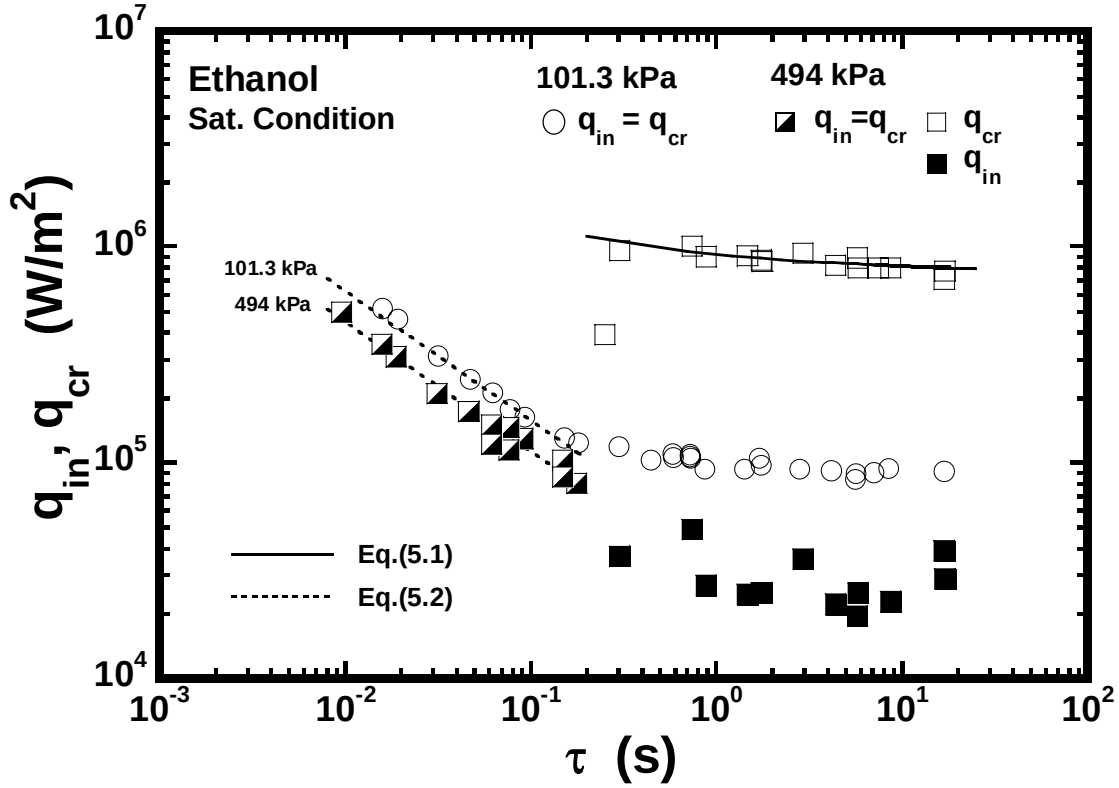

Fig. 5.1 Initial boiling heat flux q_{in}, critical heat flux q_{cr} versus period τ in saturated ethanol at pressures of 101.3 and 494 kPa.

where $h_c = (k_l \rho_l c_{pl} / \tau)^{1/2} K_{1th}(\mu D/2) / K_0(\mu D/2) \cong (k_l \rho_l c_{pl} / \tau)^{1/2}$, and $\mu = [\rho_l c_{pl} / k_l \tau]^{1/2}$. K_o and K_{1th} are the modified Bessel functions of the second kind of zero- and first-orders. h_c is the heat transfer coefficient resulting from transient heat conduction, ΔT_{sub} is liquid subcooling and $\Delta T_{in}(\tau)$ is the initial boiling surface superheat due to the HSN in conduction regime: those depend on the increasing rates of surface superheat, pressures and liquid subcoolings (Sakurai et al., 1992). Eq. (5.1) represents the CHF due to the HI belonging to the first group. Eqs. (5.1) and (5.2) are just the same with corresponding CHFs for water. Therefore, the empirical equations (5.1) and (5.2) are effective for not only water but also the highly wetting liquids such as ethanol and FC-72.

The minimum CHF for the period under the pressure of 494 kPa is observed at around 0.2 s. It should be noted that the value is about 11% of steady-state one corre-

sponding to the CHF for the period of 20 s. As a result, the minimum CHF value within the second group is much lower than the corresponding steady state CHF. This fact means that conduction heat transfer becomes more predominant as the period becomes shorter than natural convection heat transfer. Therefore, the heat transfer coefficient becomes higher due to heat conduction and a direct transition to film boiling occurs at the heat flux point that is higher than that of natural convection.

5.4 Heat transfer processes under saturated condition in water

Typical boiling heat transfer processes due to exponentially increasing heat inputs in water are shown in Fig. 5.2 on a graph of heat flux, q, versus surface superheat, ΔT_{sat}. The surface superheat ΔT_{sat} is defined by the difference between the surface temperature, T_w, of the heater and the saturation temperature, T_{sat}, of liquid corresponding to the system pressure. The steady-state natural convection curve derived by Takeuchi et al. (1995), the heat conduction curve derived by Sakurai et al. (1977) and the steady-state film boiling curve derived by Sakurai et al. (1990) are also shown in the figure for comparison.

The heat transfer processes for periods of 10 s, 1 s, 100 ms and 10 ms at a pressure of 101.3 kPa are shown in the figure. The processes from non-boiling to film boiling are completely different from each other depending on the periods. It can be found that the processes up to initial boiling heat fluxes, q_{in}, are the natural convection regime for periods from 10 s down to around 1 s, and the heat conduction regime for periods from 100 ms down to 10 ms as shown in the figure. It is recognized that the values of initial boiling heat flux, q_{in}, increase with a decrease in period, that is, they depend on the increasing rates of heat inputs, respectively. The CHF values are almost equal to each other for the periods tested here.

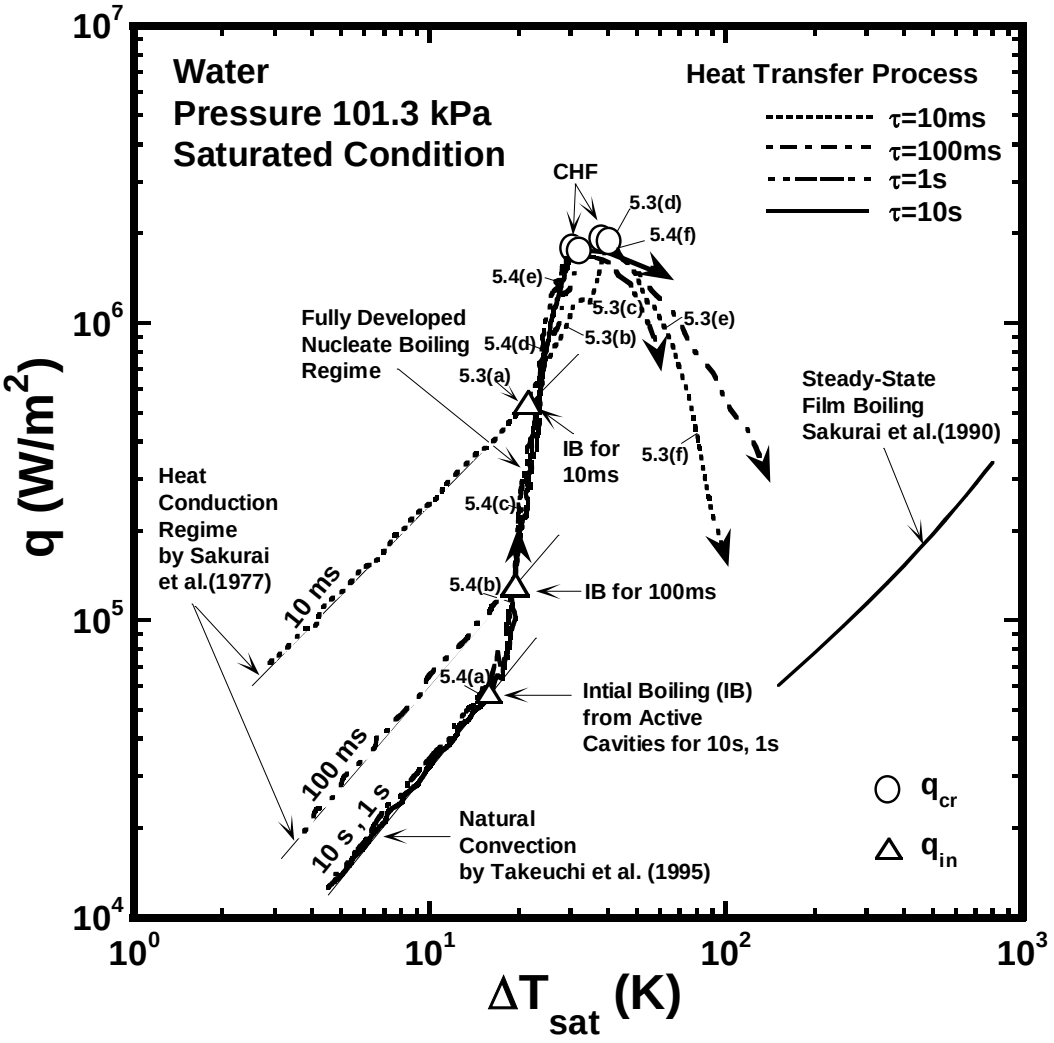

Fig. 5.2 Heat transfer process for periods of 10 ms and 10 s saturated condition at atmospheric pressure in water. Photographs shown in Figs. 5.3 & 5.4 were taken at points of 5.3(a) to (f) and 5.4(a) to (f) on the graph, respectively.

When an exponentially increasing heat input is applied to the heater immersed in the pool of water, the heater surface temperature and the heat flux increased. As shown in the figure, the heat transfer processes up to, q_{in}, show that heat flux, q, for the period of 1 s increases along the natural convection curve together with period of 10 s and natural convection heat transfer becomes predominant. As the period shortens, the heat conduction becomes predominant in heat transfer compared with the natural convection.

5.4.1 Photographs of vapor film behavior during semi-direct transition to film boiling in water

Figure 5.3 shows the semi-direct transition from transient conduction regime to film boiling with nucleate boiling due to a rapidly increasing heat input for the period of 10 ms at the pressure of 101.3 kPa in saturated water. The mechanism of semi-direct transition to film boiling with nucleate boiling from active cavities entrained vapor for the short period occurs finally due to the HSN at around the lower limit of HSN surface superheat in originally flooded cavities observed by Sakurai et al. (1992, 1993). The photographs in Fig. 5.3 are shown to confirm the assumptions. The corresponding points on the heat transfer process curve on the q versus ΔT_{sat} graph for each photograph at the points of 5.3(a) to (f) are shown in Fig. 5.2 with a dashed line. Figure 5.3(a) is the photograph at point 5.3(a), which is the onset of boiling. It shows the cylinder in transient conduction regime with a few initial vapor bubbles. The time, t, beside each photograph shows the elapsed time after the time of first photograph, Fig. 5.3(a). Figure 5.3(b) is the photograph after a time passage of 2 ms from point (a). Figures 5.3(b), 5.3(c) and 5.3(d) show vapor bubbles around the cylinder occurred from active cavities of entrained vapor which cause the rapid increase of heat flux without the detachment of vapor bubbles. The heat flux for Fig. 5.3(d) is around the CHF. A large vapor film covers the cylinder including all the vapor bubbles from active cavities as shown in Fig. 5.3(d). As seen in Fig. 5.3(e), the large vapor film with the Taylor unstable wave on the top of the vapor film moves upward with a decrease in heat flux and an increase in surface superheat. After that, the large vapor bubbles are separated from the vapor film with the approximate interval of the most dangerous Taylor wave length, and levitate in the liquid as seen in Fig. 5.3(f). The heat flux approaches around minimum film boiling heat flux and then increases along the steady-state film boiling heat flux with an

increase in surface superheat.

(f) t=49ms

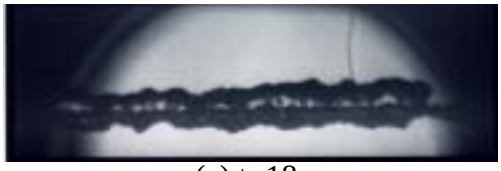

(e) t=18ms

(d) t=9ms

(c) t=5ms

(b) t=2ms

(a) t=0ms

Fig. 5.3 Vapor film behavior during semi-direct transition to film boiling for a period of 10 ms at a pressure of 101.3kPa in saturated water.

(f) t=31.2s

(e) t=28.2s

(d) t=23.6s

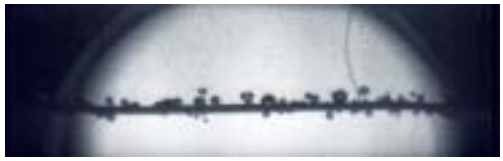

(c) t=12.8s

(b) t=6.8s

(a) t=0s

Fig. 5.4 Vapor film behavior during transition to fully-developed nucleate boiling for a period of 10 s at a pressure of 101.3kPa in saturated water.

5.4.2 Photographs of vapor film behavior during transition to nucleate boiling in water

Figure 5.4 is taken using a high-speed video camera for the vapor behavior on a horizontal cylinder during transition to nucleate boiling due to a slowly increasing heat input for a period of 10 s at a pressure of 101.3 kPa in saturated water. The photographs in the figure are shown to confirm the assumptions where the corresponding points on the heat transfer process curve at the points of 5.4(a) to (f) are shown in Fig. 5.2 with a solid line. Figure 5.4(a) is the onset of boiling and it can be seen with a few initial vapor bubbles. Figures 5.4(b) and 5.4(c) are the photographs after the time passage of 6.8 s and 12.8 s from point (a), respectively. It takes a long time for the vapor bubbles to spread to the whole surface of the test heater as shown in the figure. The vapor bubbles around the heater occur from active cavities of entrained vapor that cause the increase of heat flux. After incipient boiling at a point that corresponds to the q_{in}, the surface superheat, ΔT_{sat}, does not change so much with an increase in heat input. As shown in Fig. 5.4(d), the small bubble nucleus commences to coalesce in the nucleate boiling region to form coalesced bubbles. The detached coalesced bubbles continuously increase in size with increases in the heat flux at the points of 5.4(e) to (f).

5.5 Heat transfer processes with a constant period at pressures of 101.3 and 494 kPa under saturated condition in ethanol

Figure 5.5 shows the transient phenomenon on a graph of heat flux, q, versus surface superheat, ΔT_{sat}, for the period of 10 s at each pressure. The heat transfer process at a pressure of 494 kPa is shown with a dashed chain line: heat flux, q, increases along the natural convection curve at first and after the occurrence of initial boiling at a surface

superheat of 60 K, the surface superheat rapidly decreases, and the transition to fully-developed nucleate boiling occurs and reaches the CHF point, q_{cr}. On the other hand, the process at a pressure of 101.3 kPa is shown with a dashed line where photographs were taken at the points of 5.6(a) to (g): the curve shows that the q increases along the natural convection curve, and the boiling occurs at a surface superheat point of 100 K, which is higher than that in the case of the process at 494 kPa, and then shows a transition directly to film boiling without passing the nucleate boiling. In the case of the boiling process shown with a dashed line, it is considered that the direct boiling transition on the heater surface from non-boiling to film boiling is due to the heterogeneous spontaneous nucleation (HSN) in previously flooded cavities on heater surface as suggested by Sakurai et al. (1992, 1993, 1995).

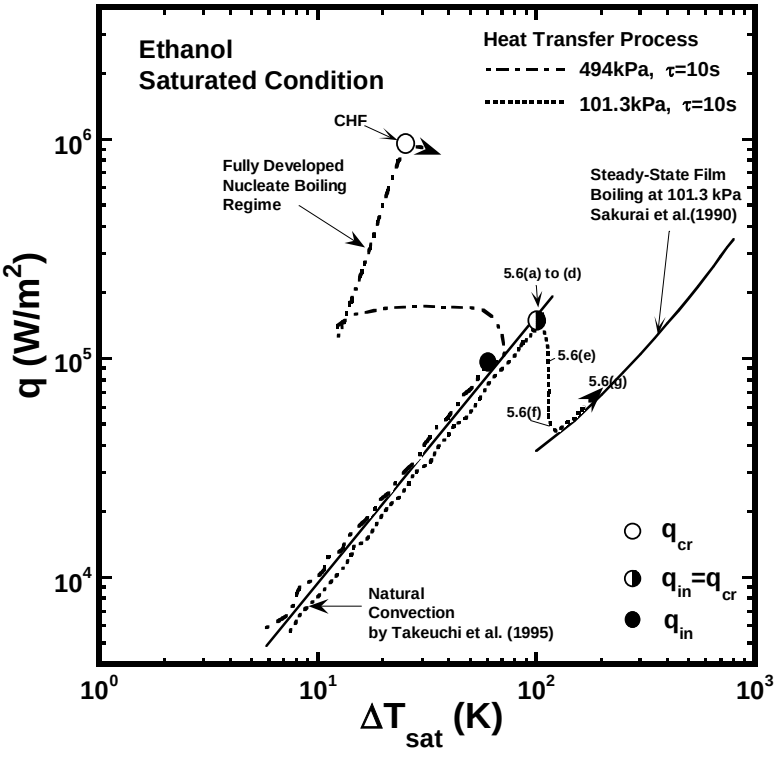

Fig. 5.5 Boiling heat transfer processes from non-boiling to film boiling or to fully developed nucleate boiling under saturated condition in ethanol. Photographs shown in Fig. 5.6 were taken at points of 5.6(a) to (g) on the graph.

Figure 5.6 gives a series of subsequent photographs from the moment of onset of a vapor phase to film boiling on a surface at a pressure of 101.3 kPa in saturated ethanol.

(g) t=141ms

(f) t=61ms

(e) t=21ms

(d) t=6ms

(c) t=2ms

(b) t=1ms

(a) t=0ms

Fig. 5.6 Vapor film behavior during direct transition to film boiling for a period of 10 s at a pressure of 101.3kPa in saturated ethanol.

Figure 5.6(a) is the onset of boiling on the cylinder. The figure 5.6(b) taken at 1 ms

after the first one shows a vapor tube due to the explosive-like HSN in flooded cavities, and it covers the whole cylinder surface by the large vapor tube. Figure 5.6(c) taken at 2 ms after the first one shows thick vapor film concentrically covering the cylinder. The vapor bubbles rapidly grow and completely cover the surface of the cylinder within just a few milliseconds. The temperature difference of the surface superheat between corresponding to Figs. 5.6(a) to (c) is almost the same. Figure 5.6(d) taken at 6 ms after the first one shows that the vapor bubbles collapse from the boiling initiation bubbles. Then, large vapor bubbles are broken away from the large vapor film by buoyancy force and move upward as shown in Figs. 5.6(e) to (f). After detachment of the large vapor bubbles, solid-liquid contacts occurs, and then new thin vapor film with the Taylor unstable wave on the upper part of the vapor-liquid interface covering the cylinder is formed by the explosive-like HSN on the places of solid-liquid contact and thin film boiling. At this moment the surface temperature starts increasing rapidly as a result of heat transfer deterioration. As shown in figure 5.6(g), the behavior of vapor-liquid interface in film boiling on the cylinder similar to that for steady-state film boiling on the cylinder is clearly observed after the detachment of large vapor bubbles.

5.6 Heat transfer processes during transitions to fully-developed nucleate boiling or to film boiling at a pressure of 101.3 kPa in saturated ethanol

Figure 5.7 shows the heat transfer processes in saturated ethanol on a graph of heat flux, q, versus surface superheat, ΔT_{sat}, for the periods of 50 s and 100 ms at atmospheric pressure. It is confirmed that the initial boiling in highly wetting liquid such as ethanol occurs in previously flooded cavities on heater surface, because the superheat temperature of initial boiling is much higher than that of water. The heat transfer process for a period of 50 s is shown with a solid line where photographs were taken at

the points of 5.8(a) to (f). On the other hand, the process for a period of 100 ms is shown with a dashed line where photographs were taken at the points of 5.9(a) to (f): the boiling occurs at a surface superheat point of 100 K, which is higher than that in the case of the process at period of 50 s, and then shows a transition directly to film boiling without passing the nucleate boiling. It is considered that the direct boiling transition from non-boiling to film boiling is due to the heterogeneous spontaneous nucleation (HSN) as mention before.

Then the Figs 5.8 and 5.9 give a series of subsequent photographs at this condition. In the case of a period of 100ms at first, the photo no. 5.9(b) taken at 2 ms shows a vapor tube due to the explosive boiling in flooded cavities, the vapor bubbles are rapidly growing and covering the heater surface within just a few milliseconds. A photo no. 5.9(d) taken at 27 ms shows the vapor bubbles collapse from the boiling initiation bubbles. Then, large vapor bubbles are broken away from the large vapor film by buoyancy force and move upward. On the other hand, in the case of a period of 50 s, it covers the whole heater surface by the large vapor tube. The occurrence behavior of initial boiling is just similar to that of the direct transition for 100 ms. This vapor film behavior that are rapidly growing and covering the heater surface during boiling initiation could never be seen in the water experiment with quasi-steadily increasing exponential heat input. After the detachment of large vapor bubbles, transition to fully-developed nucleate boiling occurs.

5.7 Heat transfer processes during transitions to fully-developed nucleate boiling or to film boiling at atmospheric pressure in saturated FC-72

As shown in the Fig. 5.10, the heat transfer process for a period of 10 s at a pressure of 101.3 kPa is shown with a dashed chain line where photographs were taken at the points

of 5.12(a) to (f), and with the steady-state natural convection curve derived by Takeuchi et al. (1995) and the steady-state film boiling curve derived by Sakurai et al. (1990) for comparison. On the other hand, the heat transfer process including direct transition point for a period of 100 ms at the same pressure is also shown with a dashed line where photographs were taken at the points of 5.11(a) to (f), and with the heat conduction curve derived by Sakurai et al. (1977). As shown in the figure, the transition processes to film boiling are completely different from each other due to the exponential period: namely the heat inputs correspond to those with the increasing rates from quasi-steady to rapid ones.

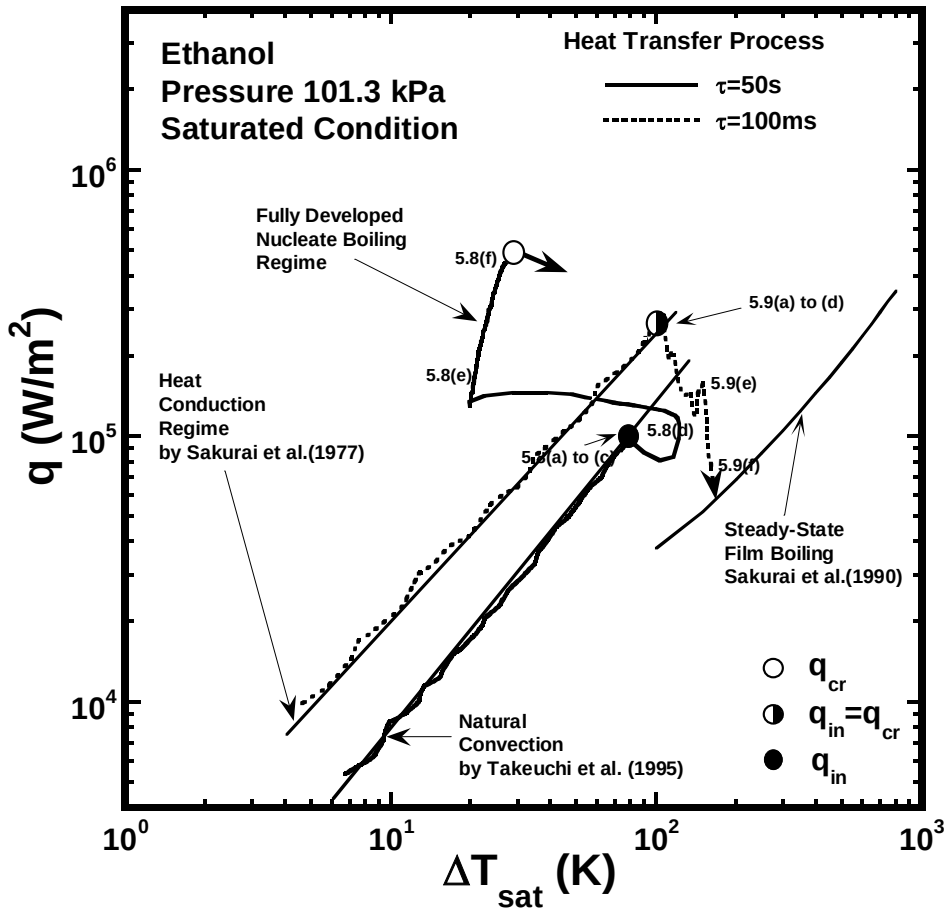

Fig. 5.7 Boiling heat transfer processes for periods of 50 s and 100 ms under saturated condition at atmospheric pressure in ethanol from non-boiling to film boiling or to fully developed nucleate boiling. Photographs were shown in Figs. 5.8 & 5.9.

(f)=64.4s

(e)=14.3s

(d)=807ms

(c)=52ms

(b)=5ms

(a)=0ms

Fig. 5.8 Vapor film behavior during transition to fully developed nucleate boiling for a period of 50 s at a pressure of 101.3kPa in saturated ethanol.

(f) t=127ms

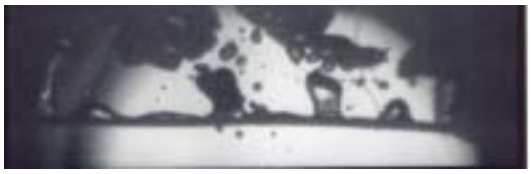

(e) t=67ms

(d) t=27ms

(c) t=5ms

(b) t=2ms

(a) t=0ms

Fig. 5.9 Vapor film behavior during direct transition to film boiling for a period of 100 ms at a pressure of 101.3kPa in saturated ethanol.

In the case of the boiling process with a period of 100 ms, it is considered that the direct boiling transition from non-boiling to film boiling is due to the heterogeneous spontaneous nucleation (HSN) as mentioned before. And it can be seen that the incipient surface superheat at which direct transition occurs, becomes a little higher with a decrease in period.

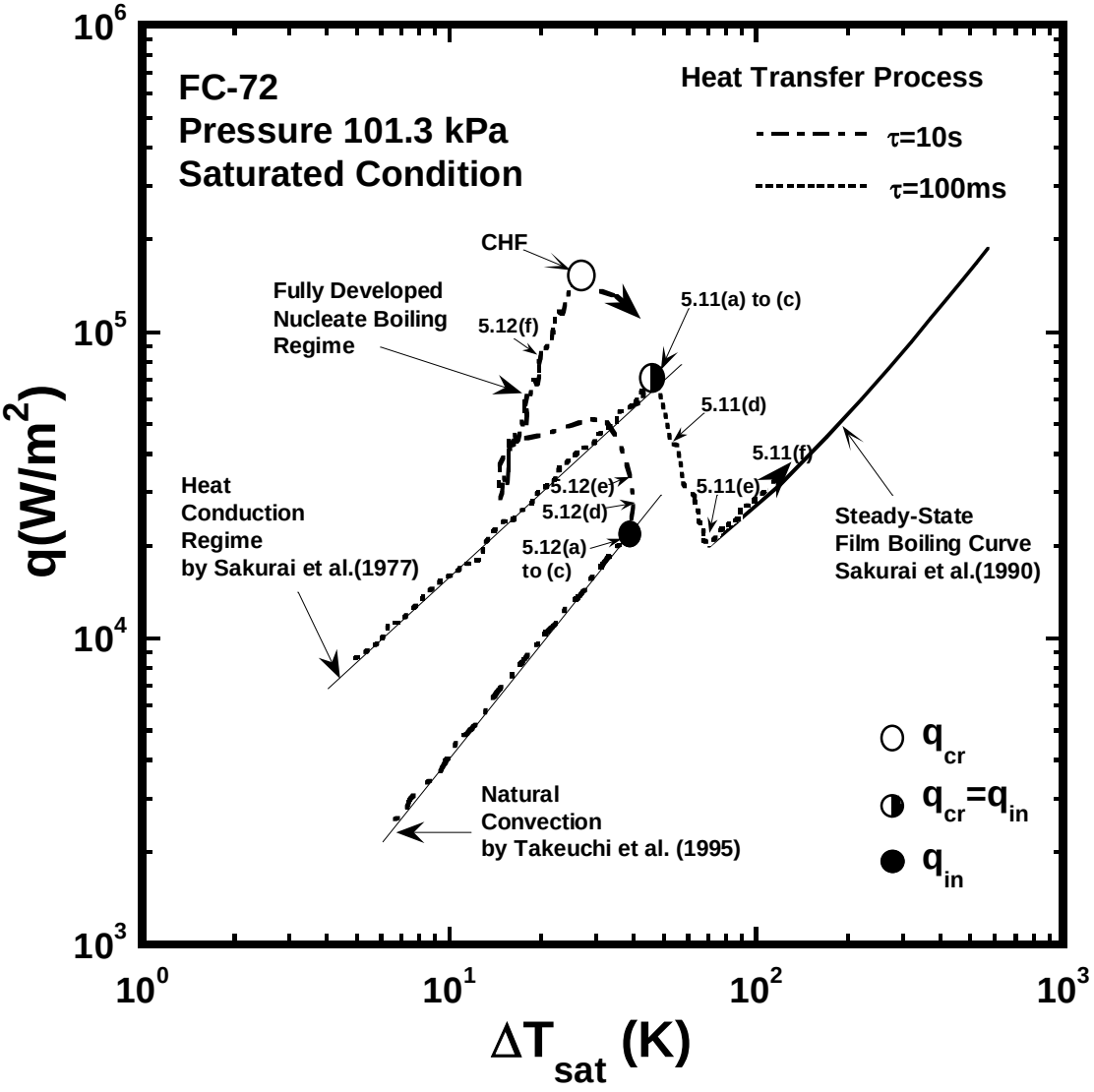

Fig. 5.10 Boiling heat transfer processes from non-boiling to film boiling or to fully developed nucleate boiling under saturated condition in FC-72. Photographs shown in Figs. 5.11 & 5.12 were taken at points of 5.11(a) to (f) and 5.12(a) to (f) on the graph, respectively.

5.7.1 Photographs of vapor film behavior during transition to film boiling in FC-72

Figure 5.11 shows the photographs of transient boiling behavior taken by a high-speed video camera at the corresponding points shown in Fig. 5.10. Figure 5.11(a) is the photograph at point (a), which is the onset of boiling. Figure 5.11(b) is the photograph after a time passage of 1 ms from point (a). The vapor bubbles are rapidly growing and surrounding the surface of test heater. The rapid growth of vapor bubbles is due to heterogeneous spontaneous nucleation (HSN) within the flooded cavities of test heater. As shown in the Fig. 5.11(c), the vapor bubbles covered almost all the heater surface within a time less than 5 ms. Figure 5.11(d) is the photograph after a time passage of 27 ms from point (a). It is seen that the vapor bubbles are separated from the surface of test heater. The bubble size along the same direction of axis as the heater is almost equal to the size of Taylor's hydrodynamic instability wavelength. Figure 5.11(e) is the photograph of the time at which 67 ms elapsed from point (a). The film boiling appears after the departure of vapor bubbles. Figure 5.11(f) is the photograph after the time passage of 127 ms from point (a) and is the stable film boiling after passing the point (e).

5.7.2 Photographs of vapor film behavior during transition to fully-developed nucleate boiling in FC-72

Figure 5.12 shows the photographs for typical vapor film and vapor bubble behaviors in the transition to developed nucleate boiling caused by quasi-steadily increasing exponential heat input with a period of 10 s at a pressure of 101.3 kPa at the corresponding points shown in Fig. 5.10. The vapor bubbles are rapidly growing and surrounding the surface of test heater, and the test heater is almost fully covered with

(f) t=127ms

(e) t=67ms

(d) t=27ms

(c) t=4ms

(b) t=1ms

(a) t=0ms

Fig. 5.11 Vapor film behavior during direct transition to film boiling for a period of 100 ms at a pressure of 101.3kPa in saturated FC-72.

(f) t=8.8s

(e) t=87ms

(d) t=22ms

(c) t=6ms

(b) t=2ms

(a) t=0ms

Fig. 5.12 Vapor film behavior during transition to fully developed nucleate boiling for a period of 10 s at a pressure of 101.3 kPa in saturated FC-72.

the vapor bubbles as shown in the Fig. 5.12(d). The vapor film behavior shown in 5.12(a) to (d) is just similar to that of the direct transition for a period of 100 ms at the

same pressure in Fig. 5.11. The time dependence of the vapor film behavior is also similar to that shown in Figs. 5.11(a) to (d) except that after the detachment of large vapor bubbles transition to film boiling occurs. This vapor film behavior that are rapidly growing and covering the heater surface during boiling initiation could never be seen in the water experiment with quasi-steadily increasing exponential heat input. In the case of the initial boiling behavior in a pool of ethanol, of course FC-72, which are highly wetting liquids, the surface tension is lower than that of water and its contact angle between liquid and heater surface is smaller than that of water, so that it may be easy for a wetting liquid to previously flooded cavities on a heater surface. Therefore, it can be assumed that the initial boiling is due to not active cavities but flooded cavities on a heater surface.

In the case of Fig. 5.11, after the detachment of large vapor bubbles, the new film boiling is formed by the explosive-like HSN. On the other hand, as seen in Figs. 5.12(e) to (f), the nucleate boiling occurs from the cavities of entrained vapor that are formed after detachment of vapor bubbles with a slight decrease in surface superheat which prevents the growth of the HSN. If the detachment of vapor bubbles without decreasing in average surface superheat is realized, the direct or semi-direct transition occurs as in the case of rapidly increasing in heat input mentioned before.

5.8 Summary

The vapor behavior on the horizontal test cylinder during the transition from natural convection and transient conduction regimes to film boiling in water and highly wetting liquids such as ethanol and FC-72 due to various exponentially increasing heat inputs including a quasi-steadily increasing heat input to a rapid increasing one was examined by the photographs taken using a high-speed video camera.

In the case of the highly wetting liquids, the vapor film behavior during transition to fully-developed nucleate boiling was just similar to that of the direct transition to film boiling. This vapor film behavior that rapidly grew and covered the heater surface during initial boiling could never be seen in the water experiment with a quasi-steadily increasing exponential heat input. It was confirmed that the initial boiling behavior is significantly affected by the property and the wettability of the liquid. The direct transition at the CHF from non-boiling regime to film boiling one occurred without a heat flux increase for a short period within second group while semi-direct transition occurred with one. It was certain that the direct or semi-direct transition occurs in the case of rapidly increasing heat input when the detachment of vapor bubbles without decreasing of average surface superheat is realized. The transient CHFs are clearly divided into three principal groups for the periods and well dependent on subcooling at the fixed pressure. And the minimum CHF values within the second group at each pressure were much lower than the corresponding steady state CHF. Also the ratio of minimum CHF to steady state one was different depending on the liquids.

6. Conclusions

Steady-state and transient boiling heat transfer characteristics caused by an exponential heat generation rates with various period were investigated. Steady-state and transient critical heat fluxes (CHFs) were measured using a 1.0 mm diameter horizontal cylinder in a pool of water and highly wetting liquids, such as ethanol and FC-72, over periods ranging from about 5 ms to 50 s for wide ranges of subcooling and pressure.

In Chapter 3, it was confirmed that boiling heat transfer processes from non-boiling to film boiling or to fully-developed nucleate boiling were completely different from each other depending on the experimental liquids. Also it is recognized they depend on the heat generation rates shown with period.

(1) The processes from non-boiling to film boiling were completely different from each other depending on the period. The values of initial boiling heat flux increased with a decrease in period, that is, as the period shortens, the heat conduction became predominant in heat transfer compared with the natural convection.

(2) The vapor behavior at initial boiling due to the HSN was considerably different from that due to active cavities; it covered the whole cylinder surface by the large vapor tube in a short time. It was considered that the direct boiling transition on the heater surface from non-boiling to film boiling was due to the HSN in previously flooded cavities on heater surface without the contribution of active cavities in general.

(3) The quasi-steady-state CHFs measured were mainly divided into two mechanisms for lower and higher subcooling at a pressure; the former and latter CHFs occur due to hydrodynamic instability (HI) and explosive-like heterogeneous spontaneous nucleation (HSN) on the cylinder surface respectively. The dependability of pressure in the high subcooling regime became different depending on the boiling liquids.

(4) The transient CHFs were clearly classified into three principal groups for the periods: first group for the longer period, second group for the shorter and third group for the intermediate. And those were dependent on subcooling whichever groups in the case of a constant pressure.

In Chapter 4, it was investigated the effect of the surface conditions of the test cylinders such as the commercially-available surface (CS) and the roughly-finished surface (RS) with different cavity size distribution and surface energy in saturated and subcooled test liquids at various pressures on the transient pool boiling CHFs caused by the exponential heat generation rate shown with the periods.

(1) The effect of surface condition on steady-state CHFs for wide range of subcoolings and pressures was investigated. The CHFs measured for the CS cylinder almost agreed with that of RS one though the data for the rough cylinder at some pressures were slightly larger than that of the CS cylinder.

(2) The transient CHFs were clearly existed into three groups in ethanol and FC-72 for the cylinders with CS and RS, though the values for the shorter periods belonging to the second group for the cylinder with CS were not observed in the case of water tested here except those for the saturated condition at around atmospheric pressure.

(3) The transient CHFs belonging to the first group for longer periods at lower and higher subcoolings at the pressure tested obtained for the cylinder with RS, expressed by Eq. (3.8) representing CHF due to the HI, and Eq. (3.9) representing CHF due to the HSN, respectively, were similar to those obtained for the cylinder with CS. On the other hand, the second groups of CHFs for the shorter periods for each cylinder were approximately expressed by Eq. (3.10) which gave the theoretical conduction heat flux corresponding to a short period at the corresponding HSN surface superheat depending on the period, though the CHF values for RS cylinder

existed at slightly higher than the CS cylinder.

(4) The period range of the third group CHF for the cylinder with RS became narrow in comparison with that for the cylinder with CS. As a result, the period range of the second group CHF became wide in the range of the periods. The minimum CHF values for the longest period for the second group at each pressure were much lower than the corresponding steady-state CHF, and the minimum CHF values obtained for CS cylinder disagreed with those obtained for RS cylinder. Consequently, the CHF values belonging to the second and third group were considerably affected by the surface conditions.

In Chapter 5, it was clarified the transition phenomena to film boiling in several liquids having different wettability by the photographic approach on the vapor bubble and vapor film behavior on the cylinder surface by using a high-speed video camera. More in detail, the vapor behavior on the horizontal test cylinder during the transition from natural convection and transient conduction regimes to film boiling in water and highly wetting liquids such as ethanol and FC-72 due to exponential heat generation rates including a quasi-steadily increasing to a rapid increasing one was examined by the photographs taken using a high-speed video camera.

In the case of the highly wetting liquids, the vapor film behavior during transition to fully-developed nucleate boiling was just similar to that of the direct transition to film boiling. This vapor film behavior that rapidly grew and covered the heater surface during initial boiling could never be seen in the water experiment with a quasi-steadily increasing exponential heat input. It was confirmed that the initial boiling behavior is significantly affected by the property and the wettability of the liquid. The direct transition at the CHF from non-boiling regime to film boiling one occurred without a heat flux increase for a short period within second group while semi-direct transition occurred with one. It was

certain that the direct or semi-direct transition occurs in the case of rapidly increasing heat input when the detachment of vapor bubbles without decreasing of average surface superheat is realized. The transient CHFs are clearly divided into three principal groups for the periods and well dependent on subcooling at the fixed pressure. And the minimum CHF values within the second group at each pressure were much lower than the corresponding steady state CHF. Also the ratio of minimum CHF to steady state one was different depending on the liquids.

References

Avksentyuk, B.P., Mamontova, N.N., 1973, "Characteristics of heat transfer crisis during boiling of alkali metals and organic fluids under free convection conditions at reduced pressure. " Prog. Heat Mass Transfer 7, pp. 355-362.

Chang, J.Y., You, S.M. & Haji-Sheikh, A., 1998, "Film boiling incipience at the departure from natural convection on flat, smooth surfaces", ASME *Journal of Heat Transfer*, Vol. 120, pp. 402-409.

Fukuda, K., Shiotsu, M. & Sakurai, A., 1995, "Transient pool boiling heat transfer due to increasing heat inputs in subcooled water at high pressures", Proceedings of the 7th Int. Meeting on Nuclear Reactor Thermal Hydraulics, Saratoga Springs, USA, pp. 554-573.

Fukuda, K., Shiotsu, M. and Sakurai, A., "Effects of surface conditions on transient critical heat fluxes for a horizontal cylinder in a pool of water at pressures due to exponentially increasing heat input," *Nuclear Engineering and Design*, 200 (2000), pp. 55-68.

Fukuda, K. and Sakurai, A., "Effects of diameters and surface conditions of horizontal test cylinders on subcooled pool boiling CHFs with two mechanisms depending on subcooling and pressure," Heat Transfer 2002, Proc. of the 12th International Conference (2002), pp. 611-616.

Fukuda, K., Liu, Q.S. and Park, J.D. and Kida, H., "Photographic study on transient critical heat flux depending on surface conditions of test heater in various liquids due to exponentially increasing heat inputs," Proceedings of 6th International Symposium on Heat Transfer, Beijing, China (2004), pp. 511-518.

J. H. Lienhard, 1988, "Burnout on Cylinders", *Journal of Heat Transfer*, Vol. 110, pp.1271-1286.

References

J. H. Lienhard & V. K. Dhir, 1973, "Hydrodynamic Prediction of Peak Pool-boiling Heat Fluxes from Finite Bodies", *Journal of Heat Transfer*, Vol. 95, No. 2, pp.1271-1286.

Kasakawa, Takashi, K., Hata, K. & Shiotsu, M., 1999, "Transient heat transfer on a horizontal cylinder in FC-72", Advances in Electronic Packaging 1999, ASME EEP Vol. 26-2, pp. 1471-1478.

Kutateladze, S.S., 1959, "Heat transfer in condensation and boiling", AEC-tr-3770, USAEC.

Kutateladze, S.S., Moskcvicheva, V.N., Bobrovich, G.I., Mamontova, N.N., Avksentyuk, B.P., 1973. "Some peculiarities of heat transfer crisis in alkali metals boiling under free convection." Int. Heat Mass Transfer 16, 705-713.

Sakurai, A. & Shiotsu, M., 1974, "Transient pool boiling heat transfer", ASME 74-WA/HT-41, pp. 1-16.

Sakurai, A. & Shiotsu, M., 1977, "Transient pool boiling heat transfer, Part 1: incipient boiling superheat", ASME *J. Heat Transfer*, Vol. 99, pp. 547-553.

Sakurai, A., Shiotsu, M. & Hata, K., 1990, "A general correlation for pool film boiling heat transfer from a horizontal cylinder to subcooled liquid, Part 2: experimental data for various liquids and its correlation", ASME *J. Heat Transfer*, Vol. 112, pp.441-450.

Sakurai, A., Shiotsu, M., Hata, K., 1992. "Heat transfer from a horizontal wire in liquid nitrogen." Heat Transfer and Super-conduction Magnetic Energy Storage, ASME HTD-Volume 211, pp. 7-18.

Sakurai, A., Shiotsu, M. & Hata, K., 1993, "New transition phenomena to film boiling due to increasing heat inputs on a solid surface in pressurized liquids", Instability in Two Phase Flow Systems, Vol. HTD-260/Fed-169. ASME, New York, pp. 27-39.

Sakurai, A., Shiotsu, M., Hata, K. & Fukuda, K., 1995, "Transition phenomena from non-boiling regime to film boiling on a cylinder surface in highly subcooled and pressu-

rized water due to increasing heat inputs", ASME Paper, 95-WA/HT-17, pp.1-11.

Sakurai, A., Shiotsu, M. & Fukuda, K., 1996, "Pool boiling critical heat flux on a horizontal cylinder in subcooled water for wide ranges of subcooling and pressure and its mechanism", Proceedings of the Thirty-first National Heat Transfer Conference, Vol. HTD-326, ASME, New York, pp. 93-104.

Sakurai, A., 2000, "Mechanisms of transitions to film boiling at CHFs in subcooled and pressurized liquids due to steady and increasing heat inputs", *Nuclear Engineering and Design*, Vol. 197, pp. 301-356.

Sakurai, A., & Fukuda, K., 2002, "Mechanisms of subcooled pool boiling CHFs depending on subcooling, pressure, and test heater configurations and surface conditions in liquids", Proceedings of ASME IMECE'02, New Orleans, pp. 1-13.

Takeuchi, Y., Hata, K., Shiotsu, M. & Sakurai, A., 1995, "A general correlation for laminar natural convection heat transfer from single horizontal cylinders in liquids and gases with all possible Prandtl numbers", International Mechanical Engineering Congress and Exposition, Vol. HTD-317-1. ASME, New York, pp. 259-270.

Zuber, N., 1959, "Hydrodynamic Aspects of Boiling Heat Transfer," AECU-4439, USAEC.

Related publications

J.D. Park, K. Fukuda and Q.S. Liu, Photographic study on transient phenomena in pool boiling CHF for various liquids, The Seventh International Symposium on Marine Engineering, ISME TOKYO 2005, Paper041, pp. 1-8, 2005.

J.D. Park, K. Fukuda and Q.S. Liu, Effects of surface conditions on transient pool boiling CHF in various liquids with different mechanisms depending on pressure and subcooling, Proceedings of 13th International Conference on Nuclear Engineering, beijin, China, ICONE13-50335, pp.1-8 2005.

J.D. Park, K. Fukuda and Q.S. Liu, Pool Boiling Critical Heat Flux of Highly Wetting Liquid, The Sixth KSME-JSME Thermal and Fluids Engineering Conference, Jeju, Korea, tfec6-448, pp. 1-4, 2005.

K. Fukuda, Q.S. Liu and J.D. Park, Transient boiling critical heat flux in a pool of freon-113 and ethanol under saturated conditions, Proceedings of 3rd International Symposium on Heat Transfer Enhancement and Energy Conservation, Guangzhou, China, Volume 1, pp.221-227, 2004.

K. Fukuda, Q.S. Liu, J.D. Park and H. Kida, Pool Boiling Critical Heat Flux of Highly Wetting Liquid, Journal of The Japan Institution of Marine Engineering (in Japanese), Vol.39, No.10, pp.25-32, 2004.

K. Fukuda, Q.S. Liu, H. Kida and J.D. Park, Boiling Heat Transfer Phenomena in Highly Wetting Liquid, Journal of The Japan Institution of Marine Engineering (in Japanese), Vol.39, No.10, pp.33-41, 2004.

K. Fukuda, Q.S. Liu, J.D. Park and H. Kida, Photographic study on transient critical heat flux depending on surface conditions of test heater in various liquids due to exponentially increasing heat inputs, Proceedings of 6th International Symposium on Heat Transfer, Beijin, China, pp.511-518, 2004.

Acknowledgements

I would like to express my sincere thank to my supervisor, Professor Fukuda, for his guidance and encouragement during my studies in Japan. I have been impressed by his excellent engineering ability and his consistent dedication to research and education. It was a wonderful opportunity for me to learn many things from him.

I would like to thank Professor Fukuoka for his judicious advice as my vice advisor, Professor Sugita for his help as a member of my thesis committee, and Assistant Professor Liu for my thesis review to the very end. I would to thank Professor K. Ishida for his help and continuous encouragement.

I would like to thank my all friends who have helped me in Japan. Thanks to Sue for her special Japanese lessons. She always gave me the lovely suggestions as my friend. Besides, I show my appreciation to Japanese Rotary Club for providing me a special scholarship for two years. I studied that Rotary provides humanitarian service, encourages high ethical standards in all vocations, and helps build goodwill and peace in the world. I give my special appreciation and greetings to Itami-Koyaike Rotary Club and Dr. Fujimoto of my counselor. They encouraged me continuously and fostered the ideal of service.

Finally, and most importantly, I thank my wife for her constant encouragement and selfless sacrifice. She makes me a father with two lovely kids during my studying abroad. It was hard for us to live in foreign country, but I think it will be very helpful for our future. I am very grateful to my daughter for her cheerful smile and lively voice and I am extremely happy to have a son of new arrival.